

The Expression, Purification and Characterization of *Escherichia coli* NudL, a Putative Coenzyme A Hydrolase

By

Sarah Maggie Kellow-Webb

Thesis presented in partial fulfilment of the requirements for the degree of Master of Science in the
Faculty of Science at Stellenbosch University.



Supervisor: Prof Erick Strauss

Co-Supervisor: Dr Marianne de Villiers

Department of Biochemistry

March 2021

Declaration

By submitting this thesis electronically, I declare that the entirety of the work contained therein is my own, original work, that I am the sole author thereof (save to the extent explicitly otherwise stated), that reproduction and publication thereof by Stellenbosch University will not infringe any third party rights and that I have not previously in its entirety or in part submitted it for obtaining any qualification

March 2021

Abstract

Coenzyme A (CoA) is an essential cofactor that is synthesized by a conserved five-step pathway from pantothenic acid (vitamin B5). The regulation of CoA levels is vital in supporting normal cellular function. In higher order organisms, CoA degradation and the recycling of CoA have proven efficient for the dynamic control of CoA levels, but in prokaryotes the contribution of CoA degradation to the regulation of CoA levels remains largely unstudied. *Escherichia coli* is known to make significant quantities of 4'-phosphopantetheine (PPanSH), a CoA biosynthesis intermediate, the excess of which is irreversibly exported to the extracellular environment. Early studies revealed that the source of the high PPanSH levels is both from the biosynthesis and the degradation of CoA. In *E. coli*, CoA degradation can be mediated via an indirect mechanism through acyl carrier protein (ACP) prosthetic group turnover, where AcpH releases the PPanSH moiety from the *holo*-ACP, or via a direct mechanism by an unidentified enzyme. One possible mechanism for direct degradation of CoA is by the action of a CoA hydrolase, a Nudix hydrolase subfamily member. Nudix hydrolases are a superfamily of housekeeping enzymes that regulate metabolic intermediates or remove toxic nucleotide metabolites. Nudix hydrolases specific for CoA are able to degrade CoA at the pyrophosphate moiety into 3',5'-ADP and PPanSH. *E. coli* has 13 predicted Nudix enzymes of which NudL is the only one yet to be characterized. NudL is encoded by the *yeaB* gene and contains both the Nudix box and NuCoA motif that points to its selectivity for CoA and strongly suggests that it is a CoA hydrolase.

The first part of this study focused on optimizing the production of pure, soluble NudL protein for testing its putative CoA hydrolase activity. The protein was found to be unstable and significant challenges were experienced with soluble recombinant protein expression. NudL could therefore only be partially purified for the purpose of activity testing.

The second part of this study focussed on characterizing NudL's activity. Both the partially purified enzyme and *E. coli* lysate containing overexpressed NudL was found to be able to degrade CoA and form PPanSH. These results provide strong evidence that CoA hydrolysis into PPanSH is mediated by NudL and confirms the presence of CoA hydrolase activity in *E. coli* lysate. CoA hydrolase activity was dependent on the presence of a metal cofactor and NudL appeared to prefer Mn^{2+} over Mg^{2+} . Following this, the physiological relevance of NudL was investigated. The results of metabolomic studies revealed that NudL contributes significantly to the intracellular PPanSH levels as a knockout mutant lacking the enzyme had considerably lower intracellular PPanSH levels. An Δ *acpH* mutant also showed a similar trend, confirming that CoA degradation contributes to the intracellular PPanSH pool. Conditions which promote CoA degradation were also investigated. Transcription of the NudL-encoding gene *yeaB* did not appear to be influenced by oxidative stress; however, a significant growth

defect was observed for the mutant strains when acetate was the carbon source, suggesting that CoA degradation by NudL is important during growth on acetate.

The results of this study support a direct mechanism of CoA degradation in *E. coli*, specifically by the NudL enzyme, being the last *E. coli* Nudix hydrolase to be experimentally characterized. Further investigations are needed to understand how this enzyme is regulated. This may provide insight into how CoA levels are regulated in *E. coli* in general.

Opsomming

Koënsiem A (KoA) is 'n noodsaaklike ko-faktor wat deur middel van 'n gekonserveerde vyf-stap-padweg vanaf pantoteensuur (vitamien B5) gesintetiseer word. Die regulering van KoA-vlakke is noodsaaklik om normale sellulêre funksie te ondersteun. In hoër orde organismes het KoA-afbraak en die herwinning van KoA effektief blyk te wees vir die dinamiese beheer van KoA-vlakke, maar in prokariote bly die bydrae van CoA-afbraak tot die regulering van KoA-vlakke grotendeels onbestudeer. Dit is wel bekend dat *Escherichia coli* beduidende hoeveelhede maak van 4'-fosfopanteteïne (PPanSH), 'n KoA-biosintese-tussenproduk, waarvan die oormaat onomkeerbaar na die ekstrasellulêre omgewing uitgevoer word. Vroeë studies het uitgewys dat die bron van die hoë PPanSH-vlakke beide die gevolg is van die biosintese en die afbraak van KoA. In *E. coli* kan KoA-afbraak plaasvind deur 'n indirekte meganisme deur die omset van die prostetiese groep van die asiel-draerproteïen (ACP), deurdat AcpH die PPanSH-groep van die *holo*-ACP vrystel, of via 'n direkte meganisme gekataliseer deur 'n ongeïdentifiseerde ensiem. Een moontlike meganisme vir direkte afbraak van KoA is deur die werking van 'n KoA-hidrolase, spesifiek 'n lid van die Nudix-hidrolase-subfamilie. Nudix-hidrolases is 'n superfamilie van huishoudingsensieme wat metaboliese tussenprodukte reguleer of toksiese nukleotiedmetaboliete verwyder. Nudix-hidrolases wat spesifiek vir KoA is kan KoA in die pirofosfaatgedeelte hidroliseer om 3',5'-ADP en PPanSH te vorm. *E. coli* het 13 voorspelde Nudix-ensieme waarvan NudL die enigste is wat nog gekarakteriseer moet word. NudL word gekodeer deur die *yeaB*-geen en bevat beide die Nudix-Koks en die NuKoA-motief, waarvan laasgenoemde die ensiem se selektiwiteit vir KoA aandui en dus sterk daarop wys dat dit 'n KoA-hidrolase is.

Die eerste gedeelte van hierdie studie het gefokus op die optimisering van die produksie van suiwer, oplosbare NudL-proteïene om die vermeende CoA-hidrolase-aktiwiteit daarvan te toets. Daar is gevind dat die proteïen onstabiel is en dat die oplosbare rekombinante proteïenuitdrukking beduidende uitdagings ondervind. NudL kon dus slegs gedeeltelik gesuiwer word om die aktiwiteit daarvan te toets.

Die tweede deel van hierdie studie het gefokus op die karakterisering van NudL se aktiwiteit. Daar is gevind dat beide die gedeeltelik gesuiwerde ensiem en *E. coli* lisaat wat ooruitdruklike NudL bevat, KoA kon afbreek en PPanSH kon vorm. Hierdie resultate lewer sterk bewyse dat KoA-hidrolase in PPanSH deur NudL bemiddel word en bevestig die teenwoordigheid van KoA-hidrolase-aktiwiteit in *E. coli* lisaat. CoA-hidrolase-aktiwiteit was afhanklik van die teenwoordigheid van 'n metaal ko-faktor, en NudL het blykbaar Mn^{2+} bo Mg^{2+} verkies. Hierna is die fisiologiese relevansie van NudL ondersoek. Die resultate van metaboliese studies het aan die lig gebring dat NudL aansienlik bydra tot die intrasellulêre PPanSH-vlakke, aangesien 'n uitklop-mutant sonder die ensiem aansienlik laer

intracellulêre PPanSH-vlakke gehad het. 'N $\Delta acpH$ -mutant het ook 'n soortgelyke neiging getoon, wat bevestig dat KoA-afbraak bydra tot die intracellulêre PPanSH-poel. Toestande wat CoA-afbraak bevorder is ook ondersoek. Transkripsie van die NudL-koderende geen *yeaB* blyk nie deur oksidatiewe stress beïnvloed te word nie; 'n beduidende groeifout is egter waargeneem vir die mutante stamme wanneer asetaat die koolstofbron was, wat daarop dui dat KoA-afbraak deur NudL belangrik is tydens die groei op asetaat.

Die resultate van hierdie studie ondersteun 'n direkte meganisme van CoA-afbraak in *E. coli*, spesifiek deur die NudL-ensiem, wat die laaste *E. coli* Nudix-hidrolase is wat eksperimenteel gekarakteriseer is. Verdere ondersoek is nodig om te verstaan hoe hierdie ensiem gereguleer word. Dit kan insig gee in hoe KoA-vlakke in *E. coli* in die algemeen gereguleer word.

Acknowledgements

I'd like to thank my supervisor Erick Strauss and my co-supervisor Marianne de Villiers. Prof for your patience and reassurance that gave me the strength to soldier on. Thank you for your financial assistance too. Dr de Villiers thank you for your guidance and for being an amazing role model for women in science.

I'd also like to thank every member of the Strauss-de Villiers lab family. I would not have survived without the encouraging and positive work environment. Helba, thank you for all the favours and keeping the ship sailing smoothly. Blake thank you for making me laugh and sharing so much of your science wisdom, you always go the extra mile. Deon, for all your insight with the microbiology aspect of this project. An additional thank you to the Rautenbach lab for coffee breaks and out of hours celebrations.

Carmen, Koketso, Konnie and Yasamin. Thank you for the physical, emotional, and virtual hugs along the way, especially through the writing process. You guys made Stellenbosch feel like home.

To my friends thank you for always giving your full support throughout my seven years in Stellenbosch. Molly and Lindsay a special thank you for the last stretch, your presence made the process infinitely better.

Thank you to my family for your unconditional support in my academic journey. Granny, Dad and Mom thank you for being patient, understanding and for funding me. Cat for being my emotional support as well as being there for the much-needed nap breaks.

Department of Biochemistry and Stellenbosch University thank you for the nurturing environment, which I could explore my curiosities as well as financial assistance.

The last two years has been the most memorable of my university experience (despite the pandemic halfway through). I'm so grateful to everyone and for all the opportunities along the way.

Table of Contents

Abstract	iii
Opsomming	v
Acknowledgements	vii
List of Abbreviations	xi
List of Figures	xiv
List of Tables	xv
Chapter 1	1
1.1 Protein superfamily: Nudix Hydrolase	1
1.1.1 <i>E. coli</i> Nudix hydrolases.....	2
1.1.2 CoA hydrolase.....	6
1.2 Regulation of CoA hydrolases	9
1.2.1 Metabolism.....	9
1.2.2 Stress.....	9
1.2.3 Divalent metal cations.....	10
1.3 CoA biosynthesis and regulating CoA levels	11
1.3.1 Role of CoA degradation and significance of PPanSH.....	14
1.3.2 Fate of 3',5'-ADP and other roles.....	15
1.4 Study Aims	16
1.5 References	17
Chapter 2	22
2.1 Introduction	22
2.2 Experimental Methods	23
2.2.1 Materials.....	23
2.2.2 Plasmid confirmation and subcloning of <i>yeaB</i>	23
2.2.3 Cloning <i>yeaB</i> into pFN29A vector.....	24
2.2.4 Expression trials of NudL.....	25
2.2.5 Purification trials.....	27

2.2.6	Activity screening.....	30
2.3	Results and discussion.....	31
2.3.1	Subcloning.....	31
2.3.2	pET28a-NudL Expression trials.....	32
2.3.3	Purification trials.....	35
2.3.4	Alternate expression systems.....	41
2.4	Conclusion.....	44
2.5	References.....	46
Chapter 3.....		48
3.1	Introduction.....	48
3.2	Experimental Methods.....	49
3.2.1	Materials.....	49
3.2.2	Confirmation of NudL's CoA hydrolase activity.....	49
3.2.3	Determination of intracellular CoA and PPanSH levels in <i>E. coli</i>	52
3.2.4	RT-qPCR analysis of <i>yeaB</i> transcription during oxidative stress and other stress conditions.....	52
3.2.5	Growth rate analysis with different carbon sources.....	53
3.3	Results and discussion.....	53
3.3.1	Confirming the CoA hydrolase activity of NudL.....	53
3.3.2	Metabolomic studies.....	58
3.3.3	Investigating the physiological relevance of NudL.....	61
3.4	Conclusion.....	64
3.5	References.....	66
Chapter 4.....		68
4.1	Summary of findings.....	68
4.1.1	Expression and purification of NudL.....	68
4.1.2	Further insight into NudL - a biological role.....	69
4.2	Future work.....	70

4.2.1	Expression and purification of NudL.....	70
4.2.2	Characterization of NudL	70
4.3	Concluding remarks.....	71
4.4	References	72

List of Abbreviations

3',5'-ADP	Adenosine 3',5'-diphosphate
ATP	Adenosine 5'-triphosphate
ACP	Acyl carrier protein
ACPS	Acyl carrier protein synthase
AcpH	Acyl carrier protein hydrolase
<i>At</i>	<i>Arabidopsis thaliana</i>
BME	β-mercaptoethanol
bp	Base pairs
BSA	Bovine serum albumin
<i>Ce</i>	<i>Caenorhabditis elegans</i>
CoA	Coenzyme A
CPM	7-Diethylamino-3-(4-maleimidophenyl)-4-methylcoumarin
dePCoA	Dephosphocoenzyme A
DNA	Deoxyribonucleic acid
DPCK	Dephosphocoenzyme A kinase
<i>Dr</i>	<i>Deinococcus radiodurans</i>
DTT	Dithiothreitol
<i>Ec</i>	<i>Escherichia coli</i>
EDTA	Ethylenediamine tetra-acetic acid
EtOH	Ethanol
GPC	Gel permeation chromatography
GST	Glutathione S-transferase
His	Histidine
HPLC	High performance liquid chromatography

Hs	Homo sapiens
IMAC	Immobilised metal affinity chromatography
IPTG	Isopropyl- β -D-thiogalactoside
KDa	Kilo Dalton
LB	Luria-Bertani
MBP	Maltose-binding protein
MeCN	Acetonitrile
MeOH	Methanol
Mm	<i>Mus musculus</i>
MW	Molecular weight
NADH	Nicotinamide adenine dinucleotide (reduced)
NH ₄ OAc	Ammonium acetate
OD ₆₀₀	Optical density at 600 nm
PBS	Phosphate-buffered saline
POI	Protein of interest
Pan	Pantothenate
PanK	Pantothenate kinase
PPanSH	4'-Phosphopantetheine
PPAT	4'-Phosphopantetheine adenylyltransferase
PPCS	Phosphopantothenoylcysteine synthetase
PPCDC	Phosphopantothenoylcysteine decarboxylase
ROS	Reactive oxygen species
Sc	<i>Saccharomyces cerevisiae</i>
SDS	Sodium dodecyl sulphate
SDS-PAGE	Sodium dodecyl sulphate polyacrylamide gel electrophoresis

SEC	Size exclusion chromatography
TAE	Tris-acetate-EDTA
TB	Terrific broth
TCA	Trichloroacetic acid
TCEP	Tris(2-carboxyethyl) phosphine
Tris-HCl	Tris(hydroxymethyl)aminomethane-HCl
WHO	World Health Organisation
WT	Wild-type
YT	Yeast-tryptone

List of Figures

Figure 1.1. General structure of a Nudix hydrolase substrate.	2
Figure 1.2. Protein sequence alignment of the <i>E. coli</i> Nudix hydrolases as well as proposed function for those that have been characterized based on the substrate specificity.	3
Figure 1.3. Structure of coenzyme A (CoA) and the two degradation products 4'-phosphopantetheine and 3',5'-ADP.....	6
Figure 1.4. Multiple sequence alignment of Nudix hydrolases from various organisms.	7
Figure 1.5. Mg ²⁺ ion coordinated to 5 water molecules and E86 of <i>Deinococcus radiodurans</i> CoA hydrolase.....	11
Figure 1.6. The five-step CoA biosynthetic pathway for <i>E. coli</i>	12
Figure 1.7. Scheme of 3',5'-ADP fate in humans.	15
Figure 2.1. PCR program for the amplification of the <i>yeaB</i> gene.....	24
Figure 2.2. Agarose gel electrophoresis of enzyme digest of pENTR-NudL.....	32
Figure 2.3. pET28a-NudL small scale expression trials analysed by 12% SDS-PAGE.	34
Figure 2.4. Soluble purification of NudL analysed by 12% SDS-PAGE.	37
Figure 2.5. Purification of NudL grown with pan supplemented media analysed by 12% SDS-PAGE..	38
Figure 2.6. Purification of NudL with different metals charged to IMAC column analysed by 12% SDS-PAGE.....	39
Figure 2.7. Purification of solubilized and purified NudL analysed by 12% SDS-PAGE.....	40
Figure 2.8. Agarose gel electrophoresis of enzyme digest of pFN29A and <i>yeaB</i>	42
Figure 2.9. pFN29A-NudL small scale expression trials analysed by 12% SDS-PAGE..	43
Figure 2.10. Cell free expression reactions analysed by 12% SDS-PAGE gel.	44
Figure 3.1. Summary of attempts to recover fluorescence signals.	55
Figure 3.2. CoA hydrolase activity in lysate obtained from cultures overexpressing NudL.	57
Figure 3.3. Determination of CoA and PPanSH levels in different <i>E. coli</i> strains grown to exponential phase.....	60
Figure 3.4. Determination of intracellular CoA/PPanSH ratios.	61
Figure 3.5. Abundance of the <i>yeaB</i> mRNA transcript in <i>E. coli</i> K12 cells at late stationary phase, with and without oxidative stress.....	62
Figure 3.6. Growth curves of <i>E. coli</i> K12; JW1802 (Δ <i>yeaB</i>), JW0394 (Δ <i>acpH</i>) in minimal media with different carbon sources.....	63

List of Tables

Table 1.1 Summary of <i>E. coli</i> Nudix hydrolases	5
Table 2.1. Summary of expression trial conditions	26
Table 2.2. Summary of purification trial conditions	28
Table 3.1. Comparison of CoA hydrolase activity in various backgrounds.....	58

Chapter 1

Escherichia coli NudL, a putative coenzyme A hydrolase

1.1 Protein superfamily: Nudix Hydrolase

Nudix hydrolases, previously annotated as the MutT family named after MutT, the first Nudix hydrolase characterized from *Escherichia coli*, are found across all domains of life (1, 2). Nudix hydrolases are classified into the “Nudix homology clan” which is often referred to as the “Nudix superfamily”. This superfamily is composed mainly of pyrophosphohydrolases (3). Nudix enzymes with pyrophosphohydrolase activity catalyse the hydrolysis of a wide variety of substrates composed of the general structure: nucleoside diphosphates that are linked to another moiety X to yield a nucleoside monophosphate and phosphate-X, hence the acronym Nudix (Figure. 1.1) (4). Nudix hydrolases are usually small proteins of 16-35 kDa (2). All members of this protein family contain a highly conserved Nudix motif (or Nudix box) of 23 residues, GX₅EX₇RE₂VX₂EEXGU, where U represents a bulky hydrophobic amino acid such as Ile, Leu, Val and X is any other amino acid (5). The Nudix box is normally located on the C-terminal domain of the enzyme whereby a loop- α helix-loop forms the active site that also binds a divalent metal such as Mg²⁺, which also forms the catalytic site (2, 6). The Nudix motif together with additional motifs distinct to the specificity of the particular Nudix hydrolase forms part of a greater $\alpha/\beta/\alpha$ sandwich also known as a Nudix fold (6). The specific conserved residues in the Nudix box that are important for catalytic activity in the *AtNUDX11* CoA hydrolase are Gly-74, Arg-89 and Glu-90 (7). Site directed mutagenesis of these residues in Nudix motifs of *AtNUDX11* (*Arabidopsis thaliana*) resulted in significantly reduced activity (7). The general mechanism by which Nudix enzymes act on their substrate is via nucleophilic substitution at one of the phosphorus atoms, usually the α -phosphorus (6). The range of substrates include NADH, CoA, mRNA caps, nucleotide sugars, dinucleoside polyphosphates as well as nucleoside di- and triphosphates and their oxidized forms (2). The majority of Nudix hydrolases have a preference for alkaline pH as well as the presence of divalent cations for activity, normally Mg²⁺ or Mn²⁺ (2). Fluoride seems to be a strong inhibitor of these enzymes as it blocks the active site with a MgF₃⁻ complex (8). Nudix hydrolases are hypothesized to play a role in the removal of toxic/mutagenic metabolites or the regulation of accumulated metabolic intermediates/cell signalling molecules in biochemical pathways (4, 6). Many Nudix enzymes also display activity for more than one type of substrate and consequently makes their biological role difficult to determine with certainty. Several Nudix enzymes have been re-characterized with substrates of greater affinity and catalytic efficiency several years after the original characterization. Consequently, studies by Nguyen et al. suggested the catalytic efficiency (k_{cat}/K_m) be used to classify the relevant substrate (9). Generally, only one of the substrates have a $k_{cat}/K_m > 10^6 \text{ M}^{-1}$

$^1.s^{-1}$, while the rest of the less relevant substrates have a $k_{cat}/K_m < 10^5 M^{-1}.s^{-1}$ (9). On the other hand, the overlapping substrate specificities of Nudix hydrolases could be advantageous from an evolutionary context to generate new substrate specificities (10).

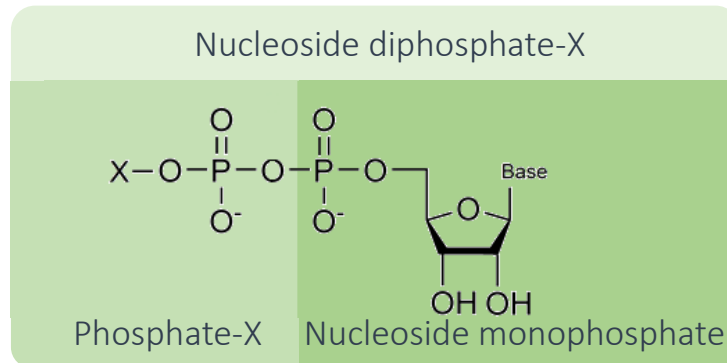


Figure 1.1. General structure of a Nudix hydrolase substrate. Nucleoside diphosphate-X, and the hydrolysis products, a nucleoside monophosphate and phosphate-X.

1.1.1 *E. coli* Nudix hydrolases

Nudix hydrolase subfamilies are arranged by substrate specificity and are classified either by specific amino acids outside of the Nudix motif or by an entirely separate motif (11). These subfamilies are found in varying numbers and combinations in individual organisms and show species-specific functions (12). *E. coli* has 13 predicted Nudix hydrolases, 12 of which have been previously characterized (13, 14) (Figure. 1.2). Amongst all prokaryotes, *E. coli* contains the second highest amount of Nudix enzymes. It was previously speculated, but not experimentally validated, that Nudix enzymes provide a fitness advantage as *Deinococcus radiodurans* has 21 Nudix hydrolases and is renowned for its resistance to stress, notably radiation (11). However, it is not necessarily true that the number of Nudix enzymes is an indication of the survivability of an organism.



* Substrate is still not conclusively determined, but Yfcd has low activity towards GPP, DAPP, and IPP.

Figure 1.2. Protein sequence alignment of the *E. coli* Nudix hydrolases as well as proposed function for those that have been characterized based on the substrate specificity. Shown in boldface type: The highly conserved amino acids of the signature sequence. Similar residues are in red and boxed with a white background. Identical residues are indicated by a solid red boxed background. Substrate is still not conclusively determined, but Yfcd has low activity towards GPP, DAPP, and IPP (*). The alignment was prepared with Clustal Omega and ESPript.

The first *E. coli* Nudix enzyme characterized was MutT. MutT was found to prefer 8-oxo-dGTP as well as dGTP as substrates, which led to the speculation that the function of MutT is to prevent A:T to C:G transversions during DNA replication (15). Orf17 (NudB) was first characterized as a canonical ribo/deoxyribonucleoside triphosphatase with a preference for dATP; however, later it was discovered that NudB was a dihydroneopterin hydrolase (DHNTPase) as the catalytic efficiency was almost 7.5 fold greater for DHNTP than for dATP (16). The true function of this enzyme is to catalyse dihydroneopterin triphosphate (DHNTP) hydrolysis in the folate biosynthesis pathway (16). The (deoxy)ribonucleoside triphosphatase Orf135 (NudG) was found to be specific for pyrimidine (deoxy)nucleotides and was most active towards 5-methyl-dCPT, CTP, dCTP respectively. This was the first example of a base specific Nudix hydrolase, in this case for cytosine. Orf141 is another *E. coli* nucleoside triphosphatase with a preference for pyrimidine deoxynucleoside triphosphates, dUTP being the preferred substrate (13). Orf153 (NudJ) is a nonspecific nucleoside tri/diphosphatase. The enzymatic mechanism of this enzyme is unique in that it differs from the other nucleoside triphosphatases by performing the phosphate hydrolysis in a stepwise manner to form P_i rather than PP_i (13).

A key example of Nudix enzyme promiscuity is Orf186 (NudE) which has three major substrates: ADP, ADP-Ribose and NADH (17). NudE also seems to be specific for nucleoside pyrophosphates with an ADP moiety (17). Orf176 (RppH) was first characterized as a diadenosine oligophosphate pyrophosphatase able to hydrolyse the larger Ap_nA (3 < n < 6 with a preference for pentaphosphate (18). However, it was later found to be a RNA pyrophosphohydrolase (19). RppH was found to degrade mRNA through the removal of the pyrophosphate from the 5' end of RNA producing monophosphorylated RNA, which is a far better substrate for ribonuclease cleavage (19).

Another Nudix enzyme with pyrophosphatase activity for NADH (NudC) was originally characterized with NADH as the main substrate and was thought to play a role in maintaining the cellular NADH/NAD⁺ ratio (20). However, more recently NudC has been identified as the second *E. coli* RNA decapping Nudix hydrolase. Prokaryotic RNA lacks the 5'-methylguanylate cap found in eukaryotic RNA, which is often responsible of RNA stability and translation efficiency (21). Furthermore, a previous study found that NAD⁺, NADH and more recently dephosphocoenzyme A (dePCoA) have been identified as 5'-methylguanylate cap initiating nucleotide equivalents in both Gram positive and Gram negative bacteria (21). NudC was able to cleave these regulatory elements *in vitro* and *in vivo* (21).

E. coli ADP-ribose pyrophosphatase is active for ADP-ribose as well as for ADP-mannose and ADP-glucose (22, 23). This enzyme plays a role in gluconeogenesis as it hydrolyses the precursor, ADP-glucose (23). The observed activity is highest in cells grown in low glucose conditions, and activity decrease with an increase of glucose and glycogen (23).

The Nudix box is conserved for the majority of the *E. coli* Nudix enzymes with only two having slight variations. Orf1.9 (GDP-mannose mannosyl hydrolase) has two replacements: a leucine at E16_N and an alanine at E19_N, as well as a missing Glu residue. Orf191 (NudK) has one replacement, a lysine at R15_N (13). NudK was predicted to be an ADP-ribose hydrolase. Although this enzyme was able to hydrolyse ADP-ribose, GDP-mannose was found to be a better substrate (13). The product of GDP-mannose hydrolysis by Orf1.9 differs to that of the NudK product. Instead of the predicted GDP-mannose + H₂O → GMP + mannose-1-phosphate, the reaction follows GDP-mannose + H₂O → GDP + mannose. NMR analysis showed the alternative mechanism involves the nucleophilic substitution on carbon instead of phosphorus (24). It has been suggested that Orf1.9 is not a true GDP-mannose hydrolase and that the enzyme is a GDP-mannosyl transferase (13).

The most recent Nudix hydrolase to be partially characterized was Orf180 (YfcD) in 2019. Since none of the nucleoside diphosphates could be hydrolysed by this enzyme, substrates for structurally related enzymes were tested (14). The Nudix box and isopentyl diphosphate isomerase (IDI) active sites' both contained a conserved α-helix and connecting loops (14). IDI is a recent addition to the Nudix clan (3). Orf180 was found to have low activity for geranyl pyrophosphate (GPP) as well as two of the IDI substrates, dimethylallyl diphosphate (DAPP) and isopentenyl diphosphate (IPP) (14). However, the primary substrate and function of Orf180 is yet to be defined.

Of all the *E. coli* Nudix enzymes that have been partially or fully characterized, YeaB (NudL) is the only one yet to be successfully expressed and kinetically characterized. NudL is predicted to be a 21.4 kDa CoA hydrolase as it contains both the Nudix motif and NuCoA motif for CoA selectivity as defined below in section 1.1.2 (25). To date, there is only one published article describing the testing of NudL

for phosphatase activity using 3-phosphooxypyruvate as substrate; however, NudL was expressed and tested as a fusion protein with Maltose-binding protein (MBP) in the above-mentioned study (26). Wenlian et al. reported that they had attempted to express NudL in “several vectors and hosts” however, they were unsuccessful in producing sufficient soluble protein for enzyme activity (13). A preprint article has also reported the expression of NudL as fusion protein with MBP (27). They found NudL-MBP was able to degrade CoA, oxidized CoA, dePCoA and oxidized dePCoA; however, after the removal of the MBP tag no activity was observed (27). The work of this study therefore did not add to the understanding CoA degradation in *E. coli* nor the role of NudL in regulating CoA levels and CoA related metabolism.

Table 1.1 Summary of *E. coli* Nudix hydrolases.

Name	Synonyms	Known substrates
NudA	MutT	8-oxo-dGTP, other (d)NTPs
NudC	Orf257	NADH, Capped RNA
NudD	Orf1.9	GDP-mannose, GDP-glucose
NudB	Orf17	dATP, DHNTP
NudE	Orf186	ADP, ADP-ribose NADH
NudF	AdpP	ADP-ribose, ADP-mannose, ADP-glucose
NudG	Orf 135	5-methyl-dCPT, CTP, dCTP
NudH	Orf176, RppH	Capped RNA, Ap ₅ A
NudI	Orf141	dTTP, dCTP, dUTP
NudJ	Orf153	(d)NTP, (d)NDP
NudK	Orf191	ADP-Ribose, GDP-mannose
YfcD	Orf180	GPP, DAPP, IPP
NudL	YeaB	CoA

In summary, *E. coli* Nudix enzymes were optimally active in an alkali environment with pH ranging from 8.5–9. Activity required the presence of a divalent metal cation in the concentration range of 0.5 mM to 10 mM (15). Mg²⁺ seemed to be the preferred metal for most of the above-mentioned Nudix enzymes, although other divalent metal cations were not always tested. The number of divalent metal cations also varied, some only requiring one, others two. Nudix enzymes do not appear to be essential (based on targeted knockout studies); however, considering the overlap of substrate specificity between Nudix hydrolases within a specific organism this is not surprising (22). Quaternary structure is rare amongst the Nudix enzymes, and only a few of those mentioned above have this structural property. Of the *E. coli* Nudix enzymes that have been characterized, GDP-mannose mannosyl

hydrolase and ADP-ribose pyrophosphatase are both homodimers in solution while Orf191 appears to be a homotrimer (13, 24).

1.1.2 CoA hydrolase

A Nudix subfamily of particular interest to this study contains an additional sequence for CoA recognition, LLTXR(SA)X₃RX₃GX₃FPGG, called the NuCoA motif (PS01293 motif) which is found directly upstream of the Nudix motif (5). This motif was first associated with substrate specificity towards CoA in a *Saccharomyces cerevisiae* Nudix hydrolase - PCD1 that hydrolyses CoA at the pyrophosphate unit to adenosine 3',5'-diphosphate (3',5'-ADP) and 4'-phosphopantetheine (PPanSH) (Figure 1.3) (28). In addition to the extra NuCoA motif, CoA hydrolases have a modified Nudix box GX₅DX₆AXREXXEEXGU. The first is a substitution of glutamate for glutamine or aspartate the second is an additional alanine (28). Mutagenesis of the NuCoA residues in AtNUDX11 Arg-58 and the overlapping Glu-90 significantly reduced CoA hydrolase activity, confirming the importance of these residues and the specificity of these motifs towards CoA and CoA esters (7). However, the binding sites between mouse isoforms Nudt7 and Nudt19 are not interchangeable and this suggests that the binding sites do differ within subfamilies (29).

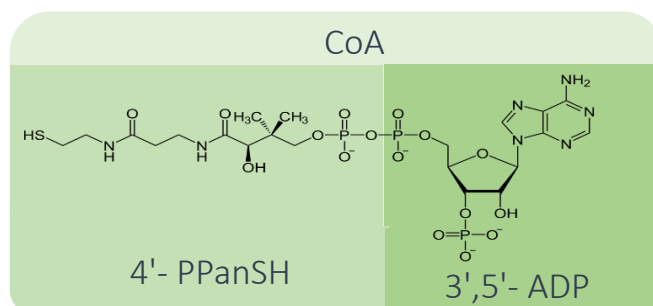


Figure 1.3. Structure of coenzyme A (CoA) and the two degradation products 4'-phosphopantetheine and 3',5'-ADP.

Partial sequence alignments show that this NuCoA motif is also found in Nudix hydrolases of various other organisms including humans, mice, *S. cerevisiae*, *Caenorhabditis elegans*, *A. thaliana*, *D. radiodurans* *Mycobacterium smegmatis*, *Mycobacterium tuberculosis* and *E. coli* (4, 7, 10–12, 28–31) (Figure. 1.4).

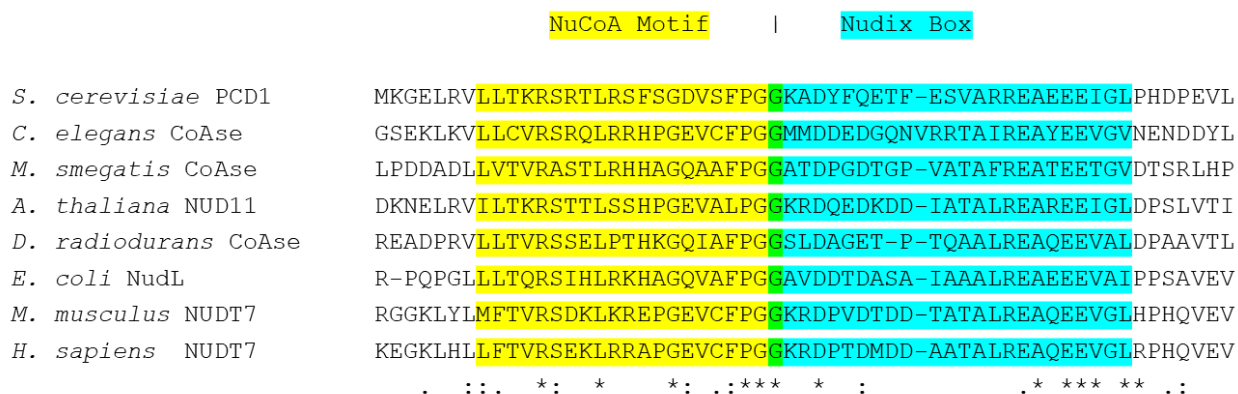


Figure 1.4. Multiple sequence alignment of Nudix hydrolases from various organisms. NuCoA motif indicated in yellow and Nudix box indicated in blue. Overlap shown in green (Gly residues). Also shown, identical residues (*), residues with strongly similar properties (:), and residues with weakly similar properties (.). Sequences used: ScPCD1 (uni/NP_Q12524), CeCoAse (uni/NP_Q9NA25), MsCoAse (uni/NP_A0R5G7) AtNud11 (uni/NP_Q8LET2), DrCoAse (uni/NP_Q9RV46), EcNudL (uni/NP_P43337), HsNudt7 (uni/NP_P0C024) and MmNudt7 (uni/NP_Q99P30). Sequence alignment performed using Clustal Omega.

To date, a number of these putative CoA hydrolases have been characterized with a range of possible substrates, all showing preferential substrate specificity towards CoA and CoA derivatives. Like other Nudix enzymes, enzyme activity is dependent on either Mg^{2+} or Mn^{2+} , an alkaline pH and are also inhibited by F^- (1, 6). Although the significance of this pathway is not entirely clear, especially in a prokaryotic model, the regulation and substrate specificity of these enzymes gives insight to the biological function. In *S. cerevisiae* the Pcd1 gene product preferred oxidized CoA over CoA, and its optimum reaction conditions were found to be pH 7.0 and 5 mM Mg^{2+} (28). *C. elegans* Y87G2A.14 favoured CoA over oxidized CoA and optimal activity was observed at pH 9.5 and 5 mM Mg^{2+} . Mouse Nudt7 showed no preference between oxidized CoA and CoA in vitro (4, 12). *M. smegmatis* and *M. tuberculosis* each have two CoA hydrolases, namely MSMEG_6185 and MSMEG_2327, and Rv3672 and Rv3040 respectively. All four of these enzymes are able to hydrolyse CoA into relevant products in the presence of 5 mM Mg^{2+} at a pH of 7.5 (10). MSMEG_6185 and Rv3672 were also able to hydrolyse oxidized CoA as well. The preferred substrate of Rv3672 was oxidized CoA as determined by the larger catalytic efficiency (k_{cat}/K_m) for oxidized CoA compared to the reduced CoA (10). MSMEG_2327 and Rv3040 had fairly low catalytic activities this could be due to the substitutions in the NuCoA motif of both these enzymes. AtNUDX11, a plant Nudix hydrolase from *A. thaliana*, was found to have hydrolase activity towards CoA in the presence of Mg^{2+} and showed minor hydrolysis of NADH in the presence of Mn^{2+} (7). Interestingly, AtNUDX15 activity was reduced by 77 % under reducing conditions (1 mM DTT); this finding is supported by a faster reaction rate observed with oxidized CoA (32). Mouse Nudt8 preferred Mn^{2+} ; the optimal reaction conditions with CoA as the substrate were at pH 8.5 with 2 mM Mn^{2+} (31). Mouse Nudt7 is active for CoA and CoA derivatives, including acetyl-CoA (4). Nudt19

was also found to degrade free CoA as well as medium and short chain acyl-CoA but not acetyl-CoA (29). Nudt19 optimum activity was found using 10 mM Mg^{2+} at pH 8.0 (29). AtNUDX22 is predicted to be a CoA hydrolase due to the presence of the NuCoA motif, but as no pyrophosphatase activity was detected towards CoA, the authors suggested that the enzyme may require eukaryotic post translational modifications for activity that the *E. coli* expression system is unable to provide (32).

In most cases, higher organisms possess two or more related CoA hydrolase sequences containing the NuCoA motif, e.g., mice, humans and *A. thaliana*. However, *S. cerevisiae* has one sequence. Furthermore, it appears that each of the isoforms have a different subcellular localisation. Animals usually have three pools of CoA: mitochondrial, cytosolic, and peroxisomal. Compartmentalisation ensures that each isoform acts independently on these specific subcellular CoA pools.

Peroxisomes are themselves unique in that they have an extremely oxidizing environment and it is hypothesized that eukaryotic CoA hydrolases are localized in the peroxisome in order to cleanse the pool of oxidatively damaged metabolites (28). The ratio of oxidized to reduced CoA is higher in peroxisomes; however, oxidized CoA is only the preferred substrate of *S. cerevisiae* PCD1 (4, 12). Peroxisomal location is encoded by either a C-terminal PTS1 or a N-terminal PTS2 targeting signal sequence (12). *S. cerevisiae* PCD1 has a PTS2_signal and *C. elegans* Y87G2A.14, mouse Nudt7 and Nudt19 have a PTS1 targeting sequence (4, 12, 28, 33). In addition to having specific subcellular localizations, Nudt7 and Nudt19 are also tissue specific: Nudt7 is expressed in the liver but are also found at lower levels in other tissues, whereas Nudt19 is the major CoA hydrolase in the kidney (4, 29).

Mitochondria also have a large pool of CoA due to it being the site of many CoA-dependent metabolic processes such as the Krebs cycle and fatty acid oxidation. AtNUDX15 and mouse Nudt8 are found to locate to the mitochondria (31, 32). Nudt8 has a broader tissue distribution compared to its peroxisomal counterparts, Nudt7 and Nudt19 (31).

AtNUDX11 (AtCoAse) is the only characterized eukaryotic cytosolic CoA hydrolase. In eukaryotes, the cytosol is where the initial steps of fatty acid synthesis take place. AtNUDX11 was found in highest amounts in flowers and shoots; these are also sites where CoA biosynthesis genes are abundantly expressed (34).

Since prokaryotes lack the cellular organization of eukaryotes, all prokaryotic CoA hydrolases are therefore by default cytosolic in nature.

1.2 Regulation of CoA hydrolases

Considering the importance of CoA hydrolases in being able to reduce the pool of CoA, their regulation is imperative to the viability of the organism. With regards to eukaryotes, compartmentalization by means of organelles (and by extension the creation of localised pools of metabolites/substrates) serves as a form of control of regulation. Prokaryotes, on the other hand, lack sub-cellular organization and therefore their CoA hydrolases would have to be more tightly regulated to avoid a futile and wasteful cycle of CoA biosynthesis and degradation. This could occur through differential expression of the enzyme, as seen in eukaryotes. For example, mouse Nudt8 expression is differentially expressed in different tissue types, expression is much lower in skeletal muscle tissue in comparison with heart and kidney tissue. In mice skeletal muscle have a lower CoA levels than the other tissues (31). Therefore, Kerr et al. suggested that Nudt8 expression might be correspondingly adjusted to the amount of the cofactor and tissue specific cofactor requirements as to avoid depletion (31).

1.2.1 Metabolism

CoA levels change in response to the metabolic state of an organism and CoA hydrolase expression levels in some organisms are found to be regulated in response to the different metabolic states.

For example in mice, Nudt7 is controlled by the nutritional state as mRNA and protein levels start to decrease during the switch from the fed to fasted state and are therefore inversely correlated to the CoA concentration in the liver (35). The expression of the two other mice isoforms, Nudt19 and Nudt8, do not change in response to the nutritional state; this suggests that the regulation of these two enzymes occurs through a different mechanism (29, 31).

In other organisms such as *M. smegmatis*, showed a consistent growth defect for the CoA hydrolase knockout strain when cultured in media containing propionate as the carbon source (10). The authors speculated that propionyl-CoA build up in the knockout strain lead to toxicity and therefore impaired growth (10). Co-culture experiments of wild-type (WT) and knockout cultures older than 3 days also showed a WT fitness advantage despite no differences in the initial growth curves when grown on glucose, acetate, or succinate (10). The most pronounced difference was again with propionate indicating that MSMEG_6185 is needed for regulation of CoA derivatives (10).

1.2.2 Stress

Nudix enzymes were originally thought to play a role in detoxifying the cell of damaged nucleotide metabolites. Consequently, the link between CoA hydrolase activity and various cellular stresses has

been investigated to determine whether CoA degradation mediated by CoA hydrolases are induced or repressed in response to such stresses. Some CoA hydrolases seem to be expressed at low levels irrespective of stress (7, 10).

A number of studies have been done in a variety of organisms investigating the role CoA hydrolases might play under various cellular stress conditions. For example, *AtNUDX11* expression was not significantly affected by salt, osmotic nor oxidative stress (7). The *AtNUDX11* knock out also showed no phenotypical differences however, over expression resulted in improved development (7). Although found throughout the plant, *AtNUDX11* is highly expressed in new shoots and flowers, therefore it could play a role in floral development (7). During normal growth (non-stress conditions) *M. smegmatis* CoA hydrolase (MSMEG_6185) is expressed at log and stationary phase but levels declined at late stationary phase leading up to cell death (10). Interestingly, under varying forms of stresses including oxidative stress, osmotic shock, temperature stress, SDS-induced stress and nutrient starvation, MSMEG_6185 was continuously expressed (10). However, during hypoxia expression was not detected (10). This suggests that CoA degradation could be part of normal dynamic regulation of the CoA pool.

1.2.3 Divalent metal cations

Divalent cations are essential for CoA hydrolyse catalysis and the metal binding site is located within the Nudix box (6). Glu residues in the centre of the REX₂EE motif usually act as the catalytic base and play a role in metal binding (1). The preferred cation is normally Mg²⁺, but activity is still observed with Mn²⁺ and other divalent cations (5). The specificity of some Nudix hydrolase, including CoA hydrolase, depends on the cofactor, this could be attributed to the different geometries within the catalytic site. Mn²⁺ has a slightly larger radius of 75 Å and Mn ligand bonds have greater flexibility in comparison to Mg²⁺ with a radius of 65 Å (36). Mn²⁺ can additionally form bidental complexes with aspartate and glutamate (31)(36). This is relevant considering the conserved Glu residues in the Nudix box as mentioned above. However, whether the Glu residues indeed leads to a preference for Mn²⁺ remains to be experimentally validated and can only be proven with crystal structures with the relevant metal bound. There are two published CoA hydrolase crystal structures (11, 37). The 1.7 Å X-ray structure of *D. radiodurans* CoA hydrolase showed one Mg²⁺ is coordinated to E86 and 5 water molecules in an octahedral coordination (Figure. 1.5) (11). However, it is important to emphasize that the *in vitro* optimized concentrations of these metals don't always align with physiological concentrations of the particular organisms. The degradation ability of the enzymes is therefore capped by *in vivo* conditions. For example, the cytoplasmic *AtNUDX11* is specific for CoA and optimum activity was observed with

5 mM Mg^{2+} ; however, the physiological concentration of Mg^{2+} is ~ 1 mM and only 80% of activity was observed at this concentration (34). *AtNUDX11* also showed activity towards NADH in the presence of 5 mM Mn^{2+} (7). Although NADH is not the main substrate, this evidence supports the hypothesis of cofactor-dependent specificity. In the case of the mitochondrial *AtNUDX15*, the activity in the presence of 5 mM Mn^{2+} was 223 % greater than the activity observed with 5 mM Mg^{2+} (32). However, the physiological Mn^{2+} concentration is 5 μ M, and activity was not detected at this lower concentration (32). The authors stated that the relevant metal is therefore most likely Mg^{2+} as activity was detected for at physiological concentrations of Mg^{2+} and not Mn^{2+} (32). Mouse *Nudt8* distinctly prefers Mn^{2+} under *in vitro* assay conditions (2 mM), which is within the physiological range for the mitochondria. The Yeast *Pcd1P* observed 83% of the optimum activity with 0.3 mM Mn^{2+} (28).

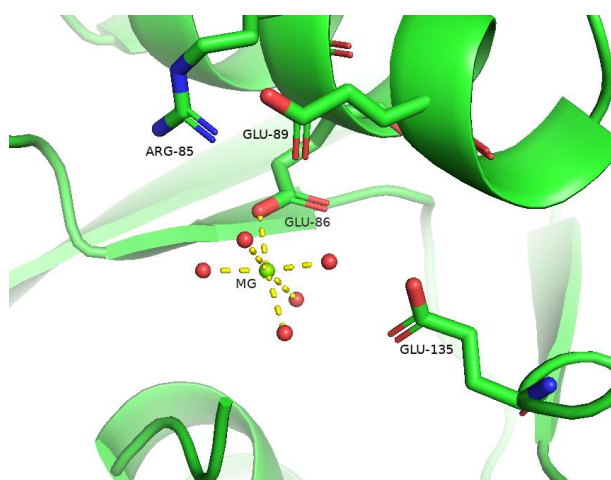


Figure 1.5. Mg^{2+} ion coordinated to 5 water molecules and E86 of *Deinococcus radiodurans* CoA hydrolase. A few of the CoA hydrolase conserved residues surrounding the ion are also shown.

1.3 CoA biosynthesis and regulating CoA levels

CoA plays an essential role in many central metabolic processes in all living organisms (38). CoA is also the main acyl carrier for key intermediates of energy metabolism like the Krebs cycle and fatty acid metabolism (39). Therefore, CoA levels need to be tightly regulated to avoid adverse effects in these pathways. In *E. coli*, reduced CoA levels results in decreased protein and phospholipid biosynthesis with protein biosynthesis being affected more (40). The biosynthesis of CoA in *E. coli* has been extensively studied and occurs via a conserved five-step enzymatic pathway from pantothenate, vitamin B5 (38, 41) (Figure. 1.6). Although the biosynthesis of CoA is universal, following the same route in both prokaryotes and eukaryotes, there are distinct differences with the specific enzymes. These differences have formed the basis of antimicrobial drug development efforts since the 1980s. It is relevant to study model prokaryote organisms, like *E. coli*, in conjunction to eukaryotic systems to

exploit these differences. CoA levels in *E. coli* were thought to be regulated by two mechanisms. First, by feedback inhibition by CoA on pantothenate kinase (PanK), the first enzyme in the biosynthesis pathway. Second, by the degradation CoA into of PPanSH, the product of the third enzyme in the biosynthesis pathway (42) (Figure. 1.6). However, a previous unpublished study from our research group suggested that the control of CoA biosynthesis by feedback inhibition of PanK is actually limited (43). This suggests a bigger role for CoA degradation in the regulation of CoA levels.

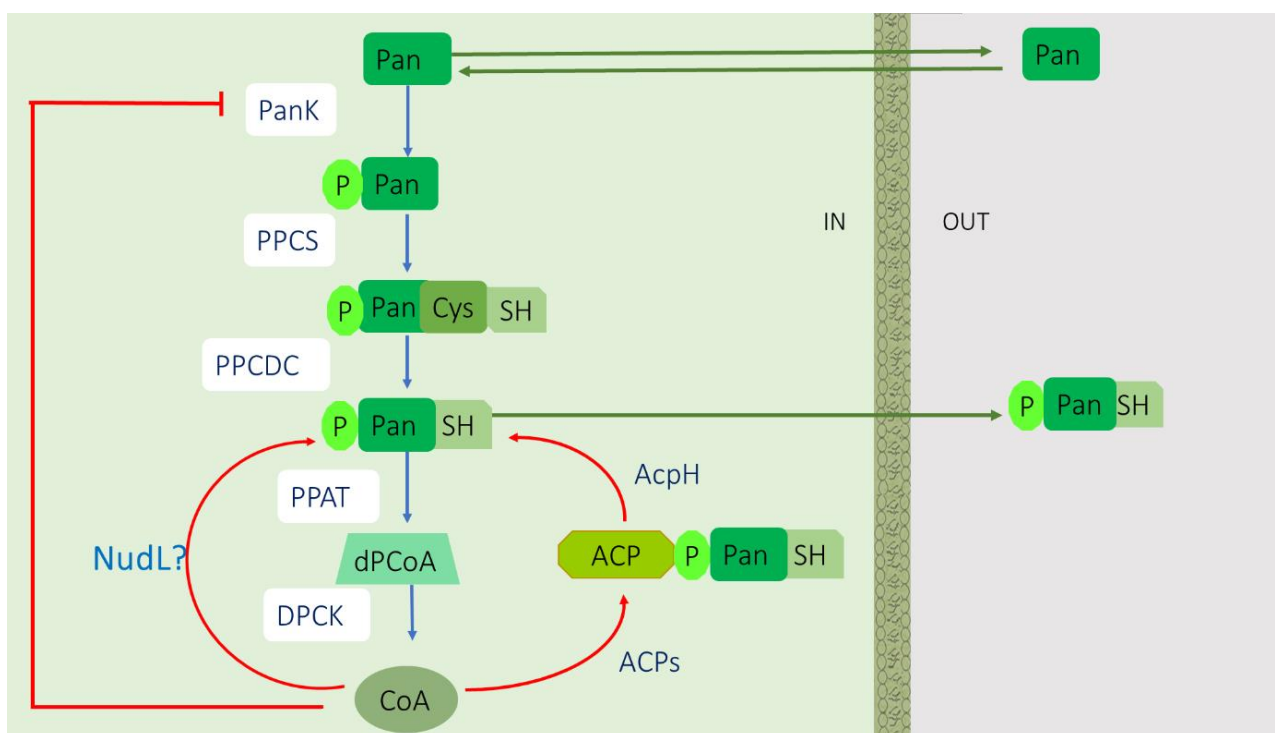


Figure 1.6. The five-step CoA biosynthetic pathway for *E. coli*. The first step is catalysed by pantothenate kinase (PanK). This enzyme is also feedback inhibited by CoA. The next two steps are catalysed by the bifunctional phosphopantocysteinyl synthetase/PPanCys decarboxylase (PPCS and PPCDC). The fourth step is catalysed by PPanSH adenyllyltransferase (PPAT) and the final step is catalysed by dephospho-CoA kinase (DPCK). CoA is directly degraded by a phosphodiesterase to 3',5'-ADP and PPanSH by an unknown enzyme, thought to be NudL. CoA is also degraded via the acyl carrier protein (ACP) prosthetic group turnover, whereby the acyl carrier protein synthase (ACPS) transfers the PPanSH moiety from CoA to the *apo*-ACP, and acyl carrier protein hydrolase (AcpH) releases PPanSH from the *holo*-ACP. Excess PPanSH is then exported out the cell.

In *E. coli*, the CoA pool consists of free CoA, acetyl-CoA, succinyl-CoA and malonyl-CoA (44, 45). The total CoA pool and well as the individual components fluctuates in response to carbon source, energy state and energy requirements (44, 46). The acetyl-CoA/CoA ratio is an indication of whether cells are saturated or starved for carbon, as a decrease in this ratio is associated with starvation and a higher ratio is associated with abundance of readily utilizable carbon (45). When glucose is the carbon source, acetyl-CoA makes up 79.8 % and free CoA makes up 13.8 % of the CoA pool, but when the

carbon is limited acetyl-CoA is converted to CoA and makes up majority of the CoA pool (44, 47). This decrease in the acetyl-CoA/CoA ratio also seems to be a trigger in *E. coli* for CoA degradation (44). Cells starved of carbon were unable to generate acetyl-CoA, and had a raise in intracellular PPanSH. These changes seem to be rapid, occurring within 5 mins, and metabolites are stable after 30 minutes (44, 45). The same is seen when a poor carbon source like acetate is used, as the CoA concentration is half of when glucose is the carbon source but becomes the major component of the CoA pool at the expense of acetyl-CoA (46). *E. coli* produces about 15 times more Pan than what is required and to prevent uncontrolled metabolism *E. coli* excretes excess pantothenate (48). The high levels of pantothenate is what originally prompted Jackowski and Rock to investigate PanK as a point of CoA biosynthesis regulation (48). The export of PPanSH could also be seen as a regulatory mechanism like in the case of Pan, however unlike Pan, export of PPanSH seems to be irreversible (48, 49).

The regulation of eukaryotic CoA levels is more complex, as in eukaryotes intracellular CoA is split between three individual pools: the cytosol, mitochondria and peroxisomes (or chloroplasts in plants), and there are separate CoA hydrolases for each subcellular compartment. Differential expression of these enzymes between tissues is also observed in higher organisms (7, 29, 31, 35). Although this seems like a futile cycle, the purpose of CoA recycling allows for the efficient and dynamic control of CoA that allows for greater metabolic flexibility.

Mitochondrial AtNUDX15 and cytosolic AtNUDX11 were found to be active on CoA as well as medium and long chain acyl CoA derivatives (32). Therefore these enzymes might function in the regulation of CoA/acyl-CoA levels in the respective organelles and by extension the maintenance of CoA associated metabolism such as the Krebs cycle (32).

In mammals the transition from fed-to-fasted state in the liver also results in an increase in the concentration of free CoA and acyl-CoA, due to the switch from glucose oxidation to fatty acid oxidation (50). CoA levels that remain too high in diabetic mice's liver results in excessive gluconeogenesis and hyperglycemia (51). The peroxisomal mouse CoA hydrolase enzymes, Nudt7 and Nudt19, are active for CoA, medium and long chain acyl-CoAs have been proposed to maintain CoA/acyl-CoA homeosis (29, 52). These independent studies suggest that CoA hydrolases may regulate the β -oxidation pathway by controlling the levels of CoA and substrate, acyl-CoAs. Another suggested function of mammalian CoA degradation is that hydrolysing CoA into small hydrophilic molecules removes excess CoA from the peroxisomes into molecules that can be exported (53). Nudt8 can hydrolyse CoA more readily than acetyl-CoA and therefore might contribute to free CoA/acetyl-CoA ratio in the mitochondria, however this is still to be proven experimentally (31).

1.3.1 Role of CoA degradation and significance of PPanSH

The CoA biosynthesis intermediate and degradation product, PPanSH, is an important molecule as it has been identified as a nexus metabolite (38). It has been suggested that it could function as a possible stable, membrane-permeable, indirect stock of CoA that is capable of influencing CoA level regulation between different cells, organelles and even different organisms (38, 54). Extracellular PPanSH was found to rescue CoA-depleted organisms that could not synthesize CoA *de novo*. These included *D. melanogaster*, *C. elegans*, or cultured human cells (54).

E. coli is known to make significant quantities of PPanSH which are found within the cell and irreversibly exported in large amounts to the extracellular environment (49). The source of the high PPanSH levels was proposed to be both from partial biosynthesis from Pan and from the degradation of CoA (42). In *E. coli*, CoA degradation remains largely uninvestigated. Two types of enzymes can hydrolyse CoA at the pyrophosphate unit to yield PPanSH, the first enzyme being a phosphodiesterase. Its manner of generating PPanSH is via the ACP prosthetic group turnover (Figure. 1.6). This is a two-step process where the ACP is first modified by covalent attachment of PPanSH to form *holo*-ACP. 4'-Phosphopantetheinyl transferases are responsible for transferring the PPanSH moiety from CoA to the hydroxyl group of a conserved serine residue of the *apo*-ACP (55). This results in free 3',5'-ADP and a protein-4'-phosphodiester linkage with PPanSH (55). *E. coli* AcpS (ACP synthase) was the first phosphopantetheinyl transferase to be characterized but ACPS are found in most other organisms. The second step is the release of the PPanSH moiety by ACPH, which regenerates the unbound *apo*-ACP form. PPanSH can be recycled for CoA biosynthesis or irreversibly exported from the cell; this has been demonstrated by two separate deuterium-labelling studies (49, 55). The rate of ACP prosthetic group turnover also depends on the intracellular CoA concentration. The prosthetic group turnover is faster at low CoA levels, but at the higher CoA concentrations that are present at exponential phase, turnover is much slower (55). It was found that most of the PPanSH in the media was from AcpH degradation but some was from direct degradation and as well as from biosynthesis (49). It is not known as to how much of each of the two degradation paths contributes to the extracellular PPanSH pool. The deletion of AcpH prevents ACP prosthetic group turnover *in vivo* and overexpression of AcpH had no effect on ACP turnover (55). The mutant strain, unlike its AcpS counterpart, was found to be non-essential (55). The mutant strain also had significantly less PPanSH exported into the media (55).

The second enzyme that is able to hydrolyse CoA at the pyrophosphate unit is a pyrophosphatase i.e., a CoA hydrolase that can directly hydrolyse CoA to 3',5'-ADP and PPanSH (Figure. 1.6). As mentioned above, a number of CoA hydrolases have already been characterized (4, 7, 10, 12, 28, 29, 31). However, as yet no enzyme has been experimentally shown to directly degrade CoA in *E. coli* (49). However, since the 1980s several studies have alluded to the existence of a direct CoA degradation mechanism

in *E. coli* that is not mediated by AcpH. CoA degradation seems to be activated when the acetyl-CoA/CoA ratio decreases. Since AcpH is inhibited equally by acetyl-CoA and CoA, a change in the ratio of CoA and acetyl-CoA would not trigger ACP hydrolysis (42). This suggests that CoA degradation plays a role in the reduction of intracellular CoA concentration after sudden changes in cell metabolism. As most of the generated PPanSH is excreted, this process is irreversible as the PPanSH released in the environment is not taken up by *E. coli* (49).

PPanSH is also formed by the extracellular hydrolysis of CoA in serum, the enzyme responsible is most likely a ENPP (ectonucleotide pyrophosphatase) (54). This is also a direct mechanism yielding the same products as CoA hydrolases. However, no ENPP has been characterized in prokaryotes.

1.3.2 Fate of 3',5'-ADP and other roles

The significance of the second degradation product, 3',5'-ADP or PAP, is less apparent. 3',5'-ADP can be generated by a number of processes. First, by CoA degradation via a Nudix hydrolase, second via the transfer of PPanSH from CoA during *holo*-ACP synthesis, and third from the transfer of the sulphate group of 3'-phosphoadenosyl-5'-phosphosulfate by sulfotransferases (42, 55, 56). In humans two enzymes, namely adenosine 3',5'-bisphosphate 3'-phosphatase (gPAPP) in the Golgi body and bisphosphate 3'-nucleotidase 1 (BPNT1) in the cytosol, can convert 3',5'-ADP into 5'-AMP, which re-enters the nucleotide pool (Figure. 1.7)(57).

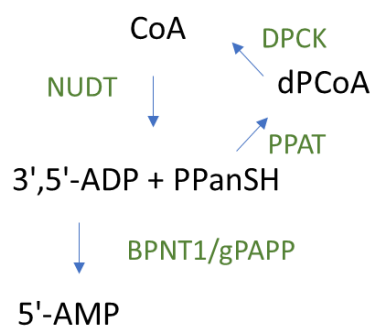


Figure 1.7. Scheme of 3',5'-ADP fate in humans. See text above for detail. NUDT refers to CoA hydrolase enzymes able of degrading CoA.

Interestingly, it has been suggested that the possible role of CoA hydrolases is not on CoA itself but rather in the downstream CoA related pathways. In bacteria RNA cap differs to eukaryotes, which have a methylguanosine that protects mRNA from degradation. In the last 10 years, NAD-capped RNA has been discovered in prokaryotes and found to serve a similar function as in eukaryotes (58). In *E. coli* both RppH and NADH hydrolase shows activity towards NAD and CoA-capped RNA (19, 59). In mammals CoA similarly attaches to proteins in a process of CoAlation; this protects protein thiols from

oxidative and metabolic stress (60). CoAlation has also been reported in *S. aureus* and *E. coli* (61). This raises the question if CoA hydrolases are also able to hydrolyse the CoA modified RNA or proteins, and if the function in prokaryotes is rather on CoA derivatives than on CoA itself. So far only one CoA hydrolase, mouse Nudt19, was shown to have some activity towards CoA-capped RNA (62).

Although these enzymes can perform the same reaction, their physiological role differs from organism to organism. What seems to be common to all of these enzymes is that they are not essential, as knockout mutants lacking these enzymes survive without severely compromised growth. The deletion mutants from *S. cerevisiae*, *C. elegans* and *A. thaliana* did not show any defect or compromised peroxisome function (7, 12, 28). Nudt19⁻¹ mice were also viable and did not display any phenotypical abnormalities (29). One notable exception was that the constitutive overexpression of AtNUDX11 in *A. thaliana* exhibited better growth, development, and life span.

1.4 Study Aims

The goal of this project was to investigate the putative pyrophosphatase activity of NudL towards CoA and to ascertain the possible biological role of this enzyme in the regulation of CoA levels in *E. coli*. This knowledge could be valuable for future studies targeting the disruption of CoA levels for potential antimicrobial development and might give greater insight on the role Nudix enzymes in a prokaryotic organism. This project goal was pursued by following three aims:

Aim 1: To optimize expression and purification of soluble NudL

NudL is yet to be successfully expressed and purified for the purpose of kinetic characterization. Therefore, the conditions that would yield soluble pure recombinant protein were investigated by optimizing both expression conditions as well as purification methods. To achieve this aim the following objectives were pursued as described in chapter 2.

Objective 1.1: To optimize expression conditions of soluble NudL from pET28a and pFN29A expression vectors.

Objective 1.2: To optimize purification of soluble recombinant NudL via immobilised metal affinity chromatography.

Objective 1.3: To solubilize insoluble NudL from inclusion bodies, followed by purification via immobilised metal affinity chromatography.

Objective 1.4: To express NudL in a cell-free expression system.

Aim 2: To assess the CoA hydrolase activity of partially purified NudL and *E. coli* lysate, using an established HPLC assay

Currently there is no published kinetic data for NudL not fused to MBP. Therefore, confirming the predicted CoA hydrolase activity of *E. coli* will give context to this previously uncharacterized CoA hydrolase. This aim was achieved by pursuing the following objectives as described in chapter 3.

Objective 2.1: To optimize reaction conditions for assaying CoA hydrolase activity with CoA as a substrate.

Objective 2.2: To determine specific CoA hydrolase activity (i) in *E. coli* lysate, (ii) in lysate in which NudL was overexpressed, and (iii) of partially purified NudL enzyme.

Aim 3: To characterize the physiological relevance of NudL

The physiological function of CoA hydrolases in prokaryotes is largely unknown. Therefore, determining conditions where NudL's activity is possibly advantageous — such as during oxidative stress and growth on various carbon sources — would give insight into the regulation of this enzyme. The role of NudL in CoA metabolism was also investigated by means of metabolic studies. The following objectives were pursued to achieve this aim as described in chapter 3.

Objective 3.1: To determine the intracellular levels of CoA and PPanSH in *E. coli* K12 and an *E. coli* NudL knockout strain (JW1802), and an *E. coli* ACP hydrolase knockout strain (JW0394).

Objective 3.2: To compare growth curves of *E. coli* K12 and, the NudL knockout strain (JW1802), and the ACP hydrolase knockout strain (JW0394) with different carbon sources.

Objective 3.3: To determine the relative transcription levels of NudL in *E. coli* K12 during physiological conditions and oxidative stress.

1.5 References

1. McLennan, A. G. (2006) The Nudix hydrolase superfamily. *Cell. Mol. Life Sci.* **63**, 123–143
2. Kraszewska, E. (2008) The plant Nudix hydrolase family. *Acta Biochim. Pol.* **55**, 663–671
3. Srouji, J. R., Xu, A., Park, A., Kirsch, J. F., and Brenner, S. E. (2017) The evolution of function within the Nudix homology clan. *Proteins Struct. Funct. Bioinforma.* **85**, 775–811
4. Gasmi, L., and McLENNAN, A. G. (2001) The mouse Nudt7 gene encodes a peroxisomal nudix hydrolase specific for coenzyme A and its derivatives. *Biochem. J.* **357**, 33

5. Bessman, M. J., Frick, D. N., and O'Handley, S. F. (1996) The MutT Proteins or "Nudix" Hydrolases, a Family of Versatile, Widely Distributed, "Housecleaning" Enzymes. *J. Biol. Chem.* **271**, 25059–25062
6. Mildvan, A. S., Xia, Z., Azurmendi, H. F., Saraswat, V., Legler, P. M., Massiah, M. A., Gabelli, S. B., Bianchet, M. A., Kang, L.-W., and Amzel, L. M. (2005) Structures and mechanisms of Nudix hydrolases. *Arch. Biochem. Biophys.* **433**, 129–143
7. Kupke, T., Caparrós-Martín, J. A., Malquichagua Salazar, K. J., and Culiáñez-Macià, F. A. (2009) Biochemical and physiological characterization of *Arabidopsis thaliana* AtCoAse: a Nudix CoA hydrolyzing protein that improves plant development. *Physiol. Plant.* **135**, 365–378
8. Fletcher, J. I., Swarbrick, J. D., Maksel, D., Gayler, K. R., and Gooley, P. R. (2002) The Structure of Ap4A Hydrolase Complexed with ATP-MgFx Reveals the Basis of Substrate Binding. *Structure.* **10**, 205–213
9. Nguyen, V. N., Park, A., Xu, A., Srouji, J. R., Brenner, S. E., and Kirsch, J. F. (2016) Substrate specificity characterization for eight putative nudix hydrolases. Evaluation of criteria for substrate identification within the Nudix family. *Proteins Struct. Funct. Bioinforma.* **84**, 1810–1822
10. Kapoor, I., Varada, R., Aroli, S., and Varshney, U. (2019) Nudix hydrolases with Coenzyme A (CoA) and acyl-CoA pyrophosphatase activities confer growth advantage to *Mycobacterium smegmatis*. *Microbiology.* **165**, 1219–1232
11. Kang, L.-W., Gabelli, S. B., Bianchet, M. A., Xu, W. L., Bessman, M. J., and Amzel, L. M. (2003) Structure of a Coenzyme A Pyrophosphatase from *Deinococcus radiodurans*: a Member of the Nudix Family. *J. Bacteriol.* **185**, 4110–4118
12. Abdelraheim, S. R., and McLennan, A. G. (2002) The *Caenorhabditis elegans* Y87G2A.14 Nudix hydrolase is a peroxisomal coenzyme A diphosphatase. *BMC Biochem.* **3**, 1–8
13. Xu, W., Dunn, C. A., O'Handley, S. F., Smith, D. L., and Bessman, M. J. (2006) Three New Nudix Hydrolases from *Escherichia coli*. *J. Biol. Chem.* **281**, 22794–22798
14. Bessman, M. J. (2019) A cryptic activity in the Nudix hydrolase superfamily. *Protein Sci.* **28**, 1494–1500
15. Bhatnagar, S. K., Bullions, L. C., and Bessman, M. J. (1991) Characterization of the mutT nucleoside triphosphatase of *Escherichia coli*. *J. Biol. Chem.* **266**, 9050–9054
16. Gabelli, S. B., Bianchet, M. A., Xu, W., Dunn, C. A., Niu, Z.-D., Amzel, L. M., and Bessman, M. J. (2007) Structure and Function of the *E. coli* Dihydroneopterin Triphosphate Pyrophosphatase: A Nudix Enzyme Involved in Folate Biosynthesis. *Structure.* **15**, 1014–1022
17. O'Handley, S. F., Frick, D. N., Dunn, C. A., and Bessman, M. J. (1998) Orf186 Represents a New Member of the Nudix Hydrolases, Active on Adenosine(5')triphospho(5')adenosine, ADP-ribose, and NADH. *J. Biol. Chem.* **273**, 3192–3197
18. Bessman, M. J., Walsh, J. D., Dunn, C. A., Swaminathan, J., Weldon, J. E., and Shen, J. (2001) The Gene ygdP, Associated with the Invasiveness of *Escherichia coli* K1, Designates a Nudix Hydrolase, Orf176, Active on Adenosine (5')-Pentaphospho-(5')-adenosine (Ap5A). *J. Biol. Chem.* **276**, 37834–37838
19. Deana, A., Celesnik, H., and Belasco, J. G. (2008) The bacterial enzyme RppH triggers messenger RNA degradation by 5' pyrophosphate removal. *Nature.* **451**, 355–358
20. Frick, D. N., and Bessman, M. J. (1995) Cloning, purification, and properties of a novel NADH

- pyrophosphatase. Evidence for a nucleotide pyrophosphatase catalytic domain in MutT-like enzymes. *J. Biol. Chem.* **270**, 1529–1534
21. Bird, J. G., Zhang, Y., Tian, Y., Panova, N., Barvík, I., Greene, L., Liu, M., Buckley, B., Krásný, L., Lee, J. K., Kaplan, C. D., Ebright, R. H., and Nickels, B. E. (2016) The mechanism of RNA 5' capping with NAD⁺, NADH and desphospho-CoA. *Nature*. **535**, 444–447
 22. Dunn, C. A., O'Handley, S. F., Frick, D. N., and Bessman, M. J. (1999) Studies on the ADP-ribose Pyrophosphatase Subfamily of the Nudix Hydrolases and Tentative Identification of *trgB*, a Gene Associated with Tellurite Resistance. *J. Biol. Chem.* **274**, 32318–32324
 23. Moreno-Bruna, B., Baroja-Fernandez, E., Munoz, F. J., Bastarrica-Berasategui, A., Zandueta-Criado, A., Rodriguez-Lopez, M., Lasa, I., Akazawa, T., and Pozueta-Romero, J. (2001) Adenosine diphosphate sugar pyrophosphatase prevents glycogen biosynthesis in *Escherichia coli*. *Proc. Natl. Acad. Sci.* **98**, 8128–8132
 24. Legler, P. M., Massiah, M. A., Bessman, M. J., and Mildvan, A. S. (2000) GDP-Mannose Mannosyl Hydrolase Catalyzes Nucleophilic Substitution at Carbon, Unlike All Other Nudix Hydrolases †. *Biochemistry*. **39**, 8603–8608
 25. Aiba, H. (1996) A 570-kb DNA Sequence of the *Escherichia coli* K-12 Genome Corresponding to the 28.0-40.1 min Region on the Linkage Map. *DNA Res.* **3**, 363–377
 26. Kim, J., Kershner, J. P., Novikov, Y., Shoemaker, R. K., and Copley, S. D. (2010) Three serendipitous pathways in *E. coli* can bypass a block in pyridoxal-5'-phosphate synthesis. *Mol. Syst. Biol.* **6**, 436
 27. Spangler, J. R., and Huang, F. (2020) The *E. coli* NudL enzyme is a Nudix hydrolase that cleaves CoA and its derivatives. *bioRxiv*. 10.1101/2020.01.31.929182
 28. Cartwright, J. L., Gasmi, L., Spiller, D. G., and McLennan, A. G. (2000) The *Saccharomyces cerevisiae* PCD1 Gene Encodes a Peroxisomal Nudix Hydrolase Active toward Coenzyme A and Its Derivatives. *J. Biol. Chem.* **275**, 32925–32930
 29. Shumar, S. A., Kerr, E. W., Geldenhuys, W. J., Montgomery, G. E., Fagone, P., Thirawatananond, P., Saavedra, H., Gabelli, S. B., and Leonardi, R. (2018) Nudt19 is a renal CoA diphosphohydrolase with biochemical and regulatory properties that are distinct from the hepatic Nudt7 isoform. *J. Biol. Chem.* **293**, 4134–4148
 30. Xu, W., Shen, J., Dunn, C. A., Desai, S., and Bessman, M. J. (2001) The Nudix hydrolases of *Deinococcus radiodurans*. *Mol. Microbiol.* **39**, 286–290
 31. Kerr, E. W., Shumar, S. A., and Leonardi, R. (2019) Nudt8 is a novel CoA diphosphohydrolase that resides in the mitochondria. *FEBS Lett.* **593**, 1873–3468.13392
 32. Ogawa, T., Yoshimura, K., Miyake, H., Ishikawa, K., Ito, D., Tanabe, N., and Shigeoka, S. (2008) Molecular characterization of organelle-type nudix hydrolases in *Arabidopsis*. *Plant Physiol.* **148**, 1412–1424
 33. Ofman, R., Speijer, D., Leen, R., and Wanders, R. J. A. (2006) Proteomic analysis of mouse kidney peroxisomes: Identification of RP2p as a peroxisomal nudix hydrolase with acyl-CoA diphosphatase activity. *Biochem. J.* **393**, 537–543
 34. Ogawa, T., Ueda, Y., Yoshimura, K., and Shigeoka, S. (2005) Comprehensive Analysis of Cytosolic Nudix Hydrolases in *Arabidopsis thaliana*. *J. Biol. Chem.* **280**, 25277–25283
 35. Shumar, S. A., Kerr, E. W., Fagone, P., Infante, A. M., and Leonardi, R. (2019) Overexpression of Nudt7 decreases bile acid levels and peroxisomal fatty acid oxidation in the liver. *J. Lipid Res.*

- 60, 1005–1019
36. Bock, C. W., Katz, A. K., Markham, G. D., and Glusker, J. P. (1999) Manganese as a Replacement for Magnesium and Zinc: Functional Comparison of the Divalent Ions. *J. Am. Chem. Soc.* **121**, 7360–7372
 37. Resnick, E., Bradley, A., Gan, J., Douangamath, A., Krojer, T., Sethi, R., Geurink, P. P., Aimon, A., Amitai, G., Bellini, D., Bennett, J., Fairhead, M., Fedorov, O., Gabizon, R., Gan, J., Guo, J., Plotnikov, A., Reznik, N., Ruda, G. F., Díaz-Sáez, L., Straub, V. M., Szommer, T., Velupillai, S., Zaidman, D., Zhang, Y., Coker, A. R., Dowson, C. G., Barr, H. M., Wang, C., Huber, K. V. M., Brennan, P. E., Ovaa, H., von Delft, F., and London, N. (2019) Rapid Covalent-Probe Discovery by Electrophile-Fragment Screening. *J. Am. Chem. Soc.* **141**, 8951–8968
 38. Sibon, O. C. M., and Strauss, E. (2016) Coenzyme A: to make it or uptake it? *Nat. Rev. Mol. Cell Biol.* **17**, 605–606
 39. Krivoruchko, A., Zhang, Y., Siewers, V., Chen, Y., and Nielsen, J. (2015) Microbial acetyl-CoA metabolism and metabolic engineering. *Metab. Eng.* **28**, 28–42
 40. Jackowski, S., and Rock, C. O. (1986) Consequences of reduced intracellular coenzyme A content in *Escherichia coli*. *J. Bacteriol.* **166**, 866–871
 41. Spry, C., Kirk, K., and Saliba, K. J. (2008) Coenzyme A biosynthesis: an antimicrobial drug target. *FEMS Microbiol. Rev.* **32**, 56–106
 42. Vallari, D. S., and Jackowski, S. (1988) Biosynthesis and degradation both contribute to the regulation of coenzyme A content in *Escherichia coli*. *J. Bacteriol.* **170**, 3961–3966
 43. Goosen, R. (2016) *A comparative analysis of CoA biosynthesis in selected organisms: a metabolite study*. Ph.D. thesis, Stellenbosch University
 44. Vallari, D. S., Jackowski, S., and Rock, C. O. (1987) Regulation of pantothenate kinase by coenzyme A and its thioesters. *J. Biol. Chem.* **262**, 2468–2471
 45. Chohnan, S., Furukawa, H., Fujio, T., Nishihara, H., and Takamura, Y. (1997) Changes in the size and composition of intracellular pools of nonesterified coenzyme A and coenzyme A thioesters in aerobic and facultatively anaerobic bacteria. *Appl. Environ. Microbiol.* **63**, 553–560
 46. Chohnan, S., Izawa, H., Nishihara, H., and Takamura, Y. (1998) Changes in Size of Intracellular Pools of Coenzyme A and Its Thioesters in *Escherichia coli* K-12 Cells to Various Carbon Sources and Stresses. *Biosci. Biotechnol. Biochem.* **62**, 1122–1128
 47. Chohnan, S., and Takamura, Y. (1991) A Simple Micromethod for Measurement of CoASH and Its Use in Measuring Intracellular Levels of CoASH and Short Chain Acyl-CoAs in *Escherichia coli* K12 Cells. *Agric. Biol. Chem.* **55**, 87–94
 48. Jackowski, S., and Rock, C. O. (1981) Regulation of coenzyme A biosynthesis. *J. Bacteriol.* **148**, 926–932
 49. Jackowski, S., and Rock, C. O. (1984) Metabolism of 4'-phosphopantetheine in *Escherichia coli*. *J. Bacteriol.* **158**, 115–120
 50. Leonardi, R., Rehg, J. E., Rock, C. O., and Jackowski, S. (2010) Pantothenate Kinase 1 Is Required to Support the Metabolic Transition from the Fed to the Fasted State. *PLoS One.* **5**, e11107
 51. Leonardi, R., Rock, C. O., and Jackowski, S. (2014) Pank1 deletion in leptin-deficient mice reduces hyperglycaemia and hyperinsulinaemia and modifies global metabolism without affecting insulin resistance. *Diabetologia.* **57**, 1466–1475

52. Reilly, S.-J., Tillander, V., Ofman, R., Alexson, S. E. H., and Hunt, M. C. (2008) The Nudix Hydrolase 7 is an Acyl-CoA Diphosphatase Involved in Regulating Peroxisomal Coenzyme A Homeostasis. *J. Biochem.* **144**, 655–663
53. Antonenkov, V. D. (2004) The rat liver peroxisomal membrane forms a permeability barrier for cofactors but not for small metabolites in vitro. *J. Cell Sci.* **117**, 5633–5642
54. Srinivasan, B., Baratashvili, M., van der Zwaag, M., Kanon, B., Colombelli, C., Lambrechts, R. A., Schaap, O., Nollen, E. A., Podgoršek, A., Kosec, G., Petković, H., Hayflick, S., Tiranti, V., Reijngoud, D.-J., Grzeschik, N. A., and Sibon, O. C. M. (2015) Extracellular 4'-phosphopantetheine is a source for intracellular coenzyme A synthesis. *Nat. Chem. Biol.* **11**, 784–792
55. Thomas, J., and Cronan, J. E. (2005) The Enigmatic Acyl Carrier Protein Phosphodiesterase of *Escherichia coli*. *J. Biol. Chem.* **280**, 34675–34683
56. Coughtrie, M. W. H. (2016) Function and organization of the human cytosolic sulfotransferase (SULT) family. *Chem. Biol. Interact.* **259**, 2–7
57. Spiegelberg, B. D., Xiong, J. P., Smith, J. J., Gu, R. F., and York, J. D. (1999) Cloning and characterization of a mammalian lithium-sensitive bisphosphate 3'-nucleotidase inhibited by inositol 1,4-bisphosphate. *J. Biol. Chem.* **274**, 13619–13628
58. Chen, Y. G., Kowtoniuk, W. E., Agarwal, I., Shen, Y., and Liu, D. R. (2009) LC/MS analysis of cellular RNA reveals NAD-linked RNA. *Nat. Chem. Biol.* **5**, 879–881
59. Höfer, K., Li, S., Abele, F., Frindert, J., Schlotthauer, J., Grawenhoff, J., Du, J., Patel, D. J., and Jäschke, A. (2016) Structure and function of the bacterial decapping enzyme NudC. *Nat. Chem. Biol.* **12**, 730–734
60. Gout, I. (2018) Coenzyme A, protein CoAlation and redox regulation in mammalian cells. *Biochem. Soc. Trans.* **46**, 721–728
61. Tsuchiya, Y., Zhyvoloup, A., Baković, J., Thomas, N., Yu, B. Y. K., Das, S., Orengo, C., Newell, C., Ward, J., Saladino, G., Comitani, F., Gervasio, F. L., Malanchuk, O. M., Khoruzhenko, A. I., Filonenko, V., Peak-Chew, S. Y., Skehel, M., and Gout, I. (2018) Protein CoAlation and antioxidant function of coenzyme A in prokaryotic cells. *Biochem. J.* **475**, 1909–1937
62. Song, M.-G., Bail, S., and Kiledjian, M. (2013) Multiple Nudix family proteins possess mRNA decapping activity. *RNA.* **19**, 390–399

Chapter 2

The expression and purification of NudL

2.1 Introduction

Escherichia coli has 13 proposed Nudix hydrolases, 11 of which have been fully characterized, one that has been partially characterized and one that remains to be characterized (1). The remaining uncharacterized *E. coli* Nudix hydrolase, NudL. NudL without a MBP fusion tag is yet to be successfully expressed, purified, and kinetically characterized. NudL (YeaB) is a small protein of 21.4 kDa and is putatively annotated as a CoA hydrolase due to the presence of a Nudix and NuCoA motifs that are characteristic to CoA hydrolases (2). CoA hydrolases are a subfamily of Nudix hydrolases specific for CoA and CoA derivatives. Several CoA hydrolases have been characterized in eukaryotes whilst only two prokaryotic CoA hydrolase has been studied to date (3–11).

Characterization of an enzyme requires pure, soluble, active protein. To date the only reports of attempts to express, purify and test NudL's activity are from a single published paper and one preprint (12, 13). Various expression vectors were used in these studies, with only the MBP (maltose-binding protein) fusion protein construct yielding some soluble NudL (1, 12, 13). Despite soluble NudL expression, the overall yields were very low and the protein was only purified to 71 % homogeneity as determined by densitometry (13). Following cleavage of the MBP fusion, no detectable phosphatase activity was observed using 3-phosphooxypyruvate(12, 13).

In this study we were also challenged with low soluble recombinant protein expression levels in our attempts to produce NudL.

There are several strategies/methods in which solubility of a recombinant protein can be increased. The first is to vary the expression conditions; this includes altering the growth media, expression time, expression temperature and the manner and intensity of induction of protein expression. Second, fusion proteins that are specifically designed to aid in solubility of the expressed protein of interest can be used. A number of the previously characterized eukaryotic CoA hydrolases have also been expressed as fusion proteins (3, 5, 6). Third, the low solubility could be attributed to toxicity due to the overexpression of the protein of interest and thus a cell free expression system may bypass this issue.

Similarly, there are various ways purification can be improved. Immobilized-metal affinity chromatography (IMAC) is the most common method of purifying recombinant protein with a poly histidine tag. IMAC can be optimized by changing the percentage of Imidazole in the wash step that removes the non-specific and histidine rich proteins. This wash step can be either be a gradient or

stepwise increase of competing imidazole. The metal charged to the column can also be varied as transition metals other than nickel have an affinity for the poly histidine tag. Detergents and additives can be added to the lysis buffer to aid the dissociation of non-specific proteins. Alternatively, to increase the yield the binding time can be increased with use of a Nickel affinity resin opposed to an automated system.

In this chapter various experimental conditions were investigated that addressed the issues of solubility and purity of NudL. This was done by attempting to improve soluble expression of NudL with the above-mentioned strategies, followed by optimization of a purification method that would yield the purest sample of NudL.

2.2 Experimental Methods

2.2.1 Materials

All chemicals, reagents, solvents, and media were sourced from Merck (Sigma-Aldrich). Restriction digest enzymes XhoI, NdeI, Accl as well quick ligation kit were obtained from New England BioLabs. The expression vector (pET28a) and the entry vector (pENTR) were sourced from Novagen. The pFN29A expression vector, the Flexi enzyme blend (SgfI & PmeI) and the S30 T7 High-Yield Protein Expression system were sourced from Promega. The KAPA HiFi HotStart ReadyMix was obtained from Roche. The HiTrap metal affinity and HiTrap gel filtration columns were obtained from GE Healthcare. GeneJET Plasmid mini prep and the GeneJET Gel Extraction Kits were obtained from Thermo Scientific. Primers were obtained from Inqaba. Bio-Rad's Quick start Bradford protein assay kit was used for protein concentration determination.

2.2.2 Plasmid confirmation and subcloning of yeaB

An existing pENTR-NudL plasmid was available in the Strauss lab from work done by Ms. Leisl Brand. First, the size of the gene of interest was confirmed by single internal enzyme restriction digestion of the pENTR-NudL plasmid with Accl. The digest reaction mixture contained the following: 2 μ L buffer, 1 μ L of Accl enzyme, 0.6 μ L acetylated BSA, 15 μ L pENTR NudL plasmid and Milli-Q water to a total volume of 20 μ L. The reaction was added in the above order to a 1.5 mL microcentrifuge tube and incubated at 37 °C for 2 hours. The reaction was heat inactivated at 65 °C for 10 minutes. The reaction was then analysed on 1% (m/v) agarose gel made up with 1 X TAE buffer. The lanes were loaded with a premixture of 20 μ L digestion reaction containing 4 μ L 6 X purple loading dye (NEB). A marker lane containing 5 μ L of KAPA Universal DNA ladder. The agarose gel electrophoresis was run at 90 V for 1

hour. The agarose gel was post stained with 1:1000 Sybr gold (Thermo Fisher Scientific) to 1 X TAE buffer. After confirmation, the gene was excised from the pENTR plasmid by double digestion with XhoI and NdeI. The digestion was performed by adding 15 µL purified plasmid (either the empty pET28a vector or pENTR-NudL), 2 µL smart cut buffer, 1 µL Milli-Q water, 1 µL XhoI and 1 µL NdeI. The reaction was incubated and analysed as per the previous restriction enzyme digest above. The *yeaB* gene and linear pET28a vector bands were cut from a 1% (m/v) agarose gel and concentrated with GeneJET Gel Extraction Kit, after which the DNA concentration was determined with a Nanodrop spectrophotometer at 260 nm. The gel-purified restriction fragments were ligated overnight at room temperature to produce the pET28a-NudL expression vector. The quick ligation kit (NEB) was used with a ratio of 1:3 (plasmid to insert) for the ligation reaction. The ligation reaction was then transformed into competent *E. coli* Mach1 cells and were plated on LB agar containing 30 mg/L kanamycin. The identity of the *yeaB* gene was confirmed by DNA sequence analysis.

2.2.3 Cloning *yeaB* into pFN29A vector

The *E. coli yeaB* gene was amplified by PCR from isolated pET28a-NudL plasmid with the following primers: 5' GGGGGGG**GCGAT**CGCCATGGAATACCGTAGCCTGACGC 3' (forward primer) to introduce a SgfI site (in bold) at the start of the gene, and 5' GGGGGGG**TTTAAACT**CAGGGTTTCACACCAATTTGCAG 3' (reverse primer) to introduce a PmeI site (in bold) to the end of the gene. 6×G were added to the 5' ends to create a larger overlap for the restriction enzymes to recognize the relevant cut sites. The PCR reaction was set up in a sterile PCR tube as follows: 0.5 µL template DNA (pET28a-NudL), 0,75 µL forward primer (10 µM), 0.75 µL reverse primer (10 µM), 12.5 µL Ready mix (Kapa HIFI hot start ready mix PCR kit) and sterile Milli-Q water to a total volume of 25 µL. The PCR product was run on a MyCycler™ Thermal Cycler (BioRad) using the following program (Figure. 2.1).

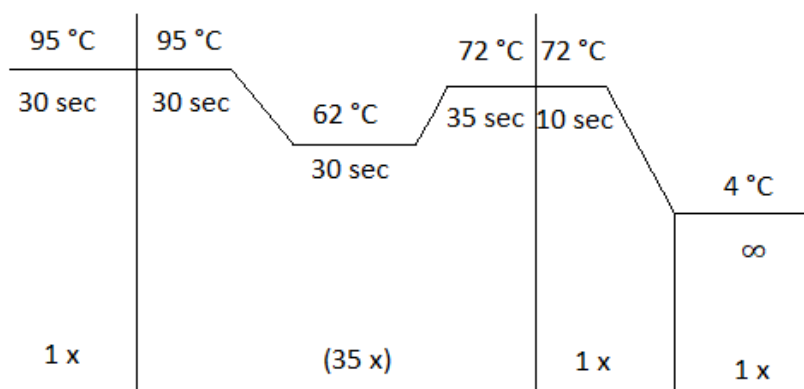


Figure 2.1. PCR program for the amplification of the *yeaB* gene

The PCR product was cleaned up in a 1% (m/v) agarose gel using the same conditions as described in the subcloning methods. The gene was excised from the PCR product by double digestion with the enzyme blend of Sgfl and Pmel. An empty pFN29A vector was also digested with Sgfl and Pmel to cut out the lethal barnase gene. The general restriction enzyme digest reaction contained 10 µL DNA (either PCR product or plasmid), 1 µL enzyme blend, 4 µL buffer and sterile Milli-Q water to a total volume of 20 µL. The digested *yeaB* gene and the linear pFN29A vector bands were cut from the agarose gel and concentrated using a GeneJET Gel Extraction Kit after which, the DNA concentration was determined at 260 nm with a µDROP plate on Multiskan Sky Microplate Spectrophotometer (ThermoFisher Scientific). The cleaned-up fragments were ligated together with a NEB quick ligation kit as per the manufacturer's instructions with a ratio of 1:3 (plasmid to insert). The ligation reaction was incubated overnight at 16 °C. The ligation reaction was then transformed into competent *E. coli* Mach1 cells and were plated on LB agar containing 100 mg/L ampicillin. Plasmid isolation was done on a sample of the colonies that grew. A preliminary restriction enzyme digest check was done with EcoRI that cuts at two sites on the pFN29A vector. The Identity of the *yeaB* gene was confirmed by DNA sequencing using the T-Terminator region.

2.2.4 Expression trials of NudL

2.2.4.1 Small scale expression trials

The expression plasmid pET28a-NudL was transformed into the expression strain *E. coli* BL21 (DE3). The colonies containing the kanamycin resistant plasmid were selected on a Luria-Bertani (LB) agar plate containing 30 mg/L kanamycin. A single colony was used to inoculate 5 mL of LB medium containing 30 mg/L kanamycin and incubated overnight at 37 °C whilst shaking at 180rpm. The overnight inoculum was diluted 1:100 in 21 × 15 mL falcon tubes, each containing 5 mL LB medium and 30 mg/L kanamycin. The cultures were grown at 37 °C until the optical density at OD₆₀₀ reached ± 0.6. IPTG was added at 0.1 mM, 0.5 mM and 1 mM and incubated at 18 °C, 25 °C and 37 °C for 3 hours or overnight (see Table 1). 2 mL of each culture was harvested by centrifugation 16 060 x g at Room temp or 4 °C for 10 min by a Heraeus Biofuge Pico and resuspended in 100 µL BugBuster®.

Table 2.1. Summary of expression trial conditions.

Temperature (°C)	[IPTG] (mM)	Induction period
18 or 25 or 37	0.0	0 hours
	0.1	3 hours
	0.1	18 hours
	0.5	3 hours
	0.5	18 hours
	1.0	3 hours
	1.0	18 hours

The cell suspension was mixed by rotation for 20 minutes at room temperature. The soluble and insoluble fractions were separated by centrifugation at $16060 \times g$ at 4°C for 20 min. Both the insoluble and soluble fraction of each trial was analysed by 12% SDS-PAGE. The soluble fraction was treated with a 1:1 ratio of lysate to 2 \times treatment buffer (0.1 M Tris-HCl pH 6.8, 4% SDS, 30% glycerol, 20% β -mercaptoethanol (BME) and 0.02% bromophenol blue). The insoluble pellet was resuspended in 100 μL treatment buffer. The samples were heated for minutes at 95°C before 15 μL samples were loaded on to the SDS-PAGE gel. The marker lane contained 3 μL of NEB Unstained Protein Standard (Broad Range). Expression trials were repeated with TB (terrific broth) and 2 \times YT (yeast-tryptone) media. LB media supplemented with 1.5% (v/v) ethanol, 2% (v/v) ethanol, 1% (m/v) sorbitol, 1% (m/v) mannitol was also tested. A second expression strain *E. coli* C41 (DE3), which has additional chloramphenicol resistance, was also tested using LB media containing 30 mg/L kanamycin and 30 mg/L chloramphenicol (dissolved in EtOH). Expression trials were repeated for the pFN29A-NudL plasmid in LB media and TB with 100 mg/L ampicillin as the antibiotic.

2.2.4.2 Cell-free expression

The S30 T7 High-Yield Protein Expression system (Promega) contained all the components for protein expression except the template DNA. In preparation, four plasmid isolations with the GeneJet plasmid mini prep kit were performed to obtain a concentration of plasmid DNA equal or greater than 100 ng/ μL . The manufacturer's protocol stated that the optimized amount of DNA is 0.5 – 1 μg per 50 μL reaction for optimal protein yield. In a sterile 1.5 mL microcentrifuge tube the following was added: 20 μL of S30 Premix plus, 18 μL T7 s30 Extract, 1 μg of DNA and Milli-Q water to a final volume of 50

μL . As per the manufacturer's instructions, the reaction was spun down with a microcentrifuge and incubated for 1 hour at 37 °C shaking on thermomixer set to 1200 RPM. The reaction was stopped placing the reactions on ice for 5 minutes. 5 μL aliquots from each reaction were analysed with SDS-PAGE.

2.2.5 Purification trials

2.2.5.1 Soluble purification

Large scale expression was conducted as per the optimal conditions determined in the expression trials. A single colony of BL21 pET28a-NudL from the LB agar plate was used to inoculate 2 \times 5 mL LB media containing 30 mg/L kanamycin. Each of the cultures were grown overnight at 37°C and used to inoculate 2 \times 500 mL LB media containing 30 mg/L kanamycin. The cultures were grown until the optical density at A_{600} reached ± 0.6 . The cultures were induced with 0.1 mM IPTG and shaken vigorously overnight at 18 °C. Cells from the 500 mL expression flasks were harvested by centrifugation for 20 min at $11305 \times g$. The basic purification method was as follows: the supernatant was discarded, and the pellet was resuspended in 10 mL lysis buffer (Binding buffer A1:20 mM Tris-HCl containing 500 mM NaCl, 5 mM imidazole, pH 7.9) per gram of wet cell mass. The cells were lysed by sonication and the cell lysate was harvested by centrifugation for 20 min at $48298 \times g$ at 4 °C. The supernatant was filtered through a 4.5 μm filter. The filtered supernatant was then loaded onto a HiTrap metal affinity purification column previously treated with 100 mM NiSO_4 (unless stated otherwise) and equilibrated with buffer A1 using an ÄKTAPrime automated protein purification system. The method selected determined the percentage of 500 mM imidazole for the wash and elution steps. The wash fractions and the purity of the elution fractions were further analysed by 12% SDS-PAGE.

The basic purification method was altered to optimize purification. The following combinations of alterations to the media and or lysis buffer and or purification were performed (Table 2).

Table 2.2. Summary of purification trial conditions. Percentage (%) refers to the percentage of 500 mM imidazole buffer used to wash or elute protein on IMAC column.

Purification	Alterations/Additives				
	Method	Lysis buffer	Media	Buffer A1	Metal charged to column
ÄKTA IMAC	10% wash, 100% elution				
	15% wash, 100% elution				
	15% wash, 100% elution	0.35% brij-35		0.35% brij-35	Ni ²⁺
	10% wash, 100% elution	0.35% brij-35 + 0.5 mM TCEP			Ni ²⁺
	5% ,8% ,10% ,15% wash, 100% elution	0.35% brij-35 + 0.5 mM TCEP			Ni ²⁺
	15% wash, 100% elution	0.5% Triton X-100			Ni ²⁺
	15% wash, 100% elution		1 mM Pan		Ni ²⁺
	5% wash, 100% elution	2 mM BME		2 mM BME	Ni ²⁺
	5% wash, 100% elution				Ni ²⁺
	5% wash, 100% elution				Co ²⁺
	5% wash, 100% elution				Zn ²⁺
Manual IMAC	15% wash, 100% elution				Ni ²⁺
Size exclusion					N/A

In addition to using an automated protein purification system, a manual purification method was also attempted. A 50% His-Select Nickel affinity gel slurry was prepared by washing the resin twice with Milli-Q water followed by equilibration with A1 binding buffer. The slurry was then incubated with filtered *E. coli* lysate for 4 hours at 4 °C by rotation. The slurry was then spun down to remove unbound proteins and excess liquid. The slurry was transferred into a 1.5 mL microcentrifuge tube and washed

three times with 1 mL A1 as in the equilibration steps. The slurry was added to a poly prep chromatography column (BioRad). The resin was allowed to pack by gravity for 5 minutes. The resin was washed again with 2 mL A1, followed by washing three times with 1 mL of 75 mM imidazole, 5 mM ATP. The flow-through was collected. A 5 μ L aliquot of each wash fraction was added to 250 μ L of the Bradford reagent, the lack of change in colour was used to monitor the protein content to ensure all the nonspecific protein was eluted. The protein of interest was eluted with 2 mL of 500 mM imidazole. The purity of the wash and elution fractions were analysed on a 12% SDS-PAGE gel.

The IMAC purified elution fractions were then pooled and subsequently subjected to size exclusion chromatography to improve the purity. Size exclusion chromatography was performed on a BioRad NGC Chromatography system. A G-75 Sephadex gel filtration column (150 mm x 20 mm) was used. The elution fractions from IMAC purification were spin concentrated with a Vivaspin 6 centrifugal concentrator to a volume of 1 mL before being loaded onto the column. The sample was eluted with buffer A6 at a flow rate of 1 mL/min.

2.2.5.2 Purification of insoluble protein

As most of the overexpressed proteins was found in the insoluble fractions, an attempt was made to solubilize the protein from inclusion bodies. Sarkosyl was used as the solubilization agent. Two solubilization methods were tested.

Method A: The pellet from a 1 L large scale culture was resuspended in 15 mL lysis Buffer (A1). The cells were lysed by sonication and the cell lysate was harvested by centrifugation for 20 mins at 25000 rpm at 4 °C. The insoluble pellet was then washed twice by resuspending the pellet with cold Milli-Q water followed by centrifugation for 20 mins at 4500 \times g at 4 °C. The pellet was then solubilized by resuspension with 15 mL A1 containing 2% (w/v) sarkosyl by rotation on low speed for two hours at room temperature.

In a second attempt, the pellet obtained from method A was solubilized with 0.2% (w/v) sarkosyl overnight at room temperature.

In a third attempt, the pellet was solubilized with 2% (w/v) sarkosyl. The supernatant was then placed in a SnakeSkin Pleated Dialysis Tubing (10000 MWCO, 3.7 mL/cm, ThermoFisherScientific). The membrane was placed into 1 L A1 and stirred at 4 °C to remove the detergent. After 30 minutes the buffer was replaced, and this was repeated twice. The last liter of buffer was not changed to allow for dialysis to occur overnight.

The supernatant from method A was then purified with ÄKTAPrime automated protein purification system as per protocol above with a stepwise method consisting of 5%, 8%, 10%, 15% imidazole wash steps followed by 100% imidazole elution.

Method B: The pellet from a 1 L large scale culture was resuspended in 15 mL lysis Buffer (A1). The cells were lysed by sonication (sonication cycle: 1 second pulses followed 1 second intervals for a total of 120 seconds. This cycle was repeated six times with 5 minute intervals between each). The cell lysate was harvested by centrifugation for 20 mins at 25 000 rpm at 4 °C. The insoluble pellet was then washed twice with cold Milli-Q water by resuspending the pellet followed by centrifugation for 20 mins at 4500 × g at 4 °C. The pellet was then solubilized by resuspension in 5 mL buffer A1 containing 2% (w/v) sarkosyl pipetting up and down on ice intermittently for 1 hour. The supernatant was then harvested by centrifugation for 20 min at 4500 × g at 4 °C. The supernatant was topped up to 20 mL with A1 and filtered through a 4.5 µm filter. The supernatant from method B was then purified with His-Select Nickel affinity gel as per protocol stated above without ATP in the wash step.

The IMAC purified samples were then loaded on a 5 mL HiTrap desalting column equilibrated with 25 mM Tris-HCl, 5 mM NaCl pH 8.0 to remove the imidazole and salts. 5% glycerol was added to the fractions containing highest protein concentration. The protein concentrations were determined with the Quick Start Bradford Protein Assay Kit (Bio-Rad).

2.2.6 Activity screening

The solubilized protein from method B was tested for activity. The reaction mixture contained 50 mM Tris-HCl pH 7.4, 5 mM (2-carboxyethyl) phosphine (TCEP), 10 mM of either MgCl₂ or MnCl₂, 0.5 mM CoA and 0.1 µg/µL NudL. The control reactions were set up in the same manner but without the addition of enzyme, using Milli-Q water to make up 50 µL. Reactions were incubated at 37°C for 60 minutes to ensure complete conversion of substrate. The reactions were then stopped, with 10 µL of 90% (w/v) trichloroacetic acid (TCA) and then neutralized with 40 µL of 2.25 M Ammonium acetate (NH₄OAc). The precipitated proteins were removed by centrifugation at 9503 × g for 10 min. The supernatant was removed and 7 µL of the aliquot was reserved for derivatization with 7-Diethylamino-3-(4-maleimidophenyl)-4-methylcoumarin (CPM). The derivatization mixture contained 21 µL MeCN, 1.3 µL CPM (10 mM in MeCN) and 7 µL supernatant, made up to 70 µL with Milli-Q. The derivatization mixture was then incubated overnight at room temperature. The CPM-labelled metabolites were analysed by HPLC using a published method (14).

2.3 Results and discussion

2.3.1 Subcloning

For the recombinant protein expression of NudL, the *yeaB* gene had to be inserted into a suitable expression vector. This was achieved by subcloning the gene insert from a cloning plasmid, pENTR-NudL that was readily available in the lab from previous studies. A restriction enzyme digest was done to confirm the size of the *yeaB* insert in the plasmid. A single digest with *Accl* that would have one internal cut site within the gene of interest was performed. The expected size of the linear DNA fragment was ~3000 bp. The *yeaB* insert was also confirmed by means of double digest of the pENTR-NudL vector with *XhoI* and *NdeI*. The restriction digest's contents were analysed on 1% agarose gel (Figure. 2.2). The uncut plasmid migrated further than the expected size of ~3000 bp, indicating that the integrity of the plasmid was supercoiled and of good quality. The single digest produced a linear DNA of the expected size. The double digest produced two fragments: the empty pENTR vector at ~2500 bp and the *yeaB* insert at ~600 bp. Subsequently, the *yeaB* gene was ligated into an expression vector, pET28a at the *XhoI* and *NdeI* sites. The transformation of the ligation reaction was successful; however, only one colony grew. The single colony was streaked out on a LB agar plate containing kanamycin, and growth was monitored. Single colonies from the streak plate were chosen for screening. For each colony, plasmid was isolated and digested with *XhoI* and *NdeI* to determine if the gene insert was present, and not an empty pET28a vector, as both would have kanamycin resistance. All the selected colonies had the gene inserted (data not shown). The plasmid obtained from one of the confirmed colonies was used for subsequent transformation into *E. coli* BL21(DE3) cells for expression trials. In the intervening period the plasmid was sent for DNA sequencing and the results showed that the insert was an exact match for the *yeaB* gene.

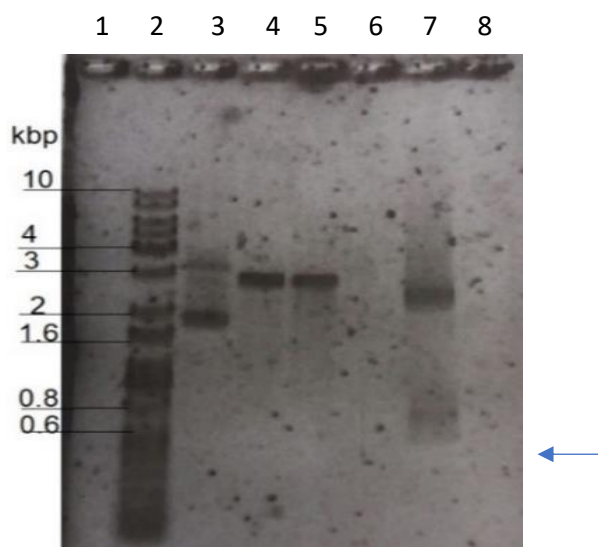


Figure 2.2. Agarose gel electrophoresis of enzyme digest of pENTR-NudL. DNA visualized with SYBR Gold post stain. Lane 2: contains Kapa universal DNA ladder. Lane 3: contains the undigested pENTR-NudL plasmid. Lane 4: contains the single digest of the pENTR-NudL with Accl restriction enzyme incubated for 1 hour. Lane 5: contains the single digest of the pENTR-NudL with Accl restriction enzyme incubated for 2 hours. Lane 7: contains the double digest of pENTR NudL with XhoI and NdeI. Lanes 1, 6, 8 do not contain anything. The *yeaB* gene indicated by an arrow.

2.3.2 pET28a-NudL Expression trials

Optimal expression conditions were determined by small scale expression trials. The newly constructed pET28a-NudL plasmid was transformed into *E. coli* BL21 (DE3) to generate an expression strain that would produce the recombinant 6× His-tagged protein. The expression conditions that were tested differed in IPTG concentration used for induction, the temperature used for expression post-induction and the expression time post-induction (Table 2.1).

Expression in LB media was tested first, and the results were analysed by 12% SDS-PAGE. NudL migrated with an apparent molecular weight of ~27 kDa (the expected molecular weight of NudL is 22.4 kDa without the His₆-tag). Most of the induced protein was found in inclusion bodies and appeared in the insoluble fraction (Figure. 2.3B). Even at higher expression temperatures, 25 °C and 37 °C, more insoluble protein was formed (data not shown). Using a lower expression temperature of 18 °C and lower IPTG concentration of 0.1 mM seemed to result in some soluble overexpression with a band at the apparent molecular weight of 27 kDa (Figure. 2.3A). In order to optimize these conditions furthermore nutrient-rich TB media was used (Table 2.1). From the SDS-PAGE analysis it appeared that although yield of the desired recombinant protein did increase more insoluble protein was observed under these conditions, even at a low the expression temperature of 18 °C (Figure. 2.3C). Furthermore, it appeared that there was less soluble expression at 18 °C when compared to when LB media was used originally (Figure. 2.3D). There also seemed to be some level of auto-induction, as the 0-hour

control showed evidence of overexpressed protein in the insoluble fraction (Figure. 2.3C). A third type of media, 2× YT was tested for expression with varying IPTG concentrations used for induction and was incubated at 18 °C overnight following induction. Unfortunately, the solubility of the desired protein was not improved (Figure. 2.3E). Following this, an alternative secondary expression strain was used in an attempt to improve solubility. The pET28a-NudL plasmid was transformed into *E. coli* C41 (DE3) + pLysS. The C41 strain is more enduring to the expression of toxic proteins; however, no significant overexpressed protein was observed at the 27 kDa mark in either the soluble and insoluble fractions following expression at 18 °C or 37 °C (Figure. 2.3F). Cultures were subsequently supplemented with mannitol and sorbitol to disrupt osmotic pressure within the *E. coli* cells, while ethanol was also added as it is hypothesised to effect the membrane fluidity and by consequence, membrane transport (15, 16). The expected effect of these reagents is therefore to shift the overexpressed protein into the soluble fraction instead of into inclusion bodies. Unfortunately, the total expression of protein from the supplemented cultures was not increased, nor was the ratio of soluble/insoluble NudL improved compared to the previously identified optimal overexpression conditions. (Figure. 2.3G-H).

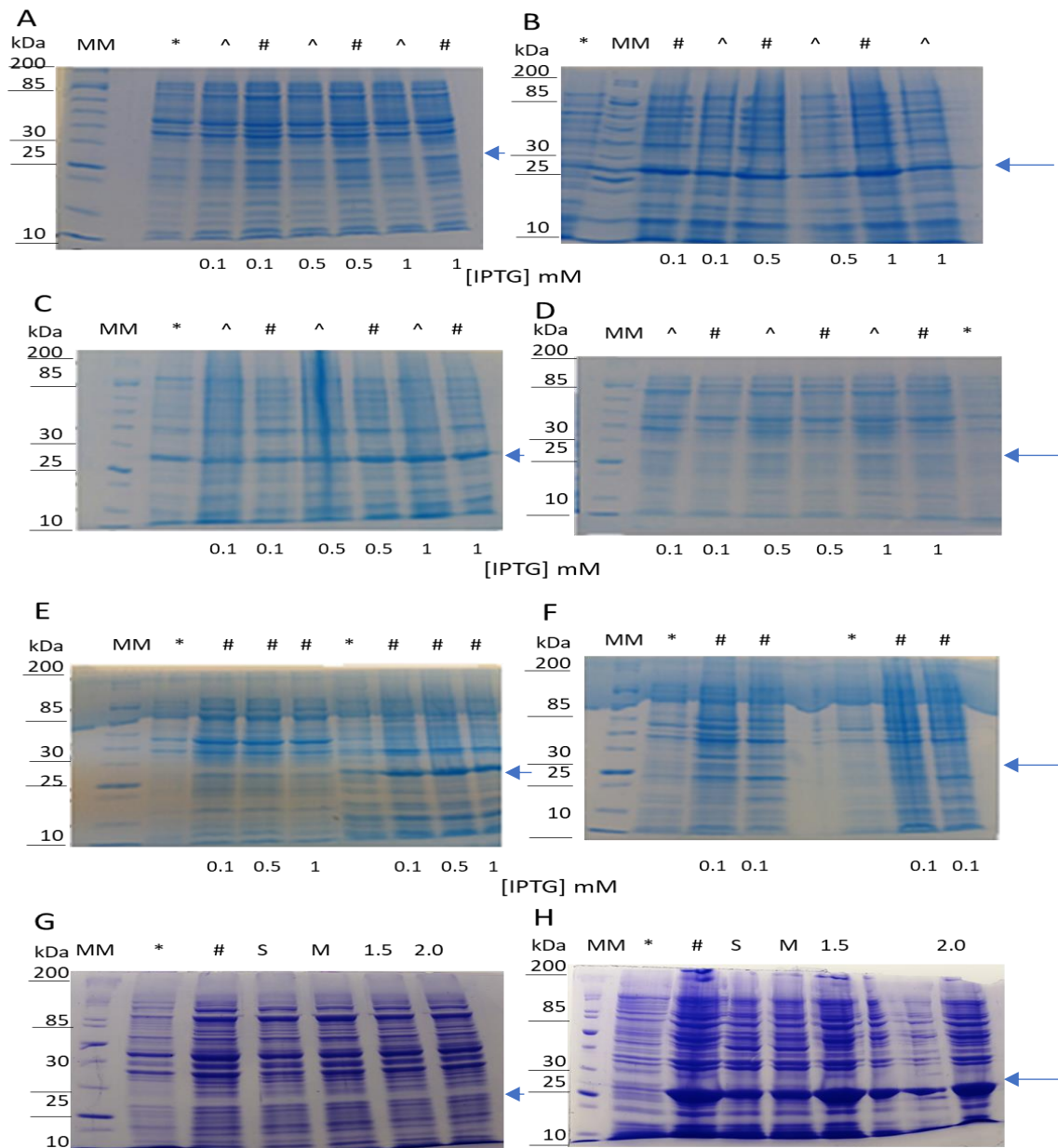


Figure 2.3. pET28a-NudL small scale expression trials analysed by 12% SDS-PAGE. The IPTG concentration used for induction is noted below each lane. Lanes containing Unstained Protein Standard indicated by (MM). Lanes containing 0-hour control (no IPTG) indicated by (*). The 3 hours expression time post-induction noted as (^), and overnight expression period noted as (#). **(A)** Soluble fractions after expression in LB media at 18 °C. **(B)** Insoluble fractions after expression in LB media at 18 °C **(C)** Insoluble fractions after expression in TB media at 18 °C **(D)** Soluble fractions after expression in TB media at 18 °C **(E)** Fractions after overnight expression in 2x YT media at 18 °C. Lane 2- 5 are soluble fractions. Lane 6- 9 are insoluble fractions. **(F)** Fractions from expression using C41 strain grown in LB media induced with 0.1 mM IPTG and expressed overnight. Lane 2: soluble control fraction. Lane 3: 18 °C soluble. Lane 4: 37 °C soluble. Lane 6: insoluble control fraction. Lane 7: 18 °C insoluble. Lane 8: 37 °C insoluble. **(G)** Soluble fractions of NudL grown at 18 °C in LB with various supplements overnight expression. Lane 3: un-supplemented. Lane 4: supplemented with 1% (m/v) sorbitol. Lane 5: supplemented with 1% (m/v) mannitol. Lane 6: supplemented with 1.5% (v/v) ethanol. Lane 7: supplemented with 2% (v/v) ethanol **(H)** Insoluble fractions of NudL grown at 18 °C in LB with various supplements with overnight. Lane 3: un-supplemented. Lane 4: supplemented with 1% (m/v) sorbitol, Lane 5: supplemented with 1% (m/v) mannitol. Lane 6: supplemented with 1.5% (v/v) ethanol. Lane 7: supplemented with 2% (v/v) ethanol. The arrows indicate those protein bands that are believed to be the desired NudL protein ~27 kDa.

2.3.3 Purification trials

2.3.3.1 Purification trials – varying imidazole concentration

Based on the expression trials, the optimum soluble expression conditions were determined to be growth in LB media, induction with 0.1 mM IPTG and expression at 18 °C overnight. These identified conditions were used for all large-scale batch expressions of NudL. Purification of NudL proved difficult as the low expression levels together with weak interactions of the His₆-tag with the IMAC column resulted in a very low yield. Contaminating proteins were also strongly associating with NudL or the IMAC column itself and resulted in 'dirty' elution fractions. Various additives were used in attempt to aid purification. First, the protein of interest was purified by Ni²⁺-IMAC on an ÄKTAPrime automated purification system. Non-specific binding histidine-rich proteins were washed off with 10% imidazole (50 mM) and NudL was eluted with 100% imidazole (500 mM). The fractions were then analysed by SDS-PAGE (Figure. 2.4A). The final elution fraction did not contain only NudL, as it also showed the presence of bands both above and below 27 kDa. Subsequently, another round of large-scale expression was performed followed by purification with a wash step in which the amount of imidazole was increased to 15% imidazole (75 mM). However, the increased imidazole concentration using in the wash step did not remove the previously observed contaminants (Figure. 2.4B).

2.3.3.2 Purification trials – detergents and additives

Next, a series of combinations of detergents and reducing agents were added to the lysis and or binding buffer to attempt to increase the yield and purity (Table 2.2). Detergents were tested as they can assist with binding and solubility by disrupting protein lipid association. Reducing agents were added to aid the dissociation of the unknown proteins that were apparently associating with NudL during expression and purification.

Brij-35 (0.35 %), an inexpensive and mild nonionic detergent was used in both lysis and binding buffers. The detergent level was below the critical micelle concentration -the concentration where the detergents form micelles around the protein -this impedes with the association of the His₆-tag associating with the column. However, it was found that in the experiments conducted in this study, the detergent concentration was too high as no protein bound to the column. The chromatogram from the IMAC purification showed no significant peaks (data not shown). Subsequently, the detergent level was lowered by only adding brij-35 to the lysis butter, and adding the reducing, agent TCEP to the lysis buffer. The lysate was purified with a stepwise increase in imidazole concentration from 5 to 100 % imidazole (Figure. 2.4C). Although purity seemed to be somewhat improved, the overall yield NudL was lower, as the band at ~27 kDa was much fainter in comparison to previous

purification attempts, and would not be sufficient for activity assays. The subsequent purification with a nonionic detergent TritonX-100 also resulted in only a wash peak, with no peak detected for elution (Figure. 2.4D). It appeared that most of the protein of interest did not bind the column as there is dark band at ~27 kDa in the flow though. The final purification attempt was with additives, using the reducing agent BME in the lysis buffer and in the binding buffer. From figure 2.3D lane 2, it is clear that under these conditions, the elution fraction contained more contaminates than the protein of interest. It was assumed that the contaminating bands were heat shock proteins, as the sizes corresponded to those of known chaperones (17). Some of these proteins can be released from the protein partner by the addition of ATP. For these tests, manual IMAC had to be performed as the automated AKTA system required a larger amount of buffer, and thus ATP. This method seemed to improve the yield of NudL due to the longer incubation time with the Ni²⁺ resin, and also improved the purity with the addition of ATP to the wash buffer. The lower amount of contaminating protein bands in the SDS-PAGE analysis compared to IMAC purification on the ÄKTAPrime automated purification system confirms that some of these contaminating bands are heat shock proteins (Figure. 2.4E).

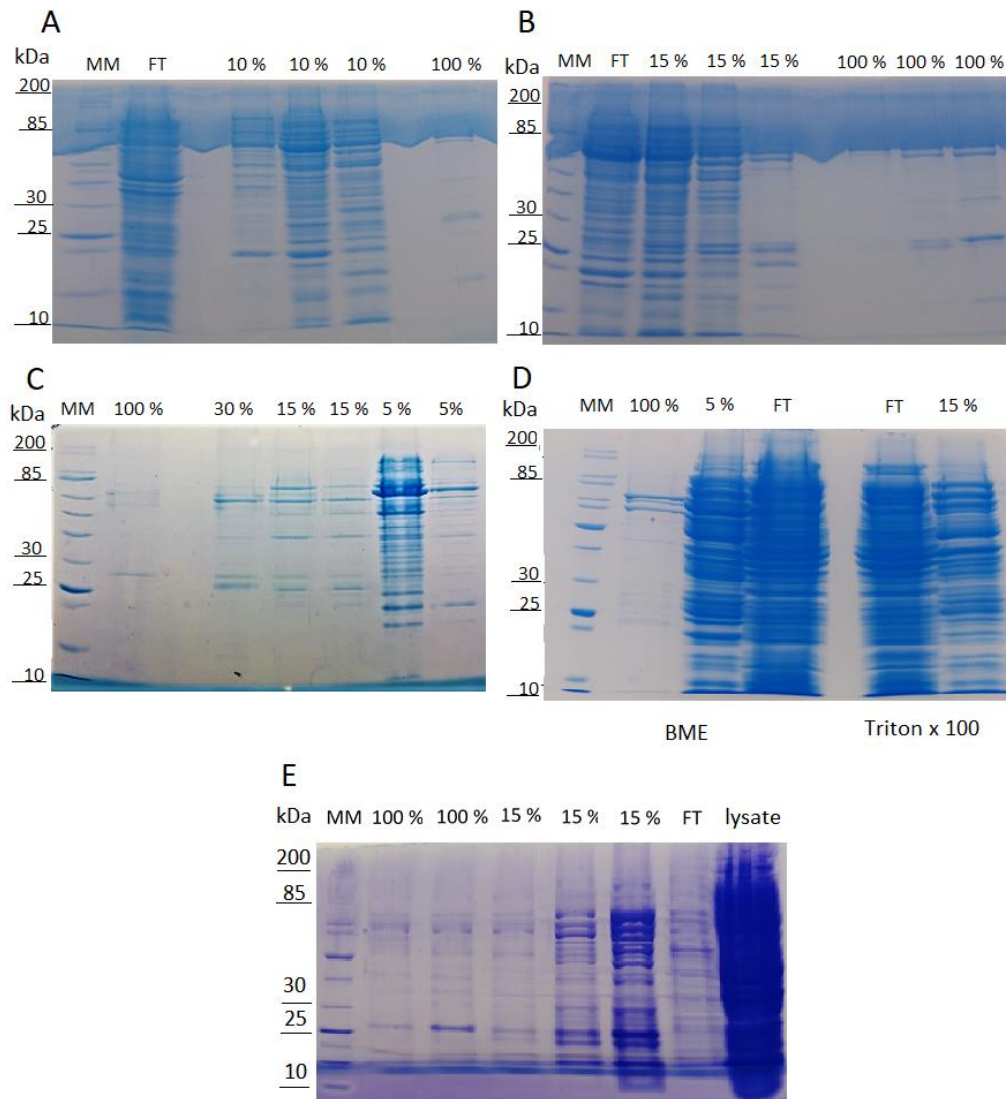


Figure 2.4. Soluble purification of NudL analysed by 12% SDS-PAGE. Lanes containing Unstained Protein Standard are indicated with MM, lanes containing Flow-through (unbound proteins) indicated with FT. Percentage (%) amounts above lanes refers to percentage of 500 mM imidazole used to obtain that specific fraction. **(A)** Result following the purification method using 10% wash and 100% elution steps. **(B)** Result following the purification method 15% wash and 100% elution steps. **(C)** Result following the purification method with 0.35% brij-35 + 0.5 mM TCEP. **(D)** Result following the purification method with 2 mM BME (Lanes 2-4) and Triton X-100 (Lanes 6 and 7). **(E)** Result following the purification method with 5 mM ATP in the 15% wash buffer.

2.3.3.3 Purification trials - supplemented media

As the addition of detergents did not aid purification, alternative approaches were explored to improve the soluble expression of NudL. We speculated that if NudL breaks down CoA as predicted, then the potential toxicity of this protein would be reduced, and its removal to inclusion bodies should also be reduced. The growth medium was therefore supplemented with 1 mM pantothenic acid as the precursor to the pathway. However, no significant increase in yield or purity was observed (Figure. 2.5).

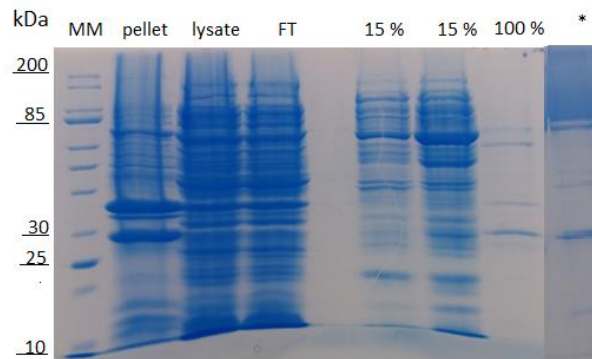


Figure 2.5. Purification of NudL grown with pan supplemented media analysed by 12% SDS-PAGE. Lane containing Unstained Protein Standard are indicated with MM. Lane containing flow-through (unbound proteins) indicated with FT. Percentage (%) amounts above lanes refers to percentage of 500 mM imidazole used to obtain that specific fraction. Result following the purification method with using 15% wash and 100 % elution steps. The lane marked with a * is to compare yield of elution fraction to standard protocol (Fig. 3B)

2.3.3.4 Purification trials – metal affinity

In an effort to optimize the IMAC-based purification on the ÄKTA system, different metals were charged to the HiTrap metal affinity purification column. The established protocol makes use of Ni^{2+} , but other transition metals also have an affinity for the poly-histidine tag (18). The metals tested were Ni^{2+} , Co^{2+} and Zn^{2+} . The affinities were compared by comparing the elution fraction from a purification method with a 5% imidazole wash step before elution with 500 mM imidazole. All purifications were loaded with the same volume of lysate from a single pellet so that batch variation did not play a role. Figure 2.5 shows that the column charged with Ni^{2+} (Figure. 2.6A) was the most effective as it had the brightest band at the expected size of 27 kDa.

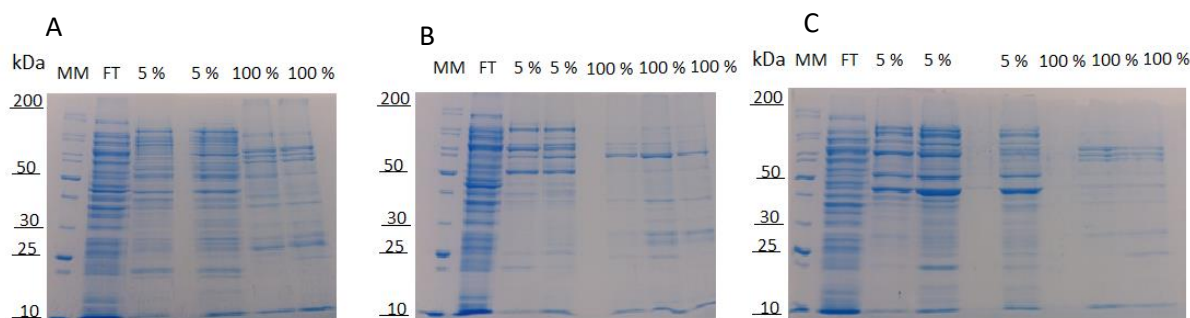


Figure 2.6. Purification of NudL with different metals charged to IMAC column analysed by 12% SDS-PAGE. Lanes containing Unstained Protein Standard noted as MM. Lanes containing flow-through (unbound proteins) indicated as FT. Percentage (%) amounts above lanes refers to percentage of 500 mM imidazole used to obtain that specific fraction. **(A)** Results from the column charged with Ni^{2+} . **(B)** Results from the column charged with Co^{2+} . **(C)**. Results from the column charged with Zn^{2+} .

2.3.3.5 Purification trials - Purification of the insoluble fraction

As most of the overexpressed protein was found in inclusion bodies, this led to an effort to recover NudL from the pellet of insoluble protein. Sarkosyl is an anionic surfactant and a mild solubilization agent that, unlike SDS would completely denature the protein (19). Sarkosyl has been widely used to solubilize natively folded proteins from inclusion bodies (20). It was assumed that NudL was natively folded but at higher concentrations became toxic to the cell, leading to its incorporation into inclusion bodies. The first solubilization attempt made use of a 2% sarkosyl solubilisation solution, followed by a stepwise purification using IMAC on an ÄKTAPrime automated protein purification system. Unfortunately, there were no significant peaks evident on the chromatogram after the initial loading of the lysate to the column (data not shown). It appeared that the detergent level was again too high and binding to the Ni^{2+} charged column was compromised. Although 2% sarkosyl was below the limit set by the manufacturer for use with the column, poor binding of NudL seemed to be a common problem with IMAC-based purification in the presence of sarkosyl (19, 20). Therefore, a second attempt at solubilization was performed, using 0.2% sarkosyl. The solubilization incubation period was increased from 2 hours to overnight to account for the lower detergent concentration and to ensure maximum solubility. The solubilized lysate was again subjected to IMAC-based purification on an ÄKTAPrime automated protein purification system with a stepwise increase in imidazole concentration from 5 to 100 % imidazole. There appeared to be no significant improvement in yield and only a slight improvement in purity for the elution (100% imidazole) fraction when compared to the soluble purification attempts (Figure. 2.7A). A third attempt was made by increasing the sarkosyl back to 2%, but by adding an additional dialysis step to remove the detergent prior to purification. The binding was still impaired as there are no bands at the expected size of 27 kDa for the elution fractions (Figure. 2.7B). This is verified by the thick band at 27 kDa in the flow through (Figure. 2.7B).

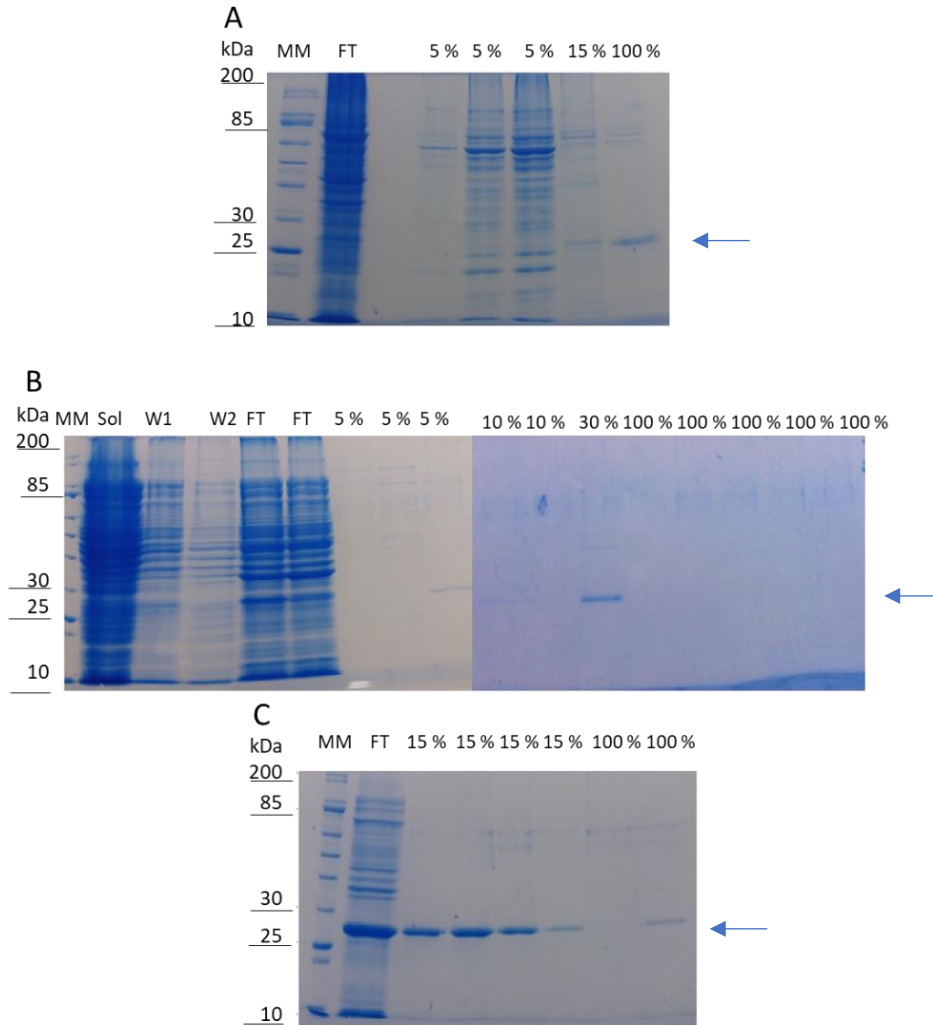


Figure 2.7. Purification of solubilized and purified NudL analysed by 12% SDS-PAGE. Lanes containing Unstained Protein Standard are indicated with MM. Lanes containing soluble fraction indicated by sol. Lanes containing flow-through (unbound proteins) indicated as FT. Percentage (%) amounts above lanes refers to percentage of 500 mM imidazole used to obtain that specific fraction. Arrows indicate the expected size of NudL following IMAC purification. W refers to the supernatant after insoluble pellet was washed with water. **(A)** Results following ÄKTA IMAC purification fractions after solubilization with 0.2% sarkosyl. **(B)** Results following ÄKTA IMAC purification fractions after solubilization with 2% sarkosyl followed by dialysis **(C)** Results following His-Select Nickel affinity gel IMAC purification fractions after solubilization with 0.5% sarkosyl.

In order to increase the binding of the protein to the metal affinity resin, a batch purification was attempted with His-Select Nickel affinity gel. The insoluble pellet was solubilized in the same amount of sarkosyl (2%) and the pellet was manually resuspended at a lower temperature of 4 °C so as to minimize distress on the protein due to heat generation from resuspension by mechanical means. The solubilized sample was diluted to a final sarkosyl concentration of 0.5% before incubation with the nickel resin. The SDS-PAGE gel suggested that this method is promising as the binding was improved as well as the purity of the eluted samples (Figure. 2.7C). The fractions containing the purest and

highest yield NudL were used for activity screening. Unfortunately, no CoA hydrolase activity was detected for any of these fractions using the HPLC assay (data not shown). NudL appears to be a very unstable protein, and it is possible that it was not natively folded prior to incorporation into the inclusion bodies. However, it is not obvious in what folded state proteins are in inclusion bodies (19).

2.3.4 Alternate expression systems

Seeing that neither soluble nor solubilized purification of NudL was yielded pure active protein, alternate expression systems were sought. The main difficulties faced was that the overall soluble expression of NudL was low, as most of the overexpressed protein was contained in the insoluble fractions. As well as low yields, upon purification with IMAC the soluble protein was contaminated with multiple unidentified proteins, assumed to be heat shock proteins. Two alternate expression systems that were available in the Strauss Laboratory which could theoretically bypass the apparent toxicity of NudL were therefore investigated. These include the pFN29A fusion vector and cell free expression systems.

2.3.4.1 Alternate expression systems - pFN29A fusion vector

The first alternate expression system tested is based on the use of an alternative expression vector, encoding a fusion protein. Many of the previously characterized CoA hydrolases have been expressed as fusion proteins; this includes NudL (6, 13). The pFN29A vector encodes a dual His₆Halo fusion protein that is meant to assist with solubility as well as have a simple two step purification process. Following the N-terminal His₆HaloTag[®] region, is a TEV protein recognition site that may be used to cleave off the tag to yield pure protein. To introduce the insert into this plasmid, primers had to be designed to introduce the unique SgfI and PmeI cut sites at the 3' and 5' ends to the *yeaB* gene respectively. The *yeaB* gene was cloned from isolated pET28a-NudL plasmid DNA with the above-mentioned primers for primer sequences see experimental section 2.2.3. The PCR product and pFN29A was digested with the SgfI and PmeI enzyme blend. *yeaB* was then ligated into the linear pFN29A vector (Figure. 2.8). Several ligation attempts were made with a lower ligation temperature of 16 °C being most effective. The plasmid was sequenced, and the insert was an exact match for the *yeaB* gene. The pFN29A-NudL plasmid was transformed into *E. coli* BL21 (DE3) to generate an expression strain and small-scale expression trials were repeated for the new plasmid construct to determine optimal expression conditions. The expression conditions tested were the same as previous

expression trials in section 2.3.2 and ranged in the concentration of IPTG used for induction, expression temperature and induction times (Table 2.1).

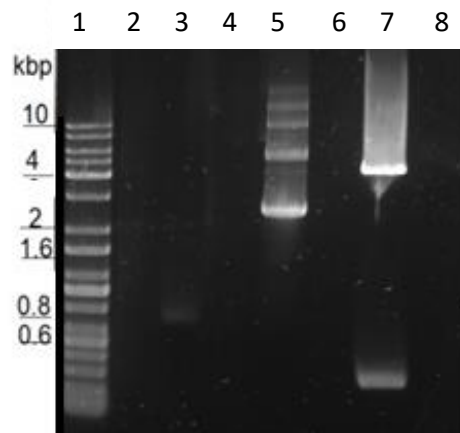


Figure 2.8. Agarose gel electrophoresis of enzyme digest of pFN29A and *yeaB*. DNA visualized with SYBR Gold post stain. Lane 1: contains Kapa universal DNA ladder. Lane 3: contains the double digested PCR product with SgfI & PmlI enzyme blend. Lane 5: contains the undigested pFN29A plasmid. Lane 7: contains the double digest of the pFN29A with SgfI & PmlI enzyme blend. Lanes 2, 4, 6, 8 do not contain anything.

The pFN29A-NudL plasmid was transformed into *E. coli* BL21 (DE3) to generate an expression strain that would produce the recombinant His₆Halo fusion protein with an expected mass of ~60 kDa (33 kDa for the fusion tag and 27 kDa for NudL). This plasmid took 4 hours to reach O.D₆₀₀ = 0.6 which is double the amount of time compared to the pET28a-NudL vector construct. Much like the previous expression trials, when grown in LB media most of the induced protein expression was found in the insoluble fraction (Figure. 2.9B). There was some soluble expression at the expected size of 60 kDa (Figure. 2.9A) but there was less overall expression at lower temperatures of 18 °C and 25 °C (data not shown). TB media was used for the second round of trials as it is more nutrient rich. The SDS-PAGE analysis shows that there was less overall (soluble and insoluble combined) expression compared to expression in LB (Figure. 2.9A-B). Again, a higher incubation temperature of 37 °C seemed to increase total expression in comparison to the lower temperature (data not shown).

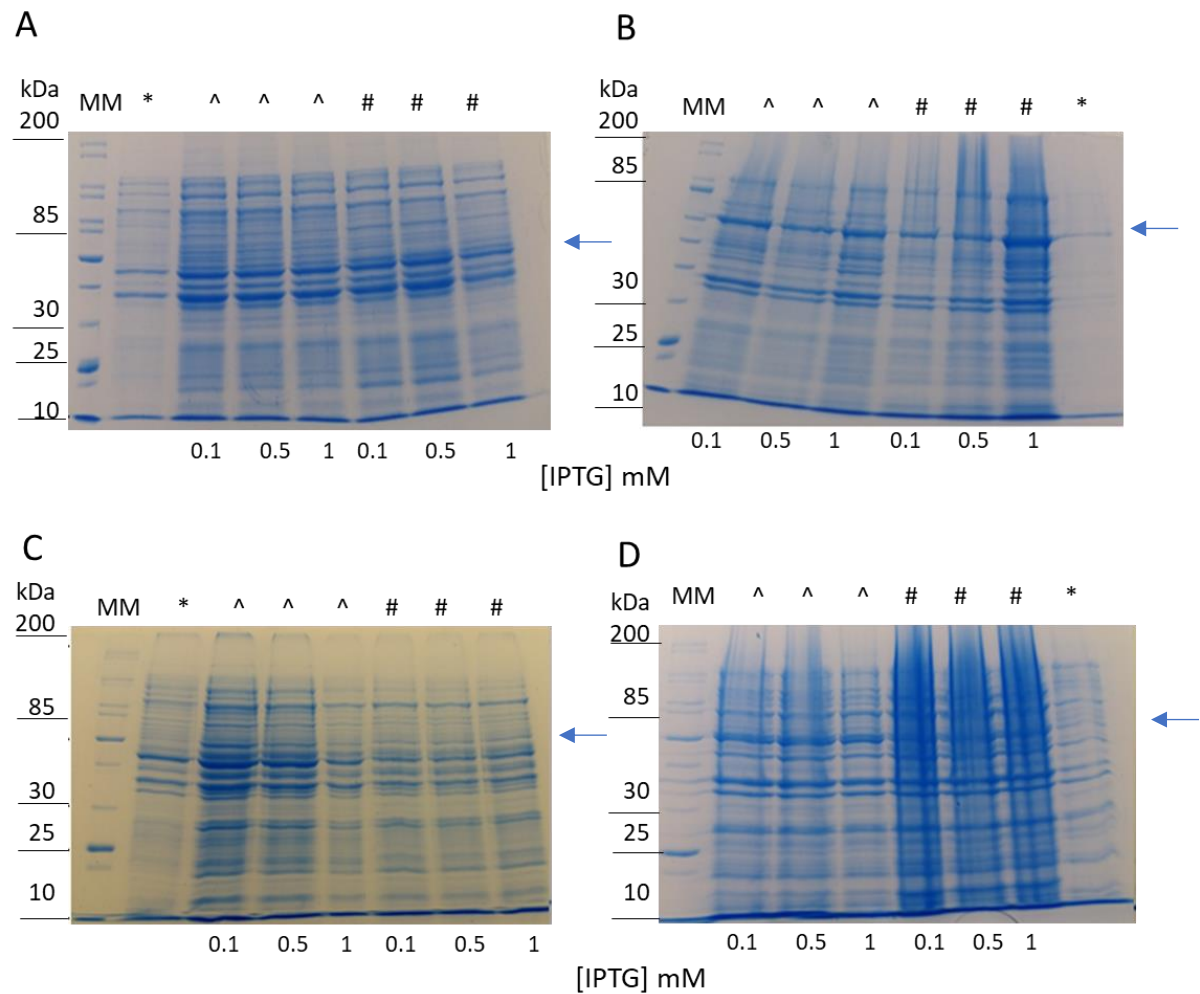


Figure 2.9. pFN29A-NudL small scale expression trials analysed by 12% SDS-PAGE. The IPTG concentration used for induction is noted below each lane. Lanes containing Unstained Protein Standard indicated by MM. Lanes containing 0-hour control (no IPTG) indicated by (*). The 3 hours expression time post induction noted as (^), and overnight post induction expression period noted as (#). **(A)** Soluble fractions after expression in LB media at 37 °C. **(B)** Insoluble fractions after expression in LB media at 37 °C. **(C)** Soluble fractions after expression in TB media at 37 °C. **(D)** Insoluble fractions after expression in TB media 37 °C. The arrows indicate those protein bands that are believed to be the desired NudL protein ~60 kDa.

Ultimately, protein expressed in cells grown in LB at the higher temperature of 37 °C, following induction with an IPTG concentration of 0.1 mM, and expression overnight seemed to show some soluble overexpression for His₆Halo-NudL. However, soluble expression was less than the amount produced using pET28a-NudL expression as identified in the previous expression trials; the bands were smaller and accounted for the fusion tag as well as the protein of interest. No further purification was attempted as it appeared that the Halo fusion protein did not increase solubility of NudL.

2.3.4.2 Alternate expression systems - cell free expression

The second alternate expression system used was based on a cell-free expression system. Cell free expression is an open system that only contains components required for transcription and translation. Therefore, metabolic and cytotoxic build up are avoided allowing for the expression of toxic proteins. In the cell-free expression system a basic reaction includes cellular extracts, template DNA, energy sources, amino acids, nucleotides and salts. There are various systems for cell-free expression, such as the wheat germ cell-free system expression system. However, cell-free expression of *E. coli* S30 extract is the most popular and was used to express NudL. The kit used was the S30 T7 High-Yield Protein Expression System and contained all the above-mentioned components except for the template for NudL. Although manufactures instructions were followed no expression was observed for the positive control protein nor the protein of interest (Figure. 2.10). Thicker over expression bands were expected at 33 kDa for the positive control and at 27 kDa for NudL. Since the positive control did not work as expected, concern arose that the kit was possibly faulty. Due to time constraints optimization of the kit could not be done. A secondary check for the positive control by means of the *Renilla* luciferase activity could have been done with the remainder of the reaction.

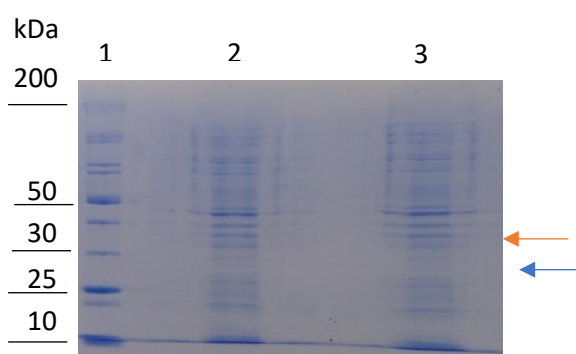


Figure 2.10. Cell free expression reactions analysed by 12% SDS-PAGE gel. Lane 1 contains the Unstained Protein Standard. Lane 2 contains the *Renilla reniformis* luciferase positive control. Lane 3 contains the standard reaction with pET28a-NudL template DNA. The orange arrow indicates the size of the expected protein band for *Renilla reniformis* luciferase and the blue arrow for NudL.

2.4 Conclusion

In this chapter attempts at the expression and partial purification of soluble NudL for activity confirmation were reported and described. Induced overexpression of soluble NudL proved challenging as most of the protein was found to be in the insoluble protein fraction. Of all the conditions tested during expression trials the lower IPTG concentrations in combination with a lower induction temperature and a longer incubation period seemed to improve the soluble yield. This was also found to be the case for the *C. elegans* protein Y87G2A.14 (6). Expression trials with more

nutrient-rich media, i.e., 2× YT and TB, did increase the total overexpression when compared to LB media. Unfortunately, solubility was not improved. The addition of neither osmolytes nor ethanol was able to shift the overexpression from the insoluble to the soluble fraction. Expression trials using the C41 strain showed no significant overexpression when compared to the control. This could be due to the use of old stocks of the expression strain, or that this strain produces very low protein yields (as have been seen in previous experiments in this laboratory). Yet, it remains surprising that an *E. coli* expression system struggled to express significant amounts of an *E. coli* protein. This suggests that overexpression of NudL was not well tolerated by the cells, which could be due to excessive NudL being able to disrupt CoA pools within the cell. Alternatively, the protein could have possible membrane association, which would greatly hinder its soluble expression.

Purification of NudL also proved to be challenging. Several other *E. coli* Nudix enzymes were reported to be easily extracted by freeze and thaw cycles (1, 21–23). However, complete cell disruption by means of sonification was required (1). SDS-PAGE analysis of the elution fractions showed that there were low yields of NudL due to several factors, including weak binding to the IMAC column, low expression levels and impurities that were present in all the soluble purification attempts. The weak interaction with the column could be attributed to possible obstruction of the histidine tag by either the protein itself or the contaminants. It is unclear why these impurities remain associated with recombinant NudL even after the 75 mM imidazole wash step. Neither the addition of the reducing agents, TCEP and BME, nor the addition of nonionic detergents, brij-35 and Triton X-100, could disrupt these interactions with interfering proteins or improve binding of the target protein. Size exclusion chromatography was performed after the standard IMAC purification to remove the contaminating proteins. This was attempted twice but both times the sample was too dilute (very low concentrations as evidenced by mAu units on chromatographs). Furthermore, the peaks that did elute were below the detection threshold settings of the instrument and hence were not automatically collected and were eluted into the waste (data not shown). Purification with the solubilized NudL did improve yield and purity, however, activity assays failed to detect the desired CoA hydrolase activity. This could be either that the protein was not natively folded in the inclusion bodies or too unstable for the lengthy solubilization and purification process. The combination of the increased binding time with the Ni²⁺ resin and the addition of 5 mM ATP purity and yield was slightly increased as the contaminating heat shock proteins were released.

As mentioned above, solubility has been a common challenge with recombinant expression of CoA hydrolases as many have been expressed as fusion proteins (3, 5, 6, 13). However, the dual His6Halo tag tested did not increase expression nor solubility. This might be a toxicity issue as mentioned before.

The unstable nature of NudL as well as the modest soluble yield and the low purity led to the exploration of the physiological role of this enzyme on a whole cell level. Since most of the overexpressed NudL was contained in inclusion bodies, it is likely that that excessive amounts of NudL is potentially toxic to the bacteria. The optimized purification method resulted in a very low yield of the protein, but the instability of NudL did not allow for the protein from multiple purification batches to be pooled to be used for full kinetic characterization. Nonetheless, the optimized purification method as determined from the studies reported in this chapter allowed for the partial purification of NudL to allow for testing of its putative CoA hydrolase activity.

2.5 References

1. Xu, W., Dunn, C. A., O'Handley, S. F., Smith, D. L., and Bessman, M. J. (2006) Three New Nudix Hydrolases from *Escherichia coli*. *J. Biol. Chem.* **281**, 22794–22798
2. Aiba, H. (1996) A 570-kb DNA Sequence of the *Escherichia coli* K-12 Genome Corresponding to the 28.0-40.1 min Region on the Linkage Map. *DNA Res.* **3**, 363–377
3. Kupke, T., Caparrós-Martín, J. A., Malquichagua Salazar, K. J., and Culiáñez-Macià, F. A. (2009) Biochemical and physiological characterization of *Arabidopsis thaliana* AtCoAse: a Nudix CoA hydrolyzing protein that improves plant development. *Physiol. Plant.* **135**, 365–378
4. Xu, W., Shen, J., Dunn, C. A., Desai, S., and Bessman, M. J. (2001) The Nudix hydrolases of *Deinococcus radiodurans*. *Mol. Microbiol.* **39**, 286–290
5. Gasmi, L., and McLENNAN, A. G. (2001) The mouse Nudt7 gene encodes a peroxisomal nudix hydrolase specific for coenzyme A and its derivatives. *Biochem. J.* **357**, 33
6. Abdelraheim, S. R., and Mclennan, A. G. (2002) The *Caenorhabditis elegans* Y87G2A.14 Nudix hydrolase is a peroxisomal coenzyme A diphosphatase. *BMC Biochem.* **3**, 1–8
7. Kang, L.-W., Gabelli, S. B., Bianchet, M. A., Xu, W. L., Bessman, M. J., and Amzel, L. M. (2003) Structure of a Coenzyme A Pyrophosphatase from *Deinococcus radiodurans*: a Member of the Nudix Family. *J. Bacteriol.* **185**, 4110–4118
8. Kapoor, I., Varada, R., Aroli, S., and Varshney, U. (2019) Nudix hydrolases with Coenzyme A (CoA) and acyl-CoA pyrophosphatase activities confer growth advantage to *Mycobacterium smegmatis*. *Microbiology.* **165**, 1219–1232
9. Cartwright, J. L., Gasmi, L., Spiller, D. G., and McLennan, A. G. (2000) The *Saccharomyces cerevisiae* PCD1 Gene Encodes a Peroxisomal Nudix Hydrolase Active toward Coenzyme A and Its Derivatives. *J. Biol. Chem.* **275**, 32925–32930
10. Kerr, E. W., Shumar, S. A., and Leonardi, R. (2019) Nudt8 is a novel CoA diphosphohydrolase that resides in the mitochondria. *FEBS Lett.* **593**, 1873-3468.13392
11. Shumar, S. A., Kerr, E. W., Geldenhuys, W. J., Montgomery, G. E., Fagone, P., Thirawatananond, P., Saavedra, H., Gabelli, S. B., and Leonardi, R. (2018) Nudt19 is a renal CoA diphosphohydrolase with biochemical and regulatory properties that are distinct from the hepatic Nudt7 isoform. *J. Biol. Chem.* **293**, 4134–4148
12. Spangler, J. R., and Huang, F. (2020) The *E. coli* NudL enzyme is a Nudix hydrolase that cleaves

CoA and its derivatives. *bioRxiv*. 10.1101/2020.01.31.929182

13. Kim, J., Kershner, J. P., Novikov, Y., Shoemaker, R. K., and Copley, S. D. (2010) Three serendipitous pathways in *E. coli* can bypass a block in pyridoxal-5'-phosphate synthesis. *Mol. Syst. Biol.* **6**, 436
14. Goosen, R., and Strauss, E. (2017) Simultaneous quantification of coenzyme A and its salvage pathway intermediates in in vitro and whole cell-sourced samples. *RSC Adv.* **7**, 19717–19724
15. Chhetri, G., Kalita, P., and Tripathi, T. (2015) An efficient protocol to enhance recombinant protein expression using ethanol in *Escherichia coli*. *MethodsX.* **2**, 385–391
16. Oganessian, N., Ankoudinova, I., Kim, S.-H., and Kim, R. (2007) Effect of osmotic stress and heat shock in recombinant protein overexpression and crystallization. *Protein Expr. Purif.* **52**, 280–285
17. Nam, S.-H., and Walsh, M. K. (2002) Affinity Purification and Characterization of the *Escherichia coli* Molecular Chaperones. *Protein Expr. Purif.* **24**, 282–291
18. Gaberc-Porekar, V., and Menart, V. (2001) Perspectives of immobilized-metal affinity chromatography. *J. Biochem. Biophys. Methods.* **49**, 335–360
19. Massiah, M. A., Wright, K. M., and Du, H. (2016) Obtaining Soluble Folded Proteins from Inclusion Bodies Using Sarkosyl, Triton X-100, and CHAPS: Application to LB and M9 Minimal Media. *Curr. Protoc. Protein Sci.* **84**, 6.13.1-6.13.24
20. Tao, H., Liu, W., Simmons, B. N., Harris, H. K., Cox, T. C., and Massiah, M. A. (2010) Purifying natively folded proteins from inclusion bodies using sarkosyl, Triton X-100, and CHAPS. *Biotechniques.* **48**, 61–64
21. O'Handley, S. F., Dunn, C. A., and Bessman, M. J. (2001) Orf135 from *Escherichia coli* Is a Nudix Hydrolase Specific for CTP, dCTP, and 5-Methyl-dCTP. *J. Biol. Chem.* **276**, 5421–5426
22. Bessman, M. J. (2019) A cryptic activity in the Nudix hydrolase superfamily. *Protein Sci.* **28**, 1494–1500
23. Frick, D. N., Townsend, B. D., and Bessman, M. J. (1995) A Novel GDP-Mannose Mannosyl Hydrolase Shares Homology with the MutT Family of Enzymes. *J. Biol. Chem.* **270**, 24086–24091

Chapter 3

Exploring the physiological role and regulation of NudL's proposed CoA hydrolase activity

3.1 Introduction

Although the degradation of coenzyme A (CoA) seems like unnecessary expenditure of energy, the cycle of CoA synthesis and degradation have been proven to be efficient in the dynamic control of CoA levels in other organisms (1, 2). While in *Escherichia coli* CoA biosynthesis is well characterized CoA degradation remains largely uninvestigated despite evidence of its existence (3–5). 4'-Phosphopantetheine (PPanSH) is the arguably the most important CoA biosynthesis intermediate as it is also found in the extracellular environment (3, 6). Investigations into CoA regulation, initiated by these findings, found that the source of PPanSH is both from biosynthesis and degradation of CoA (4). In *E. coli*, CoA can be degraded into PPanSH and 3',5'-ADP either by a direct or an indirect mechanism as detailed in chapter 1, figure 1.5, the two enzymes responsible being NudL and AcpH respectively.

Prokaryotic CoA hydrolases must have alternative regulation processes other than the subcellular localization found in their eukaryotic counterparts. Therefore, prokaryotic CoA hydrolases need to be more tightly controlled to avoid a wasteful cycle of CoA synthesis and degradation. Investigation how NudL is regulated is also important for characterization of this enzyme. All Nudix enzymes require a metal cofactor for activity, the most common being the essential nutrients magnesium or manganese. In *E. coli* excess manganese is toxic and hinders growth by inhibiting other metal import systems like iron, and is required at a much lower concentration (7). Manganese does, however, protect against reactive oxygen species (ROS) by functioning as a cofactor to enzymes that break down ROS, by reducing ROS non-enzymatically through complex formation, or by replacing iron in the active site of enzymes to prevent oxidative damage (8–10). In *Deinococcus radiodurans*, CoA hydrolase is speculated to function in restoring the reducing environment that prokaryotes would require after periods of stress (11). Given that in *E. coli* cells manganese utilization is almost exclusively associated with oxidative stress. The apparent preference for this cofactor could be a point of regulation of NudL.

In addition to the regulation of NudL, conditions where CoA degradation plays a role were investigated. In *E. coli* the pool of total CoA, as well as the ratio between free CoA and its thioesters, fluctuates depending on growth conditions and is related to the availability of nutrients, intracellular metabolites, as well as stress exposure (12). When grown on glucose, acetyl-CoA is the major component (79.8%) while the level of free CoA is significantly lower (13.8%) (13, 14). However, CoA becomes the major component (82%) of the CoA pool at the cost of acetyl-CoA in starved cells (15).

Tracking of tritium-labelled metabolites showed that after the decrease in acetyl-CoA/CoA ratio there is an increase in intracellular PPanSH followed by the excretion of PPanSH (4). The changes in the ratio of these metabolites would not trigger ACP turnover as AcpH is equally inhibited by CoA and acetyl-CoA (4). A CoA degrading enzyme, like the putative CoA hydrolase NudL, could account for the rapid hydrolysis of excess free CoA in order to restore the acetyl-CoA/CoA balance and generate PPanSH.

Investigating the CoA degrading ability of NudL in *E. coli* could increase our knowledge on the mechanism in which *E. coli* regulates its CoA levels. In this chapter the studies exploring the CoA hydrolase activity of NudL are reported. This was done by comparing the specific activity of partially pure enzyme to that of *E. coli* lysate. In addition, the physiological relevance of this enzyme was also investigated by comparing the intracellular concentration of CoA and PPanSH in *E. coli* K12, as well as in $\Delta yeaB$ and $\Delta acpH$ knockout strains. Finally, conditions like oxidative stress or alternate carbon sources which could increase NudL's activity in response to these conditions was also investigated to determine the effect on CoA levels.

3.2 Experimental Methods

3.2.1 Materials

All chemicals, reagents, solvents, and media were sourced from Merck (Sigma-Aldrich). Quick start Bradford protein assay kit Bio-Rad was used for protein concentration determination. The HiTrap gel filtration columns were from GE Healthcare. The high-pressure liquid chromatography Supelcosil LC-DP column as well as Superguard LC-DP 2 cm guard column were purchased from Merck (Sigma-Aldrich). Quick-RNA Fungal/Bacterial Miniprep kit (Zymo research). ProtoScript® II First Strand cDNA Synthesis Kit and Luna universal qPCR kit (New England Biolabs). The *E. coli* K12 strain was obtained from New England Biolabs. Mutant strains JW1802 ($\Delta yeaB$) and JW0394 ($\Delta acpH$) were obtained from National BioResource Project (NIG, Japan).

3.2.2 Confirmation of NudL's CoA hydrolase activity

3.2.2.1 Lysate preparation and protein purification for activity confirmation

Large scale batch expression of NudL was performed as per the optimal conditions determined in the expression trials described in Chapter 2. Briefly, a single colony of BL21(DE3) transformed with pET28a-NudL was picked from a Luria-Bertani (LB) agar plate and used to inoculate 2×5 mL LB media containing 30 mg/L kanamycin. Each of the cultures were grown overnight at 37 °C and used to inoculate 2×500 mL LB media containing 30 mg/L kanamycin. The cultures were grown until the optical

density at A_{600} reached ± 0.6 . The cultures were induced with 0.1 mM IPTG and incubated with shaking overnight at 18 °C. Simultaneously, BL21 (DE3) cells without the overexpression plasmid were grown up in LB without antibiotic to $OD_{600} = 0.6$ at 37 °C and then the temperature was lowered to 18 °C before growing overnight with shaking. Cells were harvested by centrifugation for 20 min at 11305 x g. The supernatant was discarded, and the pellet was resuspended in 10 mL buffer A6 (25 mM Tris-HCl, 5 mM NaCl, pH 8.0) per gram of wet cell mass. The cells were lysed by sonication and the cell lysate was harvested by centrifugation for 20 mins 48298 x g at 4 °C. The supernatant was filtered through a 4.5 μm filter prior to being desalted.

The Immobilised metal affinity chromatography (IMAC) purified samples, prepared with the His-Select Nickel affinity gel as per the method described in section 2.2.5.1, was then loaded on a 5 mL HiTrap desalting column equilibrated with 25 mM Tris-HCl, 5 mM NaCl, pH 8.0. This step was done to remove the imidazole and salts, or in the case of lysate any other contaminating small molecules. 5 % Glycerol was added to the desalted fraction containing highest protein concentration, highest UV 280 nm absorbance. The lysate used for activity testing was also desalted with the same method. The protein concentration was determined with the Quick Start Bradford Protein Assay Kit (Bio-Rad)

3.2.2.2 Sample preparation for activity analysis

The CoA hydrolase activity of NudL was assayed by monitoring the degradation of CoA and the formation of PPanSH by HPLC analysis. The reaction mixtures contained 50 mM Tris-HCl pH 7.4, 5 mM tris(2-carboxyethyl) phosphine (TCEP), 5 mM or 1 mM or 0.1 mM of either MgCl_2 or MnCl_2 , and 0.5 mM CoA. The reaction was then initiated with the addition of either 5 $\mu\text{g}/\mu\text{L}$ partially purified NudL or a lysate with a maximum of 25 μL per 50 μL . Time course assays were scaled up 6 times with a total volume of 300 μL . Control reactions were set up in the same manner but with the addition of Milli-Q water instead of enzyme/lysate to make up the final reaction volume to 50 μL . Reactions were incubated at 37°C, and 50 μL aliquots were taken at set time intervals of 5, 10, 20, 40 and 60 minutes. The reaction in a 50 μL aliquot was stopped by addition of 10 μL of 90 % (w/v) trichloroacetic acid (TCA), and the solution was then neutralized with 40 μL of 2.25 M NH_4OAc . Samples containing Mn^{2+} were incubated for an additional 10 minutes with 200 mM EDTA, 20 mM Tris-HCl pH 7 to remove excess Mn^{2+} , as this interfered with the analysis (by quenching the fluorescence signals of the derivatized analytes). The precipitated proteins were removed by centrifugation at 9503 x g for 10 min. The supernatant was removed, and a 7 μL of the aliquot was reserved for derivatization with 7-diethylamino-3-(4'-maleimidylphenyl)-4-methylcoumarin (CPM.) The derivatization mixture contained 21 μL MeCN, 1.3 μL CPM (10 mM in MeCN) and the 7 μL supernatant aliquot, made up to a

total volume of 70 μL with Milli-Q water. The derivatization mixture was then incubated overnight at room temperature.

3.2.2.3 High Performance Liquid Chromatography (HPLC) analysis

Samples were analysed by HPLC as described previously (16). Prior to HPLC analysis, the derivatization mixtures were centrifuged at $16\ 060 \times g$ for 10 min and 35 μL of the supernatant was removed for HPLC analysis. HPLC analysis was performed on an Agilent 1100 series system equipped with an in-line UV and fluorescent detector using a Supelcosil™ LC-DP (250 mm \times 4.60 mm, 5 μm particle size) reverse phase column protected with a Supelguard™ LC-DP cartridge. Analysis was performed using a ternary solvent system that consisted of Milli-Q water (solvent A), 50 mM potassium phosphate buffer, pH 6.8 (solvent B), 100% acetonitrile (solvent C) and 60% aqueous acetonitrile (solvent D). The separation method was executed as previously published (16).

Separation was monitored using fluorescence (E_m 465 nm, E_x 387 nm) of CPM. The peak areas were integrated for comparison to calibration curves prepared using pure CoA and PPanSH to quantify the concentration of the respective analytes. The CoA and PPanSH calibration curves were set up with a concentration range of 1 μM to 50 μM . The standards were used for quantification as well as determining the retention times of the specific analytes.

3.2.2.4 Optimization of Mn^{2+} fluoresce HPLC assay

Various methods were tested to alleviate the quenching of the derivatized analyte's fluorescence signal by Mn^{2+} . For the optimized method, the reaction mixtures contained 50 mM Tris-HCl pH 7.4, 5 mM TCEP, 1 mM or 0.1 mM MnCl_2 , 0.5 mM CoA with Milli-Q water added to make up a final reaction volume of 50 μL . The control reaction contained MgCl_2 instead of MnCl_2 . The reactions were incubated at 37 °C for 10 minutes, before being stopped by addition of 10 μL of 90 % (w/v) TCA. The acidified reaction was added to a pre-weighed amount of cation exchange resin equal to 1.5 or 2 equivalents of the total cation concentration. The resin was added in excess of the cation concentration as to maximize Mn^{2+} removal. The two cation exchange resins used were Dowex 50W-X8 200-400 mesh and Amberlite IR120, both in their hydrogen form. The reaction mixtures were incubated with the respective resin for 10 minutes. The resin was removed by centrifugation at $9503 \times g$ for 10 min. A 30 μL aliquot of the supernatant was then neutralized with 20 μL of 2.25 M NH_4OAc . The reaction mixtures were centrifuged again with the same conditions. Samples marked for Mn^{2+} removal with ethylenediamine tetra-acetic acid (EDTA) were neutralized immediately after acidification with 40 μL

of 2.25 M NH_4OAc . This was followed by an additional incubation of 10 minutes with 10 μL EDTA solution (200 mM EDTA, 20 mM Tris-HCl pH 7). Samples were centrifuged at $9503 \times g$ for 10 min. An aliquot of 7 μL of the remaining supernatant was used for derivatization with CPM and analysed by HPLC as described above.

3.2.3 Determination of intracellular CoA and PPanSH levels in *E. coli*

E. coli strains K12, JW1802 (ΔyeaB) and JW0394 (ΔacpH) were cultured in the same manner. For each of the strains a single colony was used to inoculate 7 mL of LB medium that was subsequently incubated overnight at 37 °C with shaking at 180 rpm. The overnight inoculum was diluted 1:100 with LB medium and cultures were grown at 37 °C. Two 45 mL aliquots of culture were removed when growth reached exponential phase ($\text{OD}_{600} = 0.6$), and the cells were pelleted by centrifugation at $4500 \times g$ at 4 °C for 20 mins. The pellets were washed twice with 45 mL cold, sterile phosphate-buffered saline (PBS) (NaCl 137 mM, KCl 2.7 mM, Na_2HPO_4 10 mM, KH_2PO_4 1.8 mM pH 7.6) by resuspension followed by centrifugation with above conditions. The washed pellets were then resuspended in the remaining PBS and transferred into pre-weighed 1.5 mL microcentrifuge tubes. The cells were centrifuged again for 5 min at $16\ 060 \times g$, and the supernatant was carefully removed and discarded. The pellets allocated for dry cell mass determination were dried on a SpeedVac for 18 hours. The pellets earmarked for extraction were resuspended in 50 μL per 20 mg wet cell mass of extraction solution (80% (v/v) MeCN, 0.1 M formic acid and 100 mM TCEP). The resuspended pellets were then mixed by rotation at 4 °C for 30 minutes. The supernatant containing the extracted metabolites was carefully removed after separation from cell debris by centrifugation at $16060 \times g$ for 5 minutes. The supernatant was then filtered through 0.22 μm syringe filters. The samples were then neutralized with a Tris-HCl buffer, the mixture contained 22.31 μL of the filtered extract, 50 mM Tris-HCl pH 7.6 and 1 mM TCEP made up to a final volume of 66.85 μL with Milli-Q water. The neutralized extracts were incubated at 10 minutes at room temperature prior to being derivatized with 3.15 μL CPM (10 mM in MeCN) to a final concentration 450 μM . The derivatization mixture was then incubated overnight at room temperature. Finally, 5 μL of the derivatized extracts were analysed HPLC, using the method described above (16).

3.2.4 RT-qPCR analysis of *yeaB* transcription during oxidative stress and other stress conditions

E. coli K12 cells were grown in LB media until late stationary phase. The pellet was then washed twice with sterile PBS. Cells were resuspended in PBS either with or without 10 mM H_2O_2 for 2 hours at 37

°C. RNA was isolated from flash frozen culture with Quick-RNA Fungal/Bacterial Miniprep kit (Zymo research). The cDNA was synthesized from the RNA with ProtoScript® II First Strand cDNA Synthesis Kit (New England Biolabs). mRNA levels were quantified in quintuplicate by RT-qPCR using the Luna universal qPCR kit (New England Biolabs) on a StepOne™ Real-Time PCR System. For the analysis, the following primers were used: 5'-ATCTGCGTAAACACGCTGGA-3' (forward) and 5'-GGCGGTATAGCGACCTCTTC-3' (reverse). The relative abundance was calculated by the C_T method using the average C_T values of one calibrator, 16S rRNA, using primers 5'-TATCCTTTGTTGCCAGCGGT-3' and 5'-CTCCAATCCGGACTACGACG-3' for the forward and reverse primer, respectively.

3.2.5 Growth rate analysis with different carbon sources

E. coli strains were grown (in two replicates) in 5 mL LB media at 37 °C with shaking at 180 rpm for 18 hours. The cells were washed twice with minimal media (M9) (Na_2HPO_4 20g/L, KH_2PO_4 12.8 g/L, NH_4Cl 1 g/L, NaCl 0.5 g/L, MgSO_4 2mM, pH 7.4) without any carbon source. The cells were then resuspended and diluted to 1:100 into fresh minimal media supplemented with either 0.4 % glucose or 1.2 % acetate before 250 μL aliquots of the culture were seeded to a 96-well plate. The plate was placed in a humidity chamber and the OD_{600} was monitored automatically every hour for 24 hours at 37 °C in a Tecan Spark Multimode Microplate reader to generate growth curves.

The growth rates of the individual *E. coli* strains were determined in LB media. Cultures grown overnight (18 hours) (two replates of each strain) at 37 °C with shaking at 180 rpm were diluted 1:100 into fresh LB media. The cultures were then grown at 37 °C with shaking. At set time intervals of 60 minutes the optical density was monitored at 600 nm. Colony Forming Units (CFUs) were determined by serially diluting cultures in PBS to 1:10⁷, in triplicate. Aliquots (20 μl) of the serial dilutions were then spot plated on square LB agar plates. CFU were quantified after plates were incubated for 18 hours at 37 °C.

3.3 Results and discussion

3.3.1 Confirming the CoA hydrolase activity of NudL

The confirmation of NudL's CoA hydrolase activity was complicated by the apparent instability of the enzyme, and since purity and yield remained an issue for the overexpressed enzyme, as detailed in Chapter 2. It was therefore decided that for all the characterizations lysate obtained from the overexpression strain (*E. coli* BL21 (DE3) transformed with the overexpression plasmid pET28a-NudL) would be used as to minimize the handling of the protein. However, the partially purified protein

would be used to allow for comparison of the specific CoA hydrolase activity found in lysate with and without the overexpressed NudL.

For the activity analysis, a previously established HPLC method would be used to quantify the decrease in CoA, the substrate, and the increase in PPanSH, the product. The assay is based on the derivatisation of thiol moieties present in CoA and PPanSH with CPM a fluorescent thiol probe

3.3.1.1 Overcoming assay interference by Mn^{2+} induced fluorescence quenching

While Mn^{2+} was predicted to be required for enzyme activity, its inclusion in the assay was found to result in quenching the fluorescence signals of the CPM-derivatized thiols. A number of attempts were made to counter this effect and recover the fluorescence signals. The conditions tested included the use of ion exchange resins, Dowex 50W-X8 200-400 mesh and Amberlite IR-120 hydrogen form, as well as EDTA in different equivalents to remove the interfering Mn^{2+} prior to analysis. Lowering the concentration of Mn^{2+} ions in the reaction mixture was also tested. Both of the ion exchange resins chosen are cation exchange resins that would remove the Mn^{2+} ions as well as any other cations in the reaction mixture. The cations in solution bind the insoluble resin beads and are physically separated when the resin is removed from the supernatant. Cation exchange resin beads can have different anionic functional groups and mesh sizes. Dowex 50W-X8 200-400 mesh and the Amberlite resin have sulfonic acid functional groups but have a slightly different total exchange capacity, 1.7 meq/mL and 1.8 meq/mL respectively. EDTA is chelating ligand which binds to metal cations like Mn^{2+} to form a strong metal-EDTA complex. The result is that Mn^{2+} ions are then no longer free in the reaction mixture to interfere with the fluorescence assay.

To test the impact of these methods, the CoA peak areas were used to quantify the apparent amount of CoA in the sample. This was then compared to a control containing 500 μ M CoA and 5 mM Mg^{2+} , which had no quenching effect. Since each reaction contained the same amount of CoA as the control, the lower the apparent CoA concentration in the sample the greater the amount of quenching observed. Figure 3.1 shows a summary of all the attempts to recover the fluorescence signal. From this result it was concluded that the quenching was proportional to the Mn^{2+} concentration. The greatest recovery was observed when 2 equivalents of Amberlite IR-120 cation exchange resin was added to the reaction mixture. Although the addition of Amberlite seemed like a promising solution, the volume recovered after acid precipitation of the proteins was found not to be sufficient for further analysis. The addition of 20 mM EDTA also showed near full recovery for samples with 0.1 mM and 1 mM Mn^{2+} . It was therefore decided that the EDTA method would be used prior to analysis of the reactions containing Mn^{2+} .

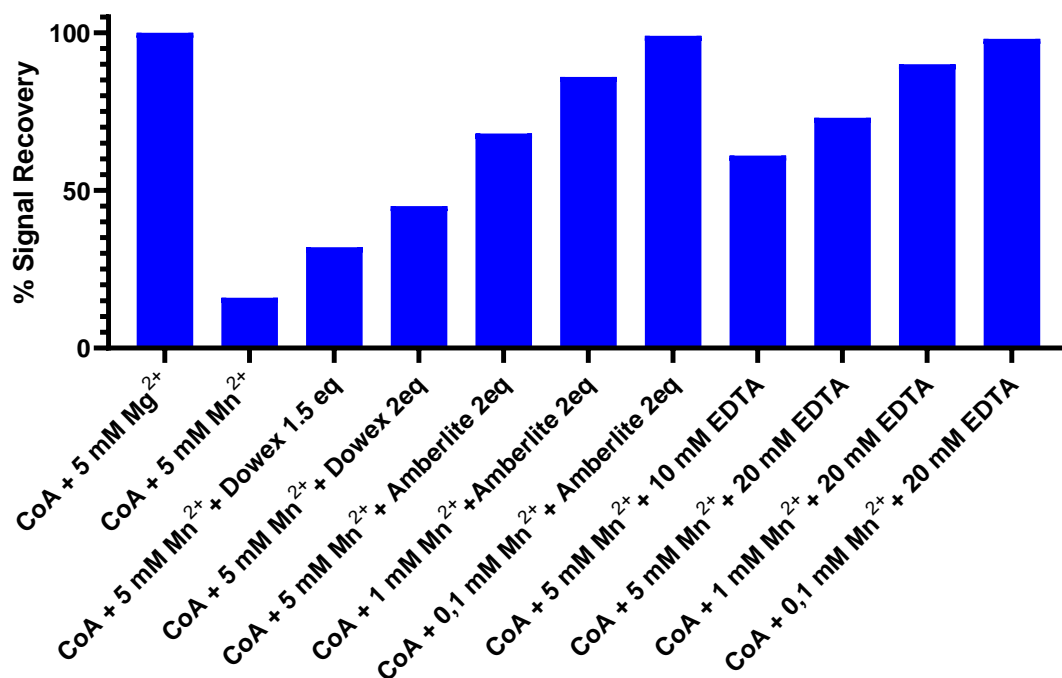


Figure 3.1. Summary of attempts to recover fluorescence signals. % signal recovery is a ratio of the apparent CoA peak area in the sample to the peak area of 0.5 mM CoA in the control with no quenching. Concentration of EDTA refers to final concentration in the reaction mixture and eq refers to number of equivalents of the cation exchange resin. n=1 and no technical replicates.

3.3.1.2 CoA hydrolase activity in lysates overexpressing NudL

Plain *E. coli* lysate (not overexpressing NudL) do not have detectable CoA-degrading activity (Table 3.4) therefore the CoA hydrolase activity present in desalted *E. coli* lysate overexpressing NudL was investigated. For these investigations, the following tests were conducted. To confirm that residual intracellular CoA and PPanSH was first removed with the desalting step, the lysate was incubated in the absence of any added substrate for 1 hour and then analyzed with the HPLC CPM assay. Neither CoA nor PPanSH could be detected in the sample (Figure. 3.2A). Next, to confirm that CoA remains stable in lysate, and that any observed CoA degradation was only due to NudL, desalted lysate and 0.5 mM CoA were incubated in the absence of any added metal cofactor for 1 hour. Subsequent analysis showed that the CoA concentration did not decrease compared to the control and no PPanSH formation was detected (Figure. 3.2A). Without the presence of metal cofactor CoA remained stable. Following this, the preferred metal cofactor for supporting CoA hydrolase activity was investigated. For these tests, activity was monitored by determining the formation of PPanSH, rather than the decrease in the substrate, CoA. There still appeared to be some quenching of the fluorescence signals and it was not clear if the decrease in CoA peak area was due to NudL activity or quenching.

Quantifying the remaining CoA seemed less reliable than quantifying the amount of PPanSH formed as there appeared to be a large variation between lysate batches. The detected activity was therefore normalized to the amount of protein in the sample as well as the incubation time. It was found that PPanSH formation was not quantifiable in lysate with only 0.1 mM Mn^{2+} or Mg^{2+} (data not shown); this could be due to the metals also being sequestered by other proteins. Nonetheless, CoA hydrolase activity was detected for both metals at a high concentration (5 mM), although Mn^{2+} clearly is the preferred cofactor. Taken together the lack of activity in the absence of a metal cofactor confirms that CoA degradation was dependent on a metal cofactor and that NudL like all other Nudix enzymes requires a metal cofactor for activity (17). However, 5 mM is also much greater than the normal physiological concentration of Mn^{2+} found in *E. coli* cells, which typically have an intracellular concentration of 5 -15 μM for Mn^{2+} (although it can withstand concentrations as high as 50 μM (18)). The normal range for free Mg^{2+} is 1-2 mM (19). Based on the initial test, a Mn^{2+} concentration was 1 mM selected for further activity assays, to minimize quenching and to be closer to the physiological range of this metal. We found that the specific activity determined with 1 mM Mn^{2+} was 6-fold greater than that observed for Mg^{2+} (Figure. 3.2B). Such a strong preference for Mn^{2+} has only been observed for Nudt8 (1). However, it is unclear what the significance of a manganese preference is, and whether it is tied to the regulation of the enzyme, whether it is linked to a specific substrate or whether it is inconsequential.

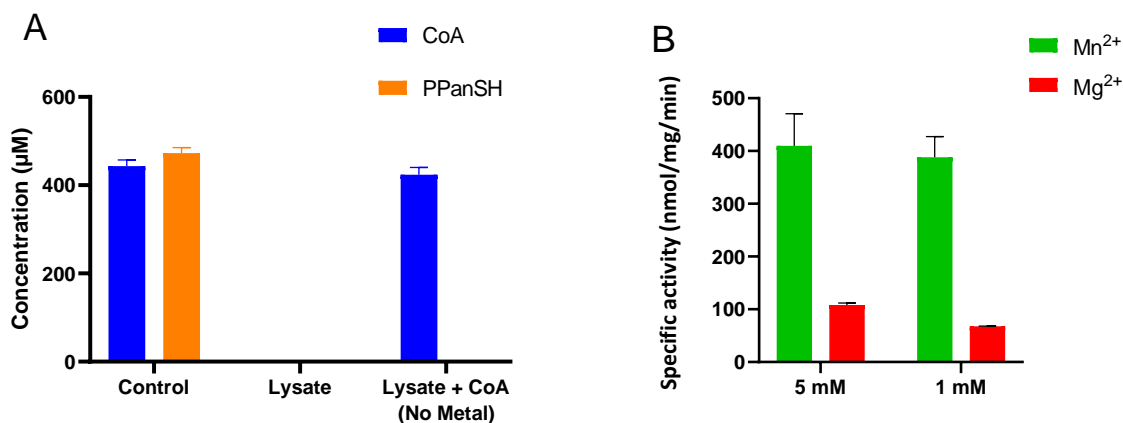


Figure 3.2. CoA hydrolase activity in lysate obtained from cultures overexpressing NudL. (A) The stability of compounds in the lysate was tested by confirming that no metabolites remained in the sample after desalting and that CoA concentration remained constant in the absence of a metal cofactor. Reactions were incubated for 1 hour. CoA displayed in blue and PPanSH displayed in orange. The control reactions were either 0.5 mM CoA or PPanSH, these samples did not experience any quenching. Bars represent the results of two-independent experiments (i.e. n = 2); error bars represent SEM (B) The effect of metal ions on NudL specific activity as represented by the rate of formation of PPanSH (product peak area) per mg protein per min. Reactions with Mn²⁺ indicated in green and reactions with Mg²⁺ indicated red. Reaction mixtures contained 50 mM Tris-HCl pH 7.4, 5 mM TCEP, 5 mM or 1 mM of either MgCl₂ or MnCl₂, 0.5 mM CoA and 25 µL of desalted lysate. Bars represent the average of three independent experiments (i.e. n = 3) and error bars represent SEM.

3.3.1.3 Purification of the CoA hydrolase activity in lysates overexpressing NudL

Seeing that the CoA hydrolase activity showed a distinct preference for Mn²⁺ as the metal cofactor, this information could be used to provide evidence that the CoA hydrolase activity is associated with NudL. This was done by determining the CoA hydrolase activity in the presence of 1 mM Mn²⁺ in various backgrounds. This included lysate from *E. coli* BI21(DE3), overexpressing and not overexpressing NudL, as well as the NudL partially purified as explained in Chapter 2. The results of this comparison are shown in Table 3.1.

Table 3.1. Comparison of CoA hydrolase activity in various backgrounds ^a

Purification step	Protein (mg)	Activity (nmol/ min)	Specific activity (nmol/min/mg)	Yield (%)	Purification (fold)
Lysate from <i>E. coli</i> BL21(DE3) cells	237	nd	nd	—	—
Lysate from BL21(DE3) overexpressing NudL	138	0.23	0.002	100	1
NudL partially purified by IMAC	0.14	0.12	0.862	0.1	517

^a Pellets from 1L batch expression grown with the optimum conditions determined in chapter 2. Protein concentration was determined after desalting 1 mL of lysate or purified protein.

CoA hydrolase activity was not detected in the *E. coli* lysate without overexpressed Nud; this could be because the native relative abundance of NudL is too low for detectable activity. However, CoA hydrolase activity was observed in the lysate from *E. coli* in which NudL was overexpressed. This provides strong evidence that NudL is responsible for the CoA hydrolase activity in *E. coli*. This is further supported by the increase in specific activity seen for the partially purified sample. Despite the low protein yield after IMAC purification (see chapter 2), the specific activity was increased 517-fold. In both cases, the increased CoA degradation can be linked to the increased relative abundance of NudL in the sample.

Throughout the expression, purification, and activity confirmation studies it became evident that NudL is not a very stable protein, as PPanSH formation from CoA was not detected in samples (either partially purified NudL, or lysates) that had been prepared previously, flash frozen and stored appropriately at -80 °C with glycerol. This apparently short half-life could be tied to a requirement that NudL is only active for a short period to rapidly alter the CoA pool after a metabolic switch.

3.3.2 Metabolomic studies

As stated in Chapter 1, in *E. coli* there are two possible mechanisms by which CoA is degraded into PPanSH, a direct and indirect mechanism. The two enzymes responsible are NudL and AcpH respectively. To determine which of these two enzymes has a greater influence on CoA degradation, and consequently on the intracellular levels of CoA and PPanSH, a reference *E. coli* strain (K12) and mutant strains in which the genes expressing these enzymes have been knocked-out were investigated. For these studies the cells were grown to specific growth phase and two aliquots were taken. The first was used to determine the dry cell mass, which was used to normalise the

concentration of metabolites measured in the extraction to the number of cells (reporting the metabolite amount as pmol/mg dry cell weight). This was done so that the results from different growth phases — as well as from the different strains — can easily be compared. The second aliquot was then used to perform the metabolite extraction, which was then analysed with the same CPM-labelling HPLC assay as was used for the activity assay.

3.3.2.1. Metabolomic studies: the relative importance of NudL and AcpH on CoA levels.

The exact amounts of the metabolites were determined at exponential phase for all three strains. In the *E. coli* K12 strain, the amount of PPanSH was greater than the amount of CoA; however, due to the limited number of replicates the statistical significance of this difference cannot be confirmed at this stage (Figure. 3.3). For the knockout strains — where one of the mechanisms for CoA degradation is blocked — one would expect an increase in the amount of CoA, as well as a decrease in the amount of its degradation product, PPanSH. Indeed, this was observed to be the case for both the $\Delta yeaB$ strain (JW1802) and the $\Delta acpH$ strain (JW0394) (Figure. 3.3). The amount of intracellular PPanSH in the $\Delta acpH$ strain was 255 ± 6 pmol/mg dry cell weight, which was approximately half that found in the K12 strain. The $\Delta yeaB$ strain had the least amount of intracellular PPanSH with 83 ± 9 pmol/mg dry cell weight (Figure. 3.4). In the $\Delta yeaB$ strain, both biosynthesis and AcpH are the main contributors to the intracellular PPanSH pool, while in the $\Delta acpH$ strain biosynthesis and NudL mainly contributes to the intracellular PPanSH pool. Interestingly, the intracellular CoA levels in both knockout strains were similar: 567 ± 119 pmol/mg dry cell weight and 574 ± 138 pmol/mg dry cell weight for the $\Delta yeaB$ and the $\Delta acpH$ strains respectively. These levels are slightly elevated compared to the CoA levels in the K12 strain, suggesting that under conditions of reduced CoA degradation, there might be a build-up of CoA. A study characterizing AcpH in *E. coli* stated that PPanSH excretion by the $\Delta acpH$ strain was significantly reduced (20). Considering the intracellular levels of these metabolites, it appears that of the two enzymes, NudL contributes more to PPanSH formation. However, the extent of PPanSH export by the $\Delta yeaB$ strain will need to be investigated before a definitive conclusion can be made in this regard.

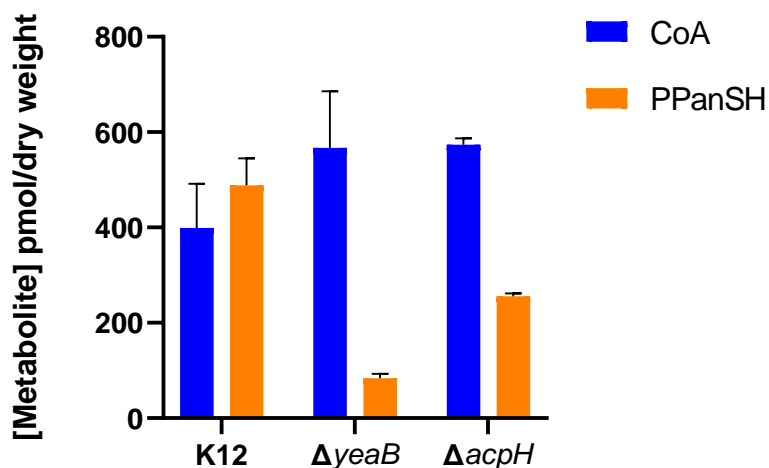


Figure 3.3. Determination of CoA and PPanSH levels in different *E. coli* strains grown to exponential phase ($OD_{600} = 0.6$). The three strains tested were: *E. coli* K12; JW1802 ($\Delta yeaB$), JW0394 ($\Delta acpH$). Bars representing CoA coloured blue and those indicating PPanSH coloured orange. Each bar represents the average of two independent repeats (i.e. $n = 2$), each performed in technical triplicates. The error bars show the data range.

The amount of CoA in *E. coli* reference strains and strains derived from these have been quantified in previous studies. Some of the first metabolomic studies in the 1980s measured the intracellular CoA concentration in *E. coli* using a radioisotope labelling method (13). Converting the amounts determined in this study from pmol/ mg dry cell mass to concentration, using a ratio of wet cell volume to dry weight of 0.0023 L/g (21) indicates that the intracellular concentration of CoA at exponential phase was 173 μM ; this is higher than what was previously found with CoA levels at exponential phase ranging between 30 μM and 118 μM depending on the carbon source (13).

Metabolomic studies conducted later made use of a CoA cycling method. For this method each metabolites is measured separately using a cycle of enzymatic conversions (22). The free CoA is converted to acetyl-CoA in the presence of acetyl-phosphate (acetyl-P) by phosphate acetyltransferase. Acetyl-CoA and malonate are enzymatically converted to malonyl-CoA by malonate decarboxylase (MD). The same enzyme decarboxylates malonyl-CoA back to acetyl-CoA, this then serves as the CoA donor for the next cycle. The acetate generated is proportional to amount of acetyl-CoA from the initial CoA added. The acetate is quantified by a spectrometric indicator reaction whereby acetate kinase phosphorylates acetate to acetyl-P, which is monitored spectrophotometrically as acetoxyacetate. This method claims to be sensitive to sudden changes in the total CoA pools (22). CoA levels were not constant throughout the growth phases and had a maximum of 300 μM at exponential phase; however, CoA levels decreased to 112 μM at late exponential phase (22). The CoA concentration determined for the K12 in this study falls within that range.

3.3.2.2. Metabolomic studies: NudL's relative importance during growth

E. coli's energy requirements — and its need for CoA — varies during its various growth phases (22). We hypothesized that the CoA hydrolase activity may therefore be relevant in modifying the cell's CoA/PPanSH ratio in response to these changes. Seeing that the NudL mutant had the greatest effect on the CoA/PPanSH ratio in the exponential phase, the ratio in the stationary phase was also investigated to determine NudL's relative importance under these conditions. Interestingly, the results showed that the ratio remained in a similar range for the two growth phases for both the K12 reference and the $\Delta yeaB$ strain (Figure. 3.4). However, as would be expected from NudL's role as a CoA hydrolase, in its absence the CoA/PPanSH ratio was increased more than 4-fold. Since the CoA/PPanSH ratios did not appear to differ much between growth phases, only exponential phase was looked at for further metabolomic studies.

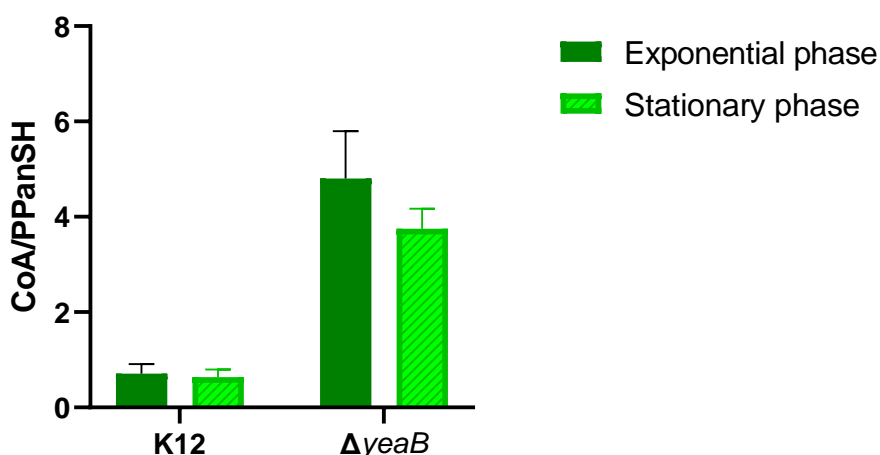


Figure 3.4. Determination of intracellular CoA/PPanSH ratios in *E. coli* K12 and $\Delta yeaB$ (JW1802) strains at exponential phase ($OD_{600} = 0.6$) and stationary phase ($OD_{600} = 1.7$). Cultures were grown in LB media at 37 °C. Exponential phase in deep green and stationary phases in light green. Bars represent one experiment (i.e. n = 1) performed in technical triplicates, with the error bars represent the standard deviation.

3.3.3 Investigating the physiological relevance of NudL

One of the research questions that this project aimed to answer was whether the CoA hydrolase activity of NudL provided a fitness advantage under different metabolic stress conditions, by allowing for a quick switch in the CoA levels. To investigate this question further, the transcription of *yeaB* (mRNA levels) were determined by RT-qPCR under various stress conditions. The first condition tested was that of an oxidative environment. Oxidative stress was investigated because the preferred metal for NudL is Mn^{2+} , and Mn^{2+} utilization is associated with oxidative stress and is known to support the

detoxification of ROS (18). An additional consideration was that in *Mycobacterium smegmatis* protein expression of its NudL homologue was detected during oxidative stress with immunoblot analysis (23).

Late stationary phase cultures were treated for 2 hours with and without oxidative stress (10 mM H₂O₂) in PBS. NudL expression seemed to be unaffected by oxidative stress when compared to the untreated control (Figure. 3.5).

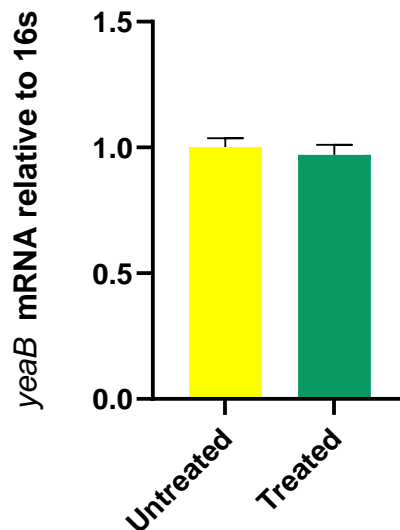


Figure 3.5. Abundance of the *yeaB* mRNA transcript in *E. coli* K12 cells at late stationary phase, with and without oxidative stress. Untreated cells were resuspended in PBS, while treated cells were resuspended in PBS with 10 mM H₂O₂, following which cells were incubated for 2 hours. Bars represent the mean of five independent experiments (i.e. n=5), each performed in technical triplicates and error bars represent SEM.

The second condition investigated was the effect of carbon source, as CoA levels are known vary on carbon source (13). A study by Chohnan et al. looked at the fluctuations in the total CoA pool for *E. coli* with different carbon sources. From these studies carbon sources were identified where either free CoA levels decreased and/or the total CoA pool decreased. This infers that CoA broken down into presumably PPanSH would not re-enter the CoA pool as it (PPanSH) is irreversibly exported and cannot serve as a source for new CoA (3). The two carbon sources chosen for these experiments were glucose and acetate. Glucose was chosen as a reference, and acetate was chosen as the total CoA pool when acetate is the carbon source is half that observed with glucose. In addition, the percentage composition of free CoA doubles (13). All the three strains tested were grown at 37 °C in a humidity chamber with the relevant carbon source. In the presence of 0.4% glucose, the knockout strains grew to a higher OD₆₀₀ but grew at the same rate, reaching stationary phase at ~10 hours (Figure. 3.6A). This suggests that there are no differences in growth rate and that CoA degradation either via NudL or AcpH does not have a significant effect on growth on glucose. With acetate as the carbon source,

the cells did not grow on 0.4 % therefore the concentration of acetate was increased to 1.2 % (data not shown). All the strains grown on acetate grew considerably slower compared to the rates of growth on glucose (Figure. 3.6B). K12 cells had the fastest growth rate suggesting that CoA degradation (i.e., the ability to limit CoA levels) is required for metabolism on acetate. This is because with acetate as a carbon source ATP is required to convert the acetate to acetyl-CoA; CoA degradation would therefore be required to regulate the rate of acetate consumption when ATP levels are low (14). The $\Delta acpH$ strain grew the slowest and $\Delta yeaB$ grew at the same rate as $\Delta acpH$ until ~ 10 h, i.e., where exponential phase started. The $\Delta yeaB$ still grew significantly slower than the reference K12 strain. Based on the growth curves, the doubling time for the strains grown in LB media were 25 minutes for K12, 44 minutes for JW1802, and 45 for JW0394 ($\Delta acpH$), suggesting that CoA degradation might also be required for optimal growth in LB media.

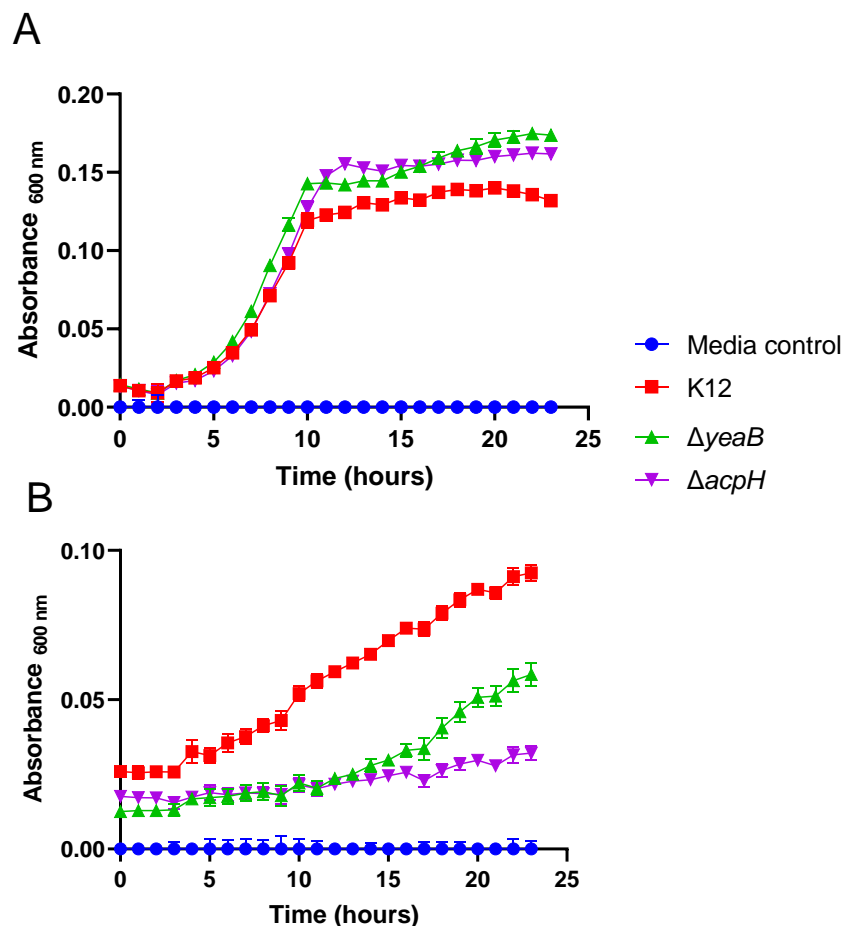


Figure 3.6. Growth curves of *E. coli* K12; JW1802 ($\Delta yeaB$), JW0394 ($\Delta acpH$) in minimal media with different carbon sources. Growth was monitored at 600 nm using a Tecan Spark Multimode Microplate reader (A) Growth curves with 0.04 % glucose as the carbon source. (B) Growth curves with 1.2 % acetate as the carbon source. Growth curves represent the mean of two independent experiments (i.e. $n = 2$), each done in technical triplicate. The error bars represent SEM.

3.4 Conclusion

In this chapter results were described confirming the presence of a CoA hydrolase activity in *E. coli* lysates, and with partially purified NudL protein. NudL is the third putative prokaryotic CoA hydrolase to be experimentally validated, the first two being the enzymes from *Deinococcus radiodurans* and *Mycobacterium smegmatis* (23, 24). The identification of the diphosphatase activity with CoA as substrate is the first step in determining the biological role of this enzyme in the regulation of CoA levels in *E. coli*.

CoA hydrolase activity was not detectable in lysate without NudL overexpression and the partially purified NudL fraction had a 517-fold increase in specific activity. This provides strong evidence that NudL is responsible for the observed CoA hydrolysis. Moreover, NudL seemed to exclusively prefer Mn^{2+} over Mg^{2+} ; only Nudt8 has the same distinction (1). No hydrolase activity was observed in the absence of a metal cofactor which further provides evidence of a Nudix enzyme being responsible for the observed activity (17). The majority of CoA hydrolases characterized to date showed activity with both divalent metal cations and with Mg^{2+} as the preferred cation. It is unclear as of yet if CoA is the relevant and/or preferred substrate, as initial rate kinetics will have to be performed with related substrates like acetyl-CoA, which forms a major part of that total CoA pool. In future studies one would need to investigate whether the metal preference provides greater substrate selectivity or some other regulatory role.

In *E. coli*, PPanSH is found in high levels both inside the cell and in the extracellular environment (3). The source of these PPanSH pools is thought to be from biosynthesis and the degradation of CoA. The two mechanisms which CoA is broken down into PPanSH in *E. coli* is directly via NudL and indirectly via AcpH. Metabolomic studies were done on the intracellular concentration of CoA and PPanSH in a reference and two mutant strains. The $\Delta yeaB$ and $\Delta acpH$ strains both had considerably less intracellular PPanSH when compared to the K12 reference strain. The CoA /PPanSH ratio in these two strains were increased more than 5-fold compared to the reference strain. This is what was expected as the knockouts had less CoA degrading ability, resulting in CoA build up and a decrease in the product, PPanSH. The physiological consequence for the loss of a CoA degrading ability was that the generation time of the knockouts were longer than the K12 reference strain. A study by Rock et al. showed that the build-up of CoA in a mutant strain without PanK feedback inhibited by CoA, results in greater intracellular PPanSH and increased export of PPanSH (25). The source of the PPanSH in the medium was found to be from both the biosynthesis pathway and CoA degradation (3). Thomas et al. reported that the $\Delta acpH$ strain had reduced PPanSH export so It would be interesting to see of the elevated CoA levels in $\Delta yeaB$ also has the same effect (20). Therefore, future work could include quantifying the extracellular PPanSH concentration would complement the metabolomics studies reported here.

The next step in determining the biological importance of NudL is to determine how its expression is regulated. The relative mRNA levels determined revealed that H₂O₂ stress does not have an influence on NudL expression in late stationary phase. This was despite of NudL's preferred metal cofactor being Mn²⁺, a metal that's utilization is associated with oxidative stress by the protection against reactive oxygen species (ROS) (10).

In addition, the growth of the reference strain compared to the knockout strains lacking CoA degradation ability was unaffected on glucose. When grown on acetate as a sole carbon source, all strains grew much slower, but the knockout strains grew significantly slower, suggesting that CoA degradation may play a role in growth regulation and overall metabolism under certain conditions as suggested by Vallari et al. (4). In future studies, this hypothesis could be tested experimentally by determining the expression of NudL with acetate as the carbon source.

Since the 1980's a mechanism of CoA degradation into 3'-5' ADP and PPanSH in *E. coli* has been alluded to, but until now no enzyme has been assigned to this activity. This study provides strong evidence that CoA hydrolysis into PPanSH is mediated by NudL. NudL seemed to exclusively prefer Mn²⁺ over Mg²⁺ and it is the second CoA hydrolases to have this distinction, the relevance of this is still to be determined (1). This study also aimed to give insight into the physiological relevance of this enzyme in a prokaryotic context. The metabolomics studies confirmed that CoA degradation mediated either via NudL or AcpH or the combination would account for the majority of the excess intracellular PPanSH as the mutant strains had significantly less intracellular PPanSH as well as slightly elevated CoA levels compared to the reference strain. The NudL mutant having the lowest intracellular PPanSH concentration during normal growth is supported by studies by Vallari et al. that demonstrated PPanSH generated from CoA degradation was not solely mediated by ACP turnover, as ACP turnover is lowest at physiological CoA levels (4, 5). The above-mentioned study also demonstrated that CoA degradation plays a role in rapid changes in metabolism where sudden changes in the acetyl-CoA/CoA ratio triggered CoA degradation (4). The acetate growth curves of the three strains as the mutants seemed to have a considerable growth defect compared to the reference stain. When acetate is the carbon source free CoA increases from 13.8 % of the total CoA pool, when grown on glucose, to 53.6 %, this results in an acetyl-CoA/CoA ratio decrease, the mutant strains would not be able to compensate for this shift (25). In conclusion, NudL is the final *E. coli* Nudix hydrolase to be experimentally validated; however, determining how this enzyme is regulated will be of greater importance to complete the model of CoA regulation in *E. coli*.

3.5 References

1. Kerr, E. W., Shumar, S. A., and Leonardi, R. (2019) Nudt8 is a novel CoA diphosphohydrolase that resides in the mitochondria. *FEBS Lett.* **593**, 1873–3468.13392
2. Shumar, S. A., Kerr, E. W., Geldenhuys, W. J., Montgomery, G. E., Fagone, P., Thirawatananond, P., Saavedra, H., Gabelli, S. B., and Leonardi, R. (2018) Nudt19 is a renal CoA diphosphohydrolase with biochemical and regulatory properties that are distinct from the hepatic Nudt7 isoform. *J. Biol. Chem.* **293**, 4134–4148
3. Jackowski, S., and Rock, C. O. (1984) Metabolism of 4'-phosphopantetheine in *Escherichia coli*. *J. Bacteriol.* **158**, 115–120
4. Vallari, D. S., and Jackowski, S. (1988) Biosynthesis and degradation both contribute to the regulation of coenzyme A content in *Escherichia coli*. *J. Bacteriol.* **170**, 3961–3966
5. Jackowski, S., and Rock, C. O. (1984) Turnover of the 4'-phosphopantetheine prosthetic group of acyl carrier protein. *J. Biol. Chem.* **259**, 1891–1895
6. Jackowski, S., and Rock, C. O. (1981) Regulation of coenzyme A biosynthesis. *J. Bacteriol.* **148**, 926–932
7. Martin, J. E., Waters, L. S., Storz, G., and Imlay, J. A. (2015) The *Escherichia coli* Small Protein MntS and Exporter MntP Optimize the Intracellular Concentration of Manganese. *PLoS Genet.* **11**, e1004977
8. Lisher, J. P., and Giedroc, D. P. (2013) Manganese acquisition and homeostasis at the host-pathogen interface. *Front. Cell. Infect. Microbiol.* **3**, 1–15
9. Anjem, A., and Imlay, J. A. (2012) Mononuclear Iron Enzymes Are Primary Targets of Hydrogen Peroxide Stress. *J. Biol. Chem.* **287**, 15544–15556
10. Sobota, J. M., and Imlay, J. A. (2011) Iron enzyme ribulose-5-phosphate 3-epimerase in *Escherichia coli* is rapidly damaged by hydrogen peroxide but can be protected by manganese. *Proc. Natl. Acad. Sci.* **108**, 5402–5407
11. Kang, L.-W., Gabelli, S. B., Bianchet, M. A., Xu, W. L., Bessman, M. J., and Amzel, L. M. (2003) Structure of a Coenzyme A Pyrophosphatase from *Deinococcus radiodurans*: a Member of the Nudix Family. *J. Bacteriol.* **185**, 4110–4118
12. Bock, C. W., Katz, A. K., Markham, G. D., and Glusker, J. P. (1999) Manganese as a Replacement for Magnesium and Zinc: Functional Comparison of the Divalent Ions. *J. Am. Chem. Soc.* **121**, 7360–7372
13. Vallari, D. S., Jackowski, S., and Rock, C. O. (1987) Regulation of pantothenate kinase by coenzyme A and its thioesters. *J. Biol. Chem.* **262**, 2468–2471
14. Chohnan, S., Izawa, H., Nishihara, H., and Takamura, Y. (1998) Changes in Size of Intracellular Pools of Coenzyme A and Its Thioesters in *Escherichia coli* K-12 Cells to Various Carbon Sources and Stresses. *Biosci. Biotechnol. Biochem.* **62**, 1122–1128
15. Tsuchiya, Y., Zhyvoloup, A., Baković, J., Thomas, N., Yu, B. Y. K., Das, S., Orengo, C., Newell, C., Ward, J., Saladino, G., Comitani, F., Gervasio, F. L., Malanchuk, O. M., Khoruzhenko, A. I., Filonenko, V., Peak-Chew, S. Y., Skehel, M., and Gout, I. (2018) Protein CoAlation and antioxidant function of coenzyme A in prokaryotic cells. *Biochem. J.* **475**, 1909–1937
16. Goosen, R., and Strauss, E. (2017) Simultaneous quantification of coenzyme A and its salvage pathway intermediates in in vitro and whole cell-sourced samples. *RSC Adv.* **7**, 19717–19724

17. Kraszewska, E. (2008) The plant Nudix hydrolase family. *Acta Biochim. Pol.* **55**, 663–671
18. Zeinert, R., Martinez, E., Schmitz, J., Senn, K., Usman, B., Anantharaman, V., Aravind, L., and Waters, L. S. (2018) Structure–function analysis of manganese exporter proteins across bacteria. *J. Biol. Chem.* **293**, 5715–5730
19. Tyrrell, J., McGinnis, J. L., Weeks, K. M., and Pielak, G. J. (2013) The Cellular Environment Stabilizes Adenine Riboswitch RNA Structure. *Biochemistry.* **52**, 8777–8785
20. Thomas, J., and Cronan, J. E. (2005) The Enigmatic Acyl Carrier Protein Phosphodiesterase of *Escherichia coli*. *J. Biol. Chem.* **280**, 34675–34683
21. Bennett, B. D., Yuan, J., Kimball, E. H., and Rabinowitz, J. D. (2008) Absolute quantitation of intracellular metabolite concentrations by an isotope ratio-based approach. *Nat. Protoc.* **3**, 1299–1311
22. Chohnan, S., and Takamura, Y. (1991) A Simple Micromethod for Measurement of CoASH and Its Use in Measuring Intracellular Levels of CoASH and Short Chain Acyl-CoAs in *Escherichia coli* K12 Cells. *Agric. Biol. Chem.* **55**, 87–94
23. Kapoor, I., Varada, R., Aroli, S., and Varshney, U. (2019) Nudix hydrolases with Coenzyme A (CoA) and acyl-CoA pyrophosphatase activities confer growth advantage to *Mycobacterium smegmatis*. *Microbiology.* **165**, 1219–1232
24. Xu, W., Shen, J., Dunn, C. A., Desai, S., and Bessman, M. J. (2001) The Nudix hydrolases of *Deinococcus radiodurans*. *Mol. Microbiol.* **39**, 286–290
25. Rock, C. O., Park, H.-W., and Jackowski, S. (2003) Role of Feedback Regulation of Pantothenate Kinase (CoaA) in Control of Coenzyme A Levels in *Escherichia coli*. *J. Bacteriol.* **185**, 3410–3415

Chapter 4

Conclusions and future work

4.1 Summary of findings

In prokaryotes such as *Escherichia coli*, CoA degradation into 4'-phosphopantetheine and 3',5'-ADP is thought to play a role in the regulation of CoA pools. However, the enzyme responsible for direct degradation of CoA has remained unidentified. Our hypothesis was that the enzyme responsible for this direct mechanism is NudL, which is the only *E. coli* Nudix hydrolase that remained to be successfully expressed, purified, and characterized. NudL has both the Nudix and NuCoA motifs distinctive for CoA recognition and is predicted to be CoA hydrolase (1). In this study the possible CoA degrading ability of NudL in *E. coli* was investigated to evaluate the role of this enzyme in the regulation of CoA levels in *E. coli*.

4.1.1 Expression and purification of NudL

NudL had only been expressed as a fusion protein with a maltose-binding protein (2). However, NudL has remained uncharacterized, we therefore attempted to express and purify NudL for the purpose for activity assays. The first challenge was the low soluble expression of NudL whereby most of the overexpressed protein was found in the insoluble fraction. Expression trials with various growth media, expression strains and solubility agents (osmolytes or ethanol) did not improve solubility. Two alternative expression systems were also explored namely the cell free expression kit and the expression vector with a dual His₆Halo tag. However, both these systems did not improve soluble expression. The low soluble expression of NudL was unexpected as an *E. coli* protein should not be difficult to overexpress in an *E. coli* expression system. This suggests that overexpression of NudL could be toxic to the cells, with the excessive amounts of NudL was disrupting the CoA pools within the cell. Alternatively, the protein could have possible membrane association, which would also result in the expressed protein shuttled to inclusion bodies. Out of all the conditions tested, expression with the pET28a-NudL vector at a lower IPTG concentrations in combination with lower induction temperatures with longer incubation time yielded the most soluble protein.

Purification attempts of pure NudL fractions were unsuccessful. Several purification attempts were made with IMAC resulting in very low yields of NudL as weak binding to the IMAC column. To complicate matters multiple contaminating proteins were also present in all the soluble purification attempts. The weak interaction with the column could be attributed to possible obstruction of the histidine tag by either the protein itself or the contaminants. Neither the addition of reducing agents

nor the addition of nonionic detergents could improve binding of NudL to the column or disrupt the interactions with the interfering proteins. Purification of the sarkosyl solubilized NudL gave the purest and highest yield however, the protein was inactive. This could be either that the protein was not natively folded in the inclusion bodies or too unstable for the lengthy solubilization and purification process. NudL could only be partially purified manually using His-Select Nickel affinity resin that increased the binding time with the addition of 5 mM ATP that released some of the contaminating proteins (presumable heat shock proteins). The optimized purification method still had very low protein yield but the instability of NudL did not allow for multiple purification batches to be pooled. Therefore, CoA hydrolase activity was characterized in *E. coli* lysate overexpressing NudL.

4.1.2 Further insight into NudL - a biological role

This study also aimed to determine the biological role of NudL. The detected pyrophosphatase activity in both lysate overexpressing NudL and the partially purified NudL fraction strongly implied that the direct degradation of CoA is due to the presence of NudL. Mn^{2+} was found to be the preferred metal cofactor but activity was still observed with Mg^{2+} as the cofactor, interestingly mouse Nudt8 also has this preference (3). The implication and importance of this is still to be determined. The only substrate tested was CoA so it is unclear as yet if it is indeed the preferred substrate or if NudL could act on related substrates like acetyl-CoA, which also forms a part of that total CoA pool. Determining the significance of the metal preference would also give insight to the role of NudL. The metal preference could provide greater substrate selectivity or some other regulatory role. The confirmed phosphatase activity of NudL for CoA together with the significantly reduced intracellular PPanSH in the NudL knockout strain is the first evidence for a direct mechanism of CoA degradation in *E. coli* that accounts for the generation of PPanSH.

The second aspect in determining the biological importance of NudL was to determine how its expression is regulated. In *E. coli* the utilization of Mn^{2+} is associated with oxidative stress by the protection against reactive oxygen species (ROS) (4). However, at late stationary phase the relative mRNA levels of NudL was not influenced by H_2O_2 stress. The growth of the three strains on glucose and acetate was also tested. The growth rate of all three strains were unaffected on glucose however, when acetate was the sole carbon source all strains grew much slower. In light of Vallari et al. demonstrating that CoA degradation is triggered by changes in metabolism that results in rapid decrease in the acetyl-CoA/CoA (5). The results of the acetate growth curves reflect this by the considerable growth defect of the NudL and AcpH mutants specifically compared to the reference

stain. When acetate is the carbon source acetyl-CoA is converted to CoA which results in a decrease in the acetyl-CoA/CoA ratio; the mutant strains would not be able to compensate for this shift (6).

4.2 Future work

4.2.1 Expression and purification of NudL

Although optimization of expression and purification was extensively explored as described in chapter 2, there is still another expression system that could be investigated, being the pCold expression vector. This system, which was recently acquired in the Strauss laboratory, allows for selective expression of target protein at low temperature of 15 °C. These conditions result in a decrease in protease activity and host protein expression. Using this system will hopefully also improve the stability of NudL as the enzyme readily becomes inactive. The multiple cloning site has the restriction enzyme sites NdeI and XhoI that would allow the *yeaB* gene to be subcloned from the pET28a-NudL vector into the pCold I vector. The resultant recombinant protein would still express with a His₆-tag and can be purified with IMAC.

Even though size exclusion chromatography (SEC) was unsuccessful in purifying NudL, it would be worthwhile to repeat this experiment with improved soluble expression of NudL. The combination of IMAC and SEC would theoretically give the purest protein for further characterization of NudL. Alternatively, the His₆-tag could be removed at the thrombin site and purified by anionic exchange as NudL has more negatively charged amino acids. Furthermore, it might also be worthwhile to assess expression and purification of NudL with methods that do not rely on the N-terminal His₆-tag like a glutathione S-transferase (GST) tag or other fusion proteins that would allow for on-column tag cleavage.

4.2.2 Characterization of NudL

The majority of the future work for the further characterization of NudL is dependent on having soluble pure protein in hand. If a pure active protein is obtained, NudL can be fully kinetically characterized with CoA as a substrate as well as other confirmed CoA hydrolase substrates such as acetyl-CoA and oxidized CoA. This would give insight into the substrate specificity of NudL. All the CoA hydrolases that have been characterized have also reported to be inhibited by F⁻ therefore to complete NudL characterization of NudL this should also be validated.

There is a lack of information with regards to the active site of CoA hydrolases as there are only two CoA hydrolases crystal structures (7, 8). NudL is only the second CoA hydrolase with a Mn²⁺ preference

therefore comparing the crystal structural of the active site with the two metals (Mg^{2+} and Mn^{2+}) might also give insight to substrate specificity. Once pure NudL is obtained, the Strauss laboratory has the tools and techniques readily available to obtain protein crystals and has regular access to Diamond Light Source in the U.K. to obtain diffraction data with which to solve the protein structure.

Future work that does not require pure enzyme would be centered around repeating experiments carried out as described in chapter 3. This includes repeating the RT-qPCR analysis with an additional reference gene. Only one reference gene was used in this study, but a second reference gene should be used for future experiments. RT-qPCR is based on the relative quantification of the gene of interest expression to an internal reference and the addition of a second reference gene improves the accuracy of this normalization. Additional conditions can also be tested to see if metabolic states that decrease acetyl-CoA/CoA ratio also results in increase NudL mRNA, for example confirming the acetate growth results. Growth rates of the K12 reference strain and the knockout mutants should be used as a preliminary screen for these conditions. Increased osmotic strength is an example of a stress that decreases the acetyl-CoA/CoA, which is linked to CoA degradation, that could also be further investigated (5, 9).

The metabolomics studies can be complimented with determining the extracellular PPanSH concentration in the media. This experiment would require optimization as the media would have to be concentrated for the PPanSH to be at detectable levels for the CPM HPLC assay. These results together with the results described in chapter 3 would indeed determine whether NudL or AcpH contributes the most to CoA degradation in *E. coli*.

4.3 Concluding remarks

The purpose of this study was to characterize a previously uncharacterized *E. coli* Nudix enzyme predicted to have CoA hydrolase activity. NudL was expressed, and partially purified and assayed for the putative CoA hydrolases activity. Despite the instability of NudL leading to a lack of pure enzyme, the results in this study provide evidence that CoA degradation in *E. coli* lysate is mediated via NudL and that this accounts for the large quantity of intracellular PPanSH, the CoA biosynthesis intermediate. NudL seems plays an integral role in the CoA cycle when acetate is the carbon source but the role of this enzyme during other metabolic stresses still remains to be explored. Determining how this enzyme is regulated will be of greater importance to complete our understanding of CoA regulation in *E. coli*.

4.4 References

1. Aiba, H. (1996) A 570-kb DNA Sequence of the *Escherichia coli* K-12 Genome Corresponding to the 28.0-40.1 min Region on the Linkage Map. *DNA Res.* **3**, 363–377
2. Kim, J., Kershner, J. P., Novikov, Y., Shoemaker, R. K., and Copley, S. D. (2010) Three serendipitous pathways in *E. coli* can bypass a block in pyridoxal-5'-phosphate synthesis. *Mol. Syst. Biol.* **6**, 436
3. Kerr, E. W., Shumar, S. A., and Leonardi, R. (2019) Nudt8 is a novel CoA diphosphohydrolase that resides in the mitochondria. *FEBS Lett.* **593**, 1873-3468.13392
4. Sobota, J. M., and Imlay, J. A. (2011) Iron enzyme ribulose-5-phosphate 3-epimerase in *Escherichia coli* is rapidly damaged by hydrogen peroxide but can be protected by manganese. *Proc. Natl. Acad. Sci.* **108**, 5402–5407
5. Vallari, D. S., and Jackowski, S. (1988) Biosynthesis and degradation both contribute to the regulation of coenzyme A content in *Escherichia coli*. *J. Bacteriol.* **170**, 3961–3966
6. Rock, C. O., Park, H.-W., and Jackowski, S. (2003) Role of Feedback Regulation of Pantothenate Kinase (CoaA) in Control of Coenzyme A Levels in *Escherichia coli*. *J. Bacteriol.* **185**, 3410–3415
7. Resnick, E., Bradley, A., Gan, J., Douangamath, A., Krojer, T., Sethi, R., Geurink, P. P., Aimon, A., Amitai, G., Bellini, D., Bennett, J., Fairhead, M., Fedorov, O., Gabizon, R., Gan, J., Guo, J., Plotnikov, A., Reznik, N., Ruda, G. F., Díaz-Sáez, L., Straub, V. M., Szommer, T., Velupillai, S., Zaidman, D., Zhang, Y., Coker, A. R., Dowson, C. G., Barr, H. M., Wang, C., Huber, K. V. M., Brennan, P. E., Ovaa, H., von Delft, F., and London, N. (2019) Rapid Covalent-Probe Discovery by Electrophile-Fragment Screening. *J. Am. Chem. Soc.* **141**, 8951–8968
8. Kang, L.-W., Gabelli, S. B., Bianchet, M. A., Xu, W. L., Bessman, M. J., and Amzel, L. M. (2003) Structure of a Coenzyme A Pyrophosphatase from *Deinococcus radiodurans*: a Member of the Nudix Family. *J. Bacteriol.* **185**, 4110–4118
9. Chohnan, S., Izawa, H., Nishihara, H., and Takamura, Y. (1998) Changes in Size of Intracellular Pools of Coenzyme A and Its Thioesters in *Escherichia coli* K-12 Cells to Various Carbon Sources and Stresses. *Biosci. Biotechnol. Biochem.* **62**, 1122–1128